MODELING THE DYNAMICS OF BLOOD PRESSURE UNDER THE SLEEP APNEA EFFECT

by

Kazım Özgün

B.S. , Industrial Engineering, Boğaziçi University, 2019

Submitted to the Institute for Graduate Studies in
Science and Engineering in partial fulfillment of the
requirements for the degree of

Master of Science

Graduate Program in Industrial Engineering
Boğaziçi University
2019

ACKNOWLEDGEMENTS

First, I would like to thank my thesis supervisor Prof. Yaman Barlas for his patience, enthusiasm and deep knowledge. It was a great honor to work under his guidance throughout my study. I cannot imagine having a better advisor and mentor.

I am also very grateful to my co-supervisor Assoc. Prof. Hakan Yaşarcan. He has taught me the methodology to present a research study as effective as possible. I would also like to thank him for his sincerity and motivation that deeply inspired me.

I would like to express my thanks to the thesis jury members Assoc. Prof. Gönenç Yücel and Assist. Prof. Özge Karanfil. Their insightful comments and intricate questions during my presentation were helpful to improve my thesis.

Finally, I express my deepest gratitude to my family members and friends for their continued support.

Kazım Özgün
May 2019

ABSTRACT

MODELING THE DYNAMICS OF BLOOD PRESSURE UNDER THE SLEEP APNEA EFFECT

In this study, a dynamic system modeling to analyze blood pressure disorders under the sleep apnea effect is carried out. As a first step, the basic variables of the blood pressure system and the causal relationship between these variables are determined with the help of previous scientific literature. Through modeling steps, these relationships are presented in a simulation environment by writing the related mathematical equations. After the equations are determined and the model is constructed, we first try to deduce the dynamics of the basic variables of blood pressure system for a healthy human. The model should generate the dynamics of the basic variables of the blood pressure system for a healthy human body, as suggested in the corresponding literature. The model indeed passes this basic test of model validity. Thereby, the model can provide insights to investigate the medical disorder scenarios such as sleep apnea, without experimenting on human beings. Increased blood pressure, hypertension, a known problem of the blood pressure system caused by sleep apnea, is obtained by simulation runs. The reason of this particular hypertension is that the sleep apnea causes oxygen deficiency in the tissues during and after apnea periods, leading to structural changes in the function of sensory cells. These changes are obtained in the simulation results. Next, by the scenario analysis, the dynamics of the fundamental variables in the blood pressure system under different intensity, frequency or distribution of the sleep apnea have been analyzed. Simulation results show that the increase in the intensity or frequency of apnea leads to more severe hypertension. Finally, receptor blocker drugs, like alpha 1 and beta 1 blockers typically used as a treatment of hypertension are also modeled and experimented with. The effect of different usage times of these drugs on the treatment of the disease has been simulated. Simulation results show that the timing of medication is important for effective control the of the hypertension associated with the sleep apnea, if drug usage time is optimal.

ÖZET

UYKU APNESİ ETKİSİ ALTINDA KAN BASINCI DİNAMİKLERİNİN MODELLENMESİ

Bu çalışmada uyku apnesi altında ortaya çıkan kan basıncı sorunlarını araştırmak için dinamik sistem modellemesi uygulanmıştır. İlk adım olarak, kan basıncı sisteminde bulunan temel değişkenler ve bu değişkenler arasındaki ilişkiler geçmiş bilimsel yayınların yardımıyla belirlenmiştir. Modelleme aşamalarında ise bu ilişkiler matematiksel denklemler halinde simülasyon ortamına aktarılmıştır. Model denklemlerinin belirlenmesi ve modelin kurulumu bittikten sonra, ilk olarak sağlıklı durumdaki bir insan için kan basıncı sistemindeki temel değişkenlerin dinamikleri çıkarılmaya çalışılmıştır. Model, sağlıklı bir insan vücudundaki kan basıncının temel değişkenlerinin dinamiğini ilgili literatürde önerildiği şekilde göstermiş ve. bu temel tutarlılık testini geçmiştir. Böylece model, insana ihtiyaç duymadan uyku apnesi gibi hastalık senaryolarının incelenmesine ışık tutabilecektir. Uyku apnesinin sebep olduğu bilinen kan basıncı yükselmesi problemi (hipertansiyon durumu) simülasyon deneylerinde elde edilmiştir. Hipertansiyonun nedeni ise, uyku apnesinin dokularda oksijen yetersizliğine yol açarak, duyu epiteli hücrelerinin işleyişinde bazı yapısal değişimlere yol açmasıdır. Bu değişimler ilgili literatürde önerildiği gibi simülasyon sonuçlarında da gözlenmiştir. Sonrasında, senaryo analizleriyle, uyku apnesinin şiddeti, sıklığı veya dağılımının farklılığına göre oluşan kan basıncı sistemindeki temel değişkenlerin dinamikleri incelenmiştir. Simülasyon sonuçlarına göre uyku apnesindeki şiddet veya sıklık artışı hipertansiyonun daha ciddi boyutlara ulaşmasına yol açmıştır. Son olarak, hipertansiyonun tıbbi tedavisinde tipik olarak kullanılan alfa 1 ve beta 1 blokerleri gibi reseptor bloker ilaçları modellenmiş ve deneyler yapılmıştır. Bu ilaçların kullanım zamanlarının farklılığının, hastalığın tedavisine olan etkisi simüle edilmiştir. Simülasyon sonuçları göstermiştir ki; doğru bir ilaç kullanım zamanlaması, uyku apnesine bağlı oluşan hipertansiyonu etkili bir biçimde kontrol altına alabilmektedir.

TABLE OF CONTENTS

LIST OF FIGURES

LIST OF TABLES

LIST OF ACRONYMS/ABBREVATIONS

A1	Alpha 1 receptor
Abs	Absorption
Adj	Adjustment
AHI	Apnea hypopnea index
ANS	Autonomous nervous system
Ar	Arterial
ASV	Average stroke volume
AT	Adjustment time
ATBP	Adjustment time of blood pressure
Aten	Atenolol
B1	Beta 1 receptor
Bal	Balance
Baro	Baroreceptor
Bio	Bioavailability
BOP	Baroreceptor operation point
BP	Blood pressure
Cap	Capacity
Chemo	Chemoreceptor
Cl	Clearance
Clr	Clear
Com	Common
Con	Converter
Conc	Concentration
DAHI	Dynamic apnea hypopnea index
Des	Desired
Dest	Destruction
dist	Distribution
EC50	Half maximal response concentration

Eff	Effect
Elim	Elimination
Ep	Epinephrine
Exp	Expected
F&L	Food and Light
Fac	Factor
HR	Heart rate
KD	Dissociation constant
L	Liter
LTBP	Long term blood pressure
Ml	Milliliter
Nep	Norepinephrine
NonAbs	Non-absorbed
O2	Oxygen
Occ	Occupancy
Perc	Percentage
Pro	Prozasin
Prod	Production
Ref	Reference
Res	Response
Resis	Resistance
Sat	Saturation
SNA	Sympathetic neuron activation
Svr	Systemic vascular resistance
Tot	Total
Trans	Transformation

1. INTRODUCTION

A system is collection of parts that interact together. A system as a whole is bigger than the sum of its elements due to their interactions. There is no way that one single part does the whole job by itself, but any dysfunction or delay of single part affects the system as a whole. A typical example is the blood pressure regulation system in human body. The individual organs or cells function together, in coordination, to maintain blood pressure homeostasis.

The blood pressure regulation system includes interactions of four main subsystems. The first subsystem is hemodynamic system. Hemodynamic variables are heart rate, stroke volume and systemic vascular resistance. They are the main determinants of blood pressure in the human body. The level of blood pressure determines amount of oxygen delivery to the tissues. Oxygen consumption amount of the tissues is determined by circadian rhythm under normal circumstances (i.e. Circadian Clock). Circadian clock is the 24-hour internal clock that is synchronized with solar time. The circadian clock determines the level of hormones (such as melatonin and growth hormones) and 24-hour sleep-wake cycles. Thus, the circadian clock determines the activity level of cells. The circadian clock regulated activity levels determine oxygen and nutrition requirements of cells. To satisfy these requirements, blood pressure adjusts itself as a response (Portaluppi & Smolensky, 2007).

The second subsystem is arterial receptor system. Arterial receptor system has two different sources of signals to warn autonomous nervous system: chemoreceptors and baroreceptors. The first source is baroreceptors. The baroreceptors are responsible for protecting body from sudden changes in the blood pressure via conveying signals to autonomous nervous system. The number of signals is determined by the ratio of blood pressure to baroreceptor operation point (Chapleau *et al.*, 1989). Under normal conditions, baroreceptor operation point is equal to the average blood pressure. The other source is chemoreceptors. A chemoreceptor is a sensory cell that is specialized in transducing

chemical substances and generating biological signals (Guyton & Hall, 2006). If there are imbalances between tissues' oxygen demand and supply, chemoreceptors are stimulated by them. Thus, the number of signals sent by chemoreceptors to autonomous nervous system is determined by the magnitude of the imbalances.

The third subsystem is autonomous nervous system. Signals that are produced by chemoreceptors and baroreceptors are transmitted to the autonomous nervous system. According to these signals, autonomous nervous system determines the level of hormones to affect the hemodynamic system (Guyton & Hall, 2006). *Catecholamines* (Epinephrine & Norepinephrine) are the most important hormones produced by autonomous nervous system. Norepinephrine is produced inside the nerve axon and released into blood. Some portion of norepinephrine is transformed into epinephrine in the adrenal medulla and released into blood. They circulate throughout the body in the blood plasma to activate the adrenergic receptors, as explained below.

The last subsystem is adrenergic receptors. Adrenergic receptors have two different subsections: alpha and beta. Epinephrine and norepinephrine hormones in the blood attach to the adrenergic receptors and stimulate them. Alpha1 receptor stimulation leads to constriction of vessel wall. Thereby, the diameter of the vessel is decreased. Diameter of the arteries is the main determinant of systemic vascular resistance. Beta1 receptor stimulation leads to an increase in heart rate. These adrenergic hormones stimulate adrenergic receptors to regulate important hemodynamic variables like heart rate, stroke volume and systemic vascular resistance.

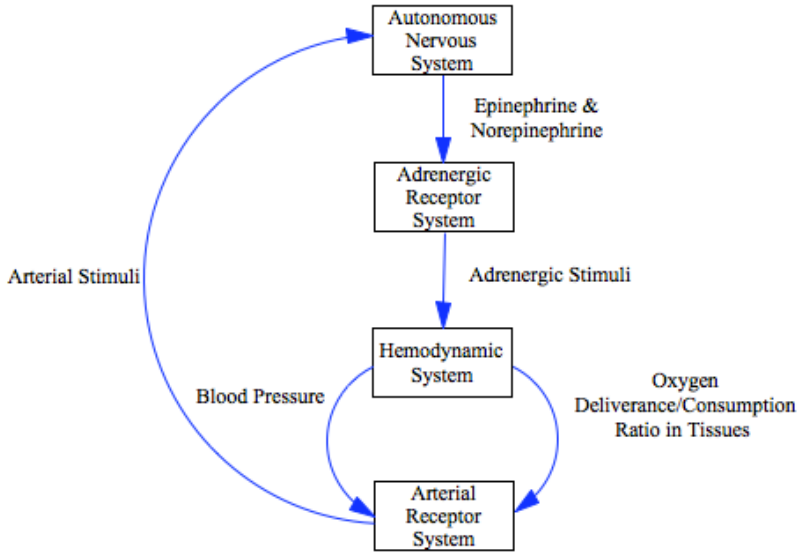

Figure 1.1. Basic structure of the blood pressure system.

These interrelationships of the subsystems constitute the main feedback control loops in the blood pressure system. The aim of the feedback loops is to ensure internal homeostasis in the human body. The basic structure of blood pressure system is shown in Figure 1.1. There are five main feedback loops. Three of them are negative feedback loops. The negative feedback loops are "Oxygenation", "Baroreceptor Anchoring" and "Chemoreceptor Sensitization" feedback loops. There are two positive feedback loops: "Baroreceflex Resetting" and "Cardiac Workload" feedback loops. The details of main feedback loops will be explained in the "Overview of the Model" section.

Hypertension is the medical term for high blood pressure, which is a common and dangerous condition. Klabunde (2004) stated that there are three different groups of blood pressure: normal blood pressure (when systolic and diastolic blood pressures are lower than 120 and 80 mmHg, respectively), high blood pressure or hypertension (when systolic and diastolic blood pressures are higher than 140 and 90 mmHg, respectively) and pre-hypertension (when systolic and diastolic blood pressures are in between 120/80 and 140/90 mmHg, respectively). At 2017, the American College of Cardiology (ACC) and American Heart Association (AHA) have added a new category: Stage 1 hypertension, which was previously known as "Pre-hypertension". Patients with systolic blood pressures of 130 to

139 mmHg and diastolic blood pressures of 80 to 89 mmHg are diagnosed with “Stage 1 hypertension”. With this new definition, the number of adults in U.S who have hypertension is increased from 72 to 103 million, or in percentage, from 32% to 46% of the adult population (Bakris & Sorrentino, 2018). The diagnosis and classification of hypertension should be done as early as possible. Early diagnosis and classification of hypertension ease treatment procedure. Hypertension is classified in two groups: Essential and secondary hypertensions. Essential hypertension has no clear cause, mostly associated with genetics, poor diet and lack of exercise. For example, unhealthy eating habits may lead to accumulation of fat in the artery walls. Medical literature defines it as “atherosclerosis” (hardening of arteries). Arteries offer more resistance to blood flow, which leads to high blood pressure, which is also known as “hypertension” (Castorena-Gonzalez *et al.*, 2014). Secondary hypertension is caused by other medical conditions such as thyroid disease , glomerular disease and sleep apnea (Grassi, 2010). It is known that hypertension can be a result of many different problems in the above mechanisms such as abnormal catecholamine secretion, chemoreceptor over-activation and imbalances between tissues’ oxygen demand/supply. One such problem can be inadequate oxygen delivery to tissues due to sleep apnea. When the inadequate oxygen delivery to tissues continuously happens, it creates problems like chemoreceptor sensitization and baroreflex resetting. For example, baroreceptor operation point is the level of blood pressure to which the system tries to bring the blood pressure. However, if blood pressure is persistent at a new level for two days, the baroreceptor system resets its operation point to this level. This phenomenon is known as baroreflex resetting (Chapleau *et al.*, 1989). Thus, these problems may cause progressive increase in blood pressure.

Sleep apnea is a disorder in which breathing is repeatedly interrupted during the sleep period. The breathing cessation throughout the sleep period decreases the percentage of hemoglobin that is saturated with oxygen. Thus, the percentage may decrease down to 80 (from the regular percentage of 97), which leads to inadequate oxygen delivery to tissues (Silverberg *et al.*, 2001). Nocturnal period is nighttime, whereas the diurnal period is daytime. In the model, nocturnal period is defined as the time interval between 11:00 PM and 07:00 AM. Diurnal period is defined as the time interval between 07:00 AM and 11:00 PM. Imbalance between oxygen supply and demand during nocturnal period may lead to

changes in the functioning of baroreceptors and chemoreceptors. In the medical literature, sleep apnea has acute and chronic effects on variables such as sympathetic neuron activation and blood pressure. Changes in the functioning of baroreceptor are known as “acute effect” of sleep apnea. Sympathetic neuron over-activity and hypertension are associated with the chronic effect of sleep apnea on chemoreceptor concentration. Even if the sleep apnea is treated, changes in the functioning of chemoreceptor could be permanent. As a result, the chronic effect of sleep apnea on the functioning of chemoreceptor may lead to resistant (permanent) hypertension.

It is claimed that more than 936 million people worldwide are affected by sleep apnea disorder (ATS 2018 International Conference). Since the world population has reached approximately 7.5 billion people, the sleep apnea disorder affects 12.48 percent of total population. Worldwide prevalence of hypertension exceeds 1.3 billion, 17.33 percent of total population (MJ Bloch, 2016). The research of Daugherty *et al.* (2012) showed that 16.52 percent of total patients with hypertension have resistant hypertension, which is nearly 214.5 million people worldwide. Konecny *et al.* (2013) stated that 64 percent of all resistant hypertension cases (approximately 137.2 million people) are induced by sleep apnea. It is claimed that the cumulative incidence of sleep apnea induced hypertension in 15 years is approximately 70 percent of total patients with sleep apnea disorder, which is approximately 630 million people (Konecny *et al.*, 2013). Obesity and age are the main drivers of sleep apnea disorder. The prevalence of sleep apnea tends to increase with age. Nearly 15% of men and 5% of women have sleep apnea. However, it is stated that the percentage for women may be underestimated (Frigy & Kocsis, 2018).

Our purpose is to model the dynamics of blood pressure under the sleep apnea disorder. Thus, it will also be possible to simulate and analyze under what conditions sleep apnea can cause high blood pressure. Secondly, it is known that blood pressure has a natural cycle dictated by circadian clock. We will also model and investigate to what extent the interactions between circadian clock and intensity or frequency of sleep apnea can make blood pressure dynamics worse. Thirdly, we will model and investigate the effectiveness of two typical medication types on blood pressure: alpha and beta-blockers. Finally, we will

investigate optimal usage times of blocker medications to effectively control the hypertension associated with the sleep apnea.

2. LITERATURE REVIEW AND RESEARCH OBJECTIVE

Our first task to start building the model is to understand the essential macro dynamics of blood pressure regulation system in the human body. Autonomous nervous system (ANS) mainly controls blood pressure regulation. ANS commands the adrenergic hormones to regulate blood pressure in the human body, and arterial receptors send some feedback information about blood pressure to autonomous nervous system (Guyton & Hall, 2006). Hence, the blood pressure regulation system has rich feedback loops (like chemoreceptor sensitization, baroreflex resetting and cardiac workload) that include different variables such as chemoreceptor concentration and baroreceptor operation point. The complexity of the relationships among variables makes it difficult to examine the dynamics of blood pressure regulation system without the help of modeling and simulation. Over the past few decades, modeling of blood pressure regulation system has become popular in scientific literature (Grassi, 2010).

Cheng *et al.* (2010) has built a highly detailed physiological control model of blood pressure regulation system. Authors included many previous research results in their mathematical model to explain blood pressure regulation via interactions between hemodynamic, arterial receptor and autonomous nervous subsystems. Authors claim that the model provides realistic physiological response even under sleep apnea.

Some of the previous research utilized in the mathematical model of Cheng *et al.* (2010) will be summarized here, as they are related to the thesis topic. The research, conducted by Ursino and Magosso (2003), shows blood pressure control through some special arterial receptors that have effects on the autonomous nervous system. Firstly, Ursino (1998) have completed a mathematical model to show the feedback effect of baroreceptor on autonomous nervous system to regulate blood pressure. Blood pressure is always observed by baroreceptors, such that, sudden changes in blood pressure are inhibited by the baroreceptor signals to maintain the level of blood pressure. Secondly, Magosso and Ursino,

(2001) constructed another mathematical model related with feedback effect of chemoreceptor signals on autonomous nervous system. Oxygen delivery to tissues is affected by blood pressure. Delivered oxygen is used in tissues to produce energy and byproducts. Those byproducts lead to change in the concentrations of arterial blood gases, observed by chemoreceptors. Thereby, chemoreceptors observe the blood pressure to send feedback signals to ANS. Lastly, Ursino and Magosso (2003) enlarged the scope of the model to show feedback relationship between autonomous nervous, arterial receptor and hemodynamic subsystems.

There is naturally extensive research about the blood pressure regulation system. Kuri *et al.* (2010) investigated the regulation of adrenergic hormone secretion under stress conditions like sleep apnea. Their paper aims to provide better understanding of interaction between autonomous nervous and adrenergic receptor system under oxygen deficiency in tissues. The works of Harvey *et al.* (2012), Meibohm (2006) and Brunton *et al.* (2011) investigate the interaction between adrenergic hormones and adrenergic receptors to stimulate hemodynamic system. The binding characteristics of hormones to receptors and effects of binding on hemodynamic system are well presented in the study.

Compared to previous mathematical models, our model includes simultaneously the autonomous nervous, adrenergic receptor, hemodynamic and arterial receptor subsystems in the regulation of blood pressure. Our model is focused on macro-level causal relationships between these subsystems to explain nonlinear feedback control of blood pressure, rather than the molecular level relationships. The interrelationships among those four subsystems maintain blood pressure homeostasis. Our model will include all relevant aspects of blood pressure regulation system, enabling us to show the characteristic behaviors of important variables associated with the change in blood pressure regulation under the sleep apnea condition. Table 2.1 includes the summary of previous studies using mathematical models.

Table 2.1. The summary of previous studies using mathematical models

Author	Objective	Main constraints	Validation Method	Year
Mauro Ursino	To model short-term arterial pressure control by the carotid baroreceptors	Elastance of the left and right heart, systemic and pulmonary circulations, vagal afferent activities and several effector mechanism	A statistical comparison between the model simulation results and experimental data on heart rate control date	1998
Magosso Elisa and Mauro Ursino	Analyzing the effects of changes in arterial CO2 tension on cardiovascular system	O_2-CO_2 interaction at the peripheral chemoreceptors, the effect of local CO_2 changes on peripheral resistances, the direct central neural system (CNS) response to CO_2, and the control of central chemoreceptors on ventilation.	A statistical comparison between model simulation results and various experimental data.	2001
Mauro Ursino and Magosso Elisa	To model the role of short-term cardiovascular regulation in heart period variability	Pulmonary circulation, the mechanical effect of respiration on venous return, two groups of receptors (arterial baroreceptors and lung stretch receptors), the sympathetic and vagal efferent branches, and a very low-frequency (LF) vasomotor noise.	A statistical comparison between model simulation results and various experimental data	2003

The simulation software *Stella* provides a platform for visualizing system structure. A main advantage of modeling physiological systems with simulation software is to carry out experiments without using humans. These experimentations are important to understand how subsystems interact with each other in order to regulate blood pressure. The experimentations will be helpful to detect the dynamics of key variables in the blood pressure regulation system. Thereby, the initial aim of the model is to provide a valid representation of the essential blood pressure control system explained above. Next, the model will be adjusted to represent blood pressure regulation system under well-known disorders. The homeostasis of blood pressure is critical for maintaining the oxygenation of tissues and organs. Sleep apnea disorder leads to breathing cessations in nocturnal period. These breathing cessations lead to decrease in oxygen delivery to tissues. Blood pressure regulation system adapts itself to sleep apnea condition in order to maintain the balance between oxygen supply and demand (i.e. oxygen delivery and consumption) determined by circadian rhythm. Sleep apnea may therefore create problems in blood pressure regulation and eventually hypertension. Apnea occurrences decrease the percentage of hemoglobin that is saturated with oxygen, whereas circadian clock determines the activity level of cell and

oxygen consumption throughout a day. Oxygen supply/demand ratio is affected by both variables. Thus, we will be able to investigate the interaction between the effects of circadian clock and sleep apnea on oxygen supply/demand ratio with the help of the simulation. We will simulate the model under different conditions such as different sleep apnea frequencies, intensities and distributions. Thereby, we will be able to comprehend the dynamics of key variables in the blood pressure regulation system under sleep apnea disorder. Understanding of these dynamics will help recognition of sleep apnea-related hypertension. Model-generated dynamics of variables will be evaluated to make sure that they are compatible with clinical data and data from other scientific research. After the model is completed and validated, the final goal of the thesis is to analyze by simulation, how and to what extent the disease can be treated with the help of receptor (alpha and beta) blocker medications, focusing specifically on the effects of different usage times of blocker medications on treatment.

3. RESEARCH METHODOLOGY

Our model aims to understand the dynamics of blood pressure regulation that includes variables like sympathetic neuron activation, blood pressure, heart rate, and vascular resistance that change over time. The blood pressure regulation is a closed system, which includes many feedback mechanisms. Basically, information about the blood pressure level is continuously sent to autonomous nervous system. In this way, the blood pressure level is adjusted by autonomous nervous system. As a whole blood pressure regulation system ensures that enough oxygen delivered to tissues. System dynamics method is an ideal tool to model dynamic feedback systems facing difficult control and management problems (Barlas, 2002).

Autonomous nervous system is only a part of the structure of the entire system that we are interested in. Many variables are interrelated so that those relationships construct the system structure. All the relationships of individual parts should serve the purpose of survival of the human body. However, the purpose cannot be met optimally under some health disorders. Sleep apnea is one of the examples of such circumstances in our case. Barlas (2002) states “main purpose of system dynamics methodology is to understand the causes of undesirable dynamics and design new policies to eliminate them”. Thus, our ultimate goal is to understand why and under what conditions sleep apnea can cause circulation and blood pressure problems and how these problems can be tackled.

In system dynamics method, one of the initial steps is to determine the causal links between all variables in the system. Secondly, important causal relations will typically be “circular” so as to create feedback causality in most dynamic systems, as will be illustrated in the following chapters in our case (see Figure 4.1 for example).

Dynamic behaviors of the system variables are primarily caused by the *internal structure* of the system. Thus, to understand the causes and cures for the blood pressure regulation problem, we will analyze the relations between internal structure of our model and its dynamic behavior, primarily by a series of simulation experiments.

The literature is reviewed to capture important causally interrelated variables to construct structure of the model. Time delays, nonlinear causal relationships between variables and feedback loops are the main elements that create complexity in the problems subject to system dynamics modeling. These complexities can be perceived and handled thanks to system dynamics modeling method.

The notions `stock` and `flow` variables are essential to represent the variables in system dynamics method. A stock variable represents quantities that accumulate over time. Meanwhile, a flow is the rate of change of stocks. Hence, stocks accumulate the net differences of their flows. There is also another intermediate variable type called 'converter' (or auxiliary) that represents quantities can be computed from stocks and flows of the system at any point in time through a computational procedure (see for instance Figure 5.2). In this research, we follow the standard main steps of system dynamics methodology as presented by Sterman (2000):

- Boundary selection
- Formulation of dynamic hypothesis
- Formulation of simulation model
- Testing
- Policy design and evaluation

4. OVERVIEW OF THE MODEL

Our model has 5 different sectors named hemodynamic sector, chemoreceptor sector, baroreceptor sector, medication sector and apnea sector, respectively. The most important variables in the circulation are *hemodynamic* ones, which are mainly controlled by autonomous nervous system. The internal structure of the model for healthy person will include the first three sectors mentioned above. The structure of model suggests that dynamics of important variables will be controlled by the interrelation of those three sectors for healthy human body. Finally, for a person suffering sleep apnea, two additional sectors, medication and apnea will be integrated to the model.

Hemodynamic sector is the one that ensures short-term regulation of oxygenation of tissues. Autonomous nervous system dictates the desired levels of adrenergic hormones that are epinephrine and norepinephrine in the blood. Adrenal medulla in hypothalamus is responsible for the adrenergic hormone secretion to blood plasma. Adrenergic hormones are also excreted from the body via urination, sweating and etc. The adrenergic hormones can bind with adrenergic receptors to regulate the functioning of special organs. The level of heart rate is regulated by beta 1 receptors, whereas the diameter of arterioles is arranged by alpha 1. Oxygen delivery to tissues is regulated by those hemodynamic variables. Each individual tissue is capable of sending signals to autonomous nervous system to redistribute blood flow.

Baroreceptor sector is one of the blood pressure control systems in the human body. The system consists of mechanoreceptors that keep homeostasis of blood pressure in the human body. Short-term regulation of blood pressure is the main responsibility of the baroreceptors. An undesirable level of blood pressure is sensed through baroreceptors to send signals to autonomous nervous system to initiate desired change in blood pressure. Chemoreceptor sector ensures the long-term control of blood pressure. In the short-term, the needs of tissues are met through hemodynamic sector; however, chemoreceptor sector is

capable of setting the level of blood pressure if the hemodynamic sector cannot ensure this action. Note that short term is defined as hours, whereas long term is defined as weeks.

Simplified causal loop diagram of the above structure is shown in Figure 4.1. The arrows represent causal relationships between variables. The variable at the tail of arrow represents causes, whereas the variables at the end of arrow represent effect. The sign at the head of the arrow shows the type of relationship between them. If the sign is plus, it means a change in the "cause" variable will lead to a change in the same direction in the "effect" variable: an increase in heart rate will lead to an increase in oxygen consumption. On the other hand, minus sign will lead to a change in reverse direction in the effect variable: an increase in alpha 1 receptor occupation will lead to decrease in arterioles diameter. (See Figure 4.1 for more examples). We modeled both epinephrine and norepinephrine stocks in the model separately. The change in epinephrine or norepinephrine amount leads to the change in alpha 1 and beta 1 receptor occupancy by hormones in the same direction. So, in simplified causal loop diagram, epinephrine and norepinephrine is denoted as a single node. Also, the "oxygen consumption" variable represents the total oxygen consumption in the body.

Also note that successions of causal links that start and end in the same variable indicate a feedback loop. The polarity (sign) of feedback loop is found by algebraic product of all signs on the loops. A reinforcing (or +) loop means that a change in a variable comes back to it, producing further change in the same direction. Such loops are unstable; they produce diverging dynamic behavior in isolation. They are naturally rare in human body (and living systems) because they would work against homeostasis and healthy, stable control of bodily functions. Reinforcing loops, particularly when they dominate the system indicate a health problem, a disorder in the body. A balancing (or -) loop on the other hand, means that a change in a variable comes back to it to induce a change in the opposite direction. Thus, a balancing loop seeks a goal, equilibrium; they produce stable dynamics in isolation. In health human body, there are countless negative feedback loops that make homeostasis possible in spite of radically changing external conditions. The ultimate dynamics of a system is determined by the nature of the loops it embodies and their relative

strengths. This notion will be important in analyzing the dynamics of the model in later chapters.

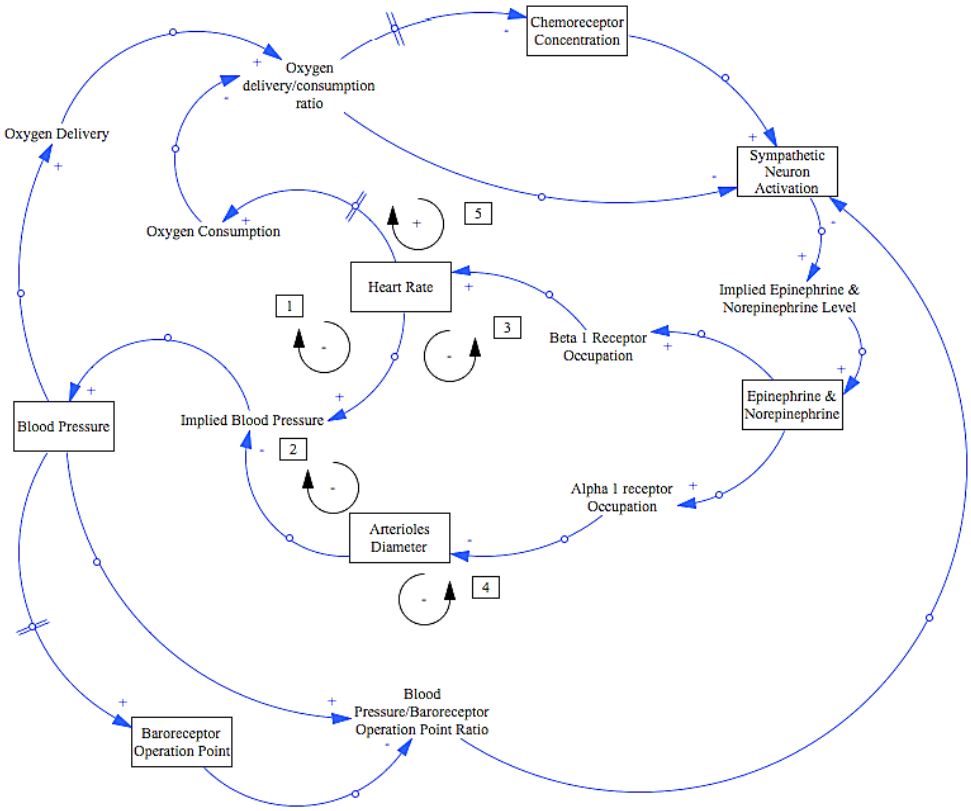

Figure 4.1. Simplified representation of the causal feedback structure of the model for healthy human body.

The relationship between oxygen supply/demand ratio and sympathetic neuron activation level is well defined in the medical literature (Koeners *et al.*, 2016). The lack of oxygen or the abundance of it is sensed by chemoreceptors in carotid body. Nerves carry messages from carotid body to autonomous nervous system, as tiny electrical signals. Autonomous nervous system arranges the level of sympathetic neuron activation according to the messages from carotid body to ensure that cells get enough oxygen. The secretion rates of adrenergic hormones are affected by sympathetic neuron activation level. Sympathetic neural mechanism and its effects on the levels of adrenergic hormones are well documented in the research of Charkaudian & Rabbitts (2019). Norepinephrine secretion in adrenal gland is affected by sympathetic neuron activation level. Norepinephrine is

converted to epinephrine in Adrenal medulla (Guyton & Hall, 2006). A receptor is a molecule on the cell surface that recognizes specific hormone molecules and binds to them. The mathematical formulations for receptor occupancy by hormones is well defined in the medical literature (Motulsky & Neubig, 2002;Sanders, 2010). The effects of receptor occupancy by hormones on hemodynamic variables such as the effect of beta1 receptor occupancy by adrenergic hormones on the heart rate and the effect of alpha1 receptor occupancy by adrenergic hormones on the diameter of arterioles are given in medical literature (Harvey *et al.*, 2012;Katzung & Trevor, 2015). Blood pressure is equal to multiplication of hemodynamic variables (stroke volume, heart rate and resistance). The amount of oxygen delivered to tissues is determined by two conditions: the level of blood pressure and oxygen saturation level (Pittman, 2011). The circadian clock determines the total Oxygen consumption. Oxygenation is our main negative feedback loop in the model.

There are baroreceptor anchoring and baroreflex resetting feedback loops in our model. Baroreceptors store the value of normal blood pressure level. Deviations from normal level of blood pressure is counteracted by negative “baroreceptor anchoring” feedback loops initially. The aim is to protect the body from sudden changes in blood pressure (Chapleau *et al.*, 1989). Baroreceptors gradually make less effort to bring blood pressure back to regular level under persistent blood pressure change, which is called "Baroreflex resetting”. According to medical literature, baroreceptors accept the new level of blood pressure as normal after two days (Dicarlo & Bishop, 2001; Albaghdadi, 2007). Thus, the change in blood pressure is reinforced by positive baroreflex resetting loops in our model.

There is also positive cardiac workload feedback loop. Sometimes the heart has to work harder to deliver more oxygen mostly during physical activities. The heart is capable of increasing oxygen delivery in two ways: increasing heart rate or stroke volume. However, if the heart works inefficiently, it may not contract with required power. Thus, the stroke volume may not be increased. So, the only way is to increase heart rate. However, increasing the heart rate means increasing the oxygen consumption by heart. So, the heart needs to deliver extra oxygen due to its own consumption. In the end, the heart cannot keep up with

its workload. The cardiac workload feedback loop explains the pathophysiology of heart failure (Westheim & Sivertssen, 1986).

The time unit used in the model is hour; so, all changes are per hour. This time unit is chosen as an optimal balance to avoid too short or too long-time units. Our purpose is to simulate the model for a time horizon ranging from a couple of days to a couple of weeks. A shorter time unit (such as a minute) would make it nearly impossible to run and analyze the model for a couple of weeks. A longer time unit (such a day) would make it impossible to trace the relevant dynamics of main hemodynamic, baroreceptor and chemoreceptor variables. So, an hour was selected as an optimal time unit that meets the model purpose.

5. DESCRIPTION OF THE MODEL

5.1. Hemodynamic Sector

5.1.1. Medical Fundamentals and Assumptions

Autonomous nervous system (ANS) is responsible to make organs function properly by controlling main variables in a desired range. Some examples are hormone levels, body temperature, arterial pressure and etc. Some of these are totally controlled by autonomous nervous system while others are controlled partially. The intervention time of ANS to the organs is very fast (a couple of minutes), compared to other control systems in the body (Guyton and Hall, 2006). The system is vital to maintain blood pressure homeostasis in short or long-term in face of external changes.

The autonomous nervous systems are stimulated from the centers in hypothalamus: medulla spinals and brain stem. (Guyton and Hall, 2006) The centers receive signals from specific arterial receptors that are stimulated by the changes in blood pressure and gas content of blood. These stimulated receptors transmit signals to autonomous nervous system, to inhibit or to promote sympathetic stimulation. Sympathetic stimulation dictates the level of adrenergic hormones. These adrenergic hormones stimulate adrenergic receptors to arrange hemodynamic variables and blood pressure. As a result, they create a feedback system to keep homeostasis of blood pressure.

Autonomous nervous system is responsible for dictating epinephrine and norepinephrine secretion into the blood plasma. While norepinephrine can be secreted from other centers, as mentioned previously, epinephrine is only secreted in adrenal medulla that converts norepinephrine to epinephrine Guyton and Hall (2006). It was assumed that the total amount of norepinephrine in the blood plasma is converted to epinephrine per hour in the adrenal medulla. Blood plasma levels of epinephrine and norepinephrine may rise and

fall irregularly due to sudden physiological or environmental changes like being excited, frightened etc. Such short-term sudden variations in hormone levels are outside the scope of the model purpose. Their average hourly values of these two hormones are represented in the model.

Hormones are cleared from the blood with specific ratio, called the clearance ratio of epinephrine and norepinephrine (*Clr rat EP* and *Clr rat NEP*). Half-lives of hormones denote durations before the hormones are decreased to half of their initial amount. The clearance ratios of hormones are determined by half-lives of the hormones that are calculated in Equation 5.1.

$$Clearance\ ratio = ln2 / t_{half} \tag{5.1}$$

where t_{half} is the half-life of a hormone. Thereby, the units of clearance ratios are found per hour. The half-lives of noradrenaline and adrenaline are given as 4.5 and 4 minutes in the medical literature. The clearance ratios of noradrenaline and adrenaline are 9 and 10 per hour, respectively.

The molecules of adrenergic hormones are able to bind to the molecules of adrenergic receptors (Katzung & Trevor, 2015). Most of the theories about the interaction between hormone and receptor molecule are deduced from scientific experiments in vitro. In vitro means, the related components of an organism, which are isolated from its usual surroundings, are used in the scientific experiments. In-vitro studies are more popular compared to others, because they prevent possibility of other undesirable factors such as hormone elimination or metabolization to interfere with the results (Burns *et al.*, 1981). These experiments help to find the concentration of hormone, which occupies half of the receptors or produces half maximum effect on associated hemodynamic variables such as heart rate, stroke volume or systemic vascular resistance.

Receptor is a molecule on the cell surface that recognizes and binds to specific hormone molecules (ligand). The hormone-receptor complex produces a response (The American Heritage Medical Dictionary, 2007). The exploration of concentration-effect curve is completed by A.V. Hill at 1909. The researcher suggests that the response produced by the hormone-receptor complex is determined by an individual function of hormone concentration. A. J Clark (1933) generalized the observation of Hill and hypothesized the classical receptor theory. A J Clark claims that the effect of the hormone-receptor complex is proportional to the ratio of receptor occupancy by the hormone; the receptors should be occupied by hormone ligand completely to produce maximum response.

Lastly, R P Stevenson (1956) showed that maximum response might be achieved without full occupancy of the receptor. The author claims that every hormone ligand has its own efficacy, which is the quantitative effect of unit hormone-receptor complex. Paton (1961) assumes that the hormone molecules only hits and leaves the receptor simultaneously (in terms of milliseconds), which can be ignored.

The importance of these researches for our model can be summarized shortly. Firstly, it was assumed that the receptor occupancy ratio is only related with the concentration of the hormones. Secondly, The magnitude of response produced by unit hormone-receptor complex is different for each complex. Lastly, the hormones are not accumulated on the receptor sites to stimulate them. A magnitude of hemodynamic response to adrenergic hormones is determined by the concentration of hormones, the binding tendency for a type of hormone to a type of receptor, and the magnitude of the response for unit receptor-hormone complex.

In the medical literature, dissociation constant (K_d) denotes the concentration of hormone in the blood plasma to occupy half of the related receptors. The percentage of occupied receptor by the hormone can be found only with concentration of the hormone and its dissociation constant for that receptor. EC_{50} denotes the concentration of hormone in the blood plasma to produce half maximal hemodynamic response. It was assumed that the magnitude of the response for unit hormone-receptor complex is equal to the ratio of K_d to

EC_{50} for that hormone-receptor complex. Table 5.1 shows related K_d values in scientific researches. EC_{50} values obtained from www.bindingdb.org are shown in Table 5.2.

Table 5.1. K_d values of adrenergic hormones for different receptors.

Hormones	Receptor	Dissociation Constant (K_d)	Reference
Epinephrine	Alpha 1 receptor	251.18 Molar	(Schwinn *et al.*, 1995)
Epinephrine	Beta 1 Receptor	3970.0 Molar	(Hoffman C. *et al.*, 2004)
Norepinephrine	Alpha 1 receptor	199.52 Molar	(Schwinn *et al.*, 1995)
Norepinephrine	Beta 1 Receptor	3570.0 Molar	(Hoffman C. *et al.*, 2004)

Table 5.2. EC_{50} values of adrenergic hormones for different receptors.

Hormones	Receptor	Half-maximal effect concentration (EC_{50})
Epinephrine	Beta 1 receptor	23.6 Molar
Norepinephrine	Beta 1 Receptor	236 Molar
Norepinephrine	Alpha 1 receptor	15 Molar

Beta1 receptors are mostly located in heart. Beta1 receptors are primarily responsible for regulating heart rate and stroke volume. It was suggested that stroke volume is regulated by heart rate, strength of heart contraction and systemic vascular resistance. Since heart rate is assumed to be main determinant of the stroke volume.

Ruffolo (2012) suggests that alpha1 receptors' stimulation by hormones lead to vasoconstriction (the smooth muscle contraction) of the arterioles. Hence, the diameters of arterioles are decreased. There are three primary factors that determine the systemic vascular

resistance to blood flow: viscosity, vessel length and vessel diameter. In the medical literature, the diameter of arterioles is primarily used to determine systemic vascular resistance. Also, the change in the value of viscosity or arterioles' length is not related with the problem of interest.

Heart rate, systemic vascular resistance and stroke volume dictate blood pressure. The blood pressure (*BP*) is determined by the multiplication of heart rate (HR), systemic vascular resistance (*SVR*) and stroke volume (*SV*) in the medical literature that can be seen in Equation 5.2.

$$Blood\ Pressure = HR * SV * SVR \tag{5.2}$$

Blood pressure is the one of the determinants of oxygen delivery to the tissues. Oxygen delivery to specific tissue has perfect analogic similarities with current to specific resistor in electric circuit (see Figure 5.1). Also, arterioles are parallel to each other like the resistors in Figure 5.1 when they distribute blood to different tissues. Current to each resistor, resistance at specific resistor, overall resistance and voltage are similar to oxygen delivery to specific tissue, resistance to specific tissue, systemic vascular resistance and blood pressure respectively. Adrenergic stimulation leads to increase in blood pressure via increasing systemic vascular resistance and heart rate when there is oxygen deficiency in a tissue.

Under the normal condition, the change in the value of each resistance is proportional to the change in the value of systemic vascular resistance. However, when there is oxygen deficiency in a tissue, systemic vascular resistance may increase and the resistance toward that specific tissue may decrease. The aim is to increase the oxygen delivery to the oxygen deficient tissue. However, after some point, the resistances to oxygen deficient tissues change proportional to systemic vascular resistance (Pittman, 2011). Equation 5.3 shows the oxygen delivery calculation to specific tissue in the medical literature.

$$Oxygen\ delivery = Sa02 * CO * SVR / R_i \quad (5.3)$$

It is known that the multiplication of cardiac output (*CO*) and systemic vascular resistance (*SVR*) is equal to blood pressure in Equation 5.3. R_i denotes specific arteriole resistance in the body. In the model, it is assumed that the oxygen delivery is regulated by blood pressure and arterial oxygen saturation. The arterial oxygen saturation will be examined in the apnea sector 5.5.

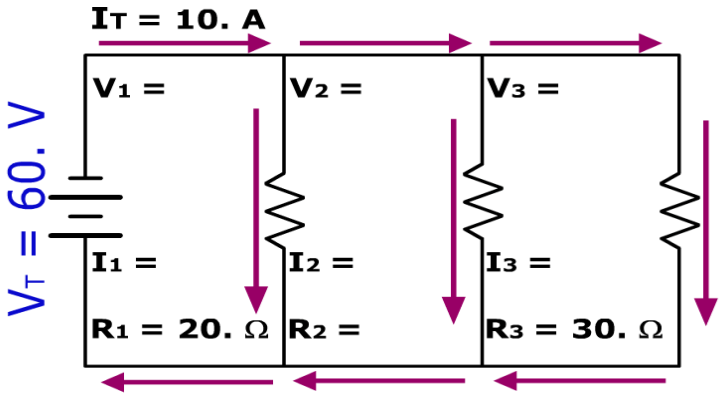

Figure 5.1. An example electric circuit.

The total oxygen consumption of the tissues is determined by tissues' energy requirements. In the model, it is assumed that energy requirements for the tissues are regulated by circadian clock and workload of the heart. The imbalances between oxygen supply and demand of tissues are observed by arterial receptors that will be explained in chemoreceptor and baroreceptor sections. Briefly, the signals produced by these receptors dictate sympathetic neuron activation via the autonomous nervous system. SNA dictates the desired levels of epinephrine and norepinephrine. Epinephrine and norepinephrine regulate the level of blood pressure to create the balance between oxygen supply and demand.

Sympathetic neuron activation unit is described as burst per min. The initial level of average sympathetic neuron activation is accepted as 40 burst/min (Charkoudian & Rabbitts, 2009). Lidco (2011) presents the reference values of main hemodynamic variables that are shown in Table 5.3.

Table 5.3. Minimum, maximum and reference values of main variables from Lidco (2011).

Variables	Min	Max	Reference Value	Unit
Blood Pressure	70	105	87	mmHg
Heart Rate	60	90	75	Beat/min
Stroke Volume	60	100	80	milliliter/beat
Systemic vascular resistance	10	19	14.5	mmHg*min/milliliter

5.1.2 Description of Hemodynamic Structure

The stock-flow diagram of hemodynamic sector is shown in Figure 5.2. It includes seven main stock variables: *Blood pressure, Heart Rate, Average Stroke Volume, Diameter of arterioles, Average Hourly Sympathetic Neuron Activation, NEP and EP*.

Average Hourly sympathetic neuron activation is measured in units called burst. The number of bursts is multiplied by *productivity of each neuron* to find *desired epinephrine level.*

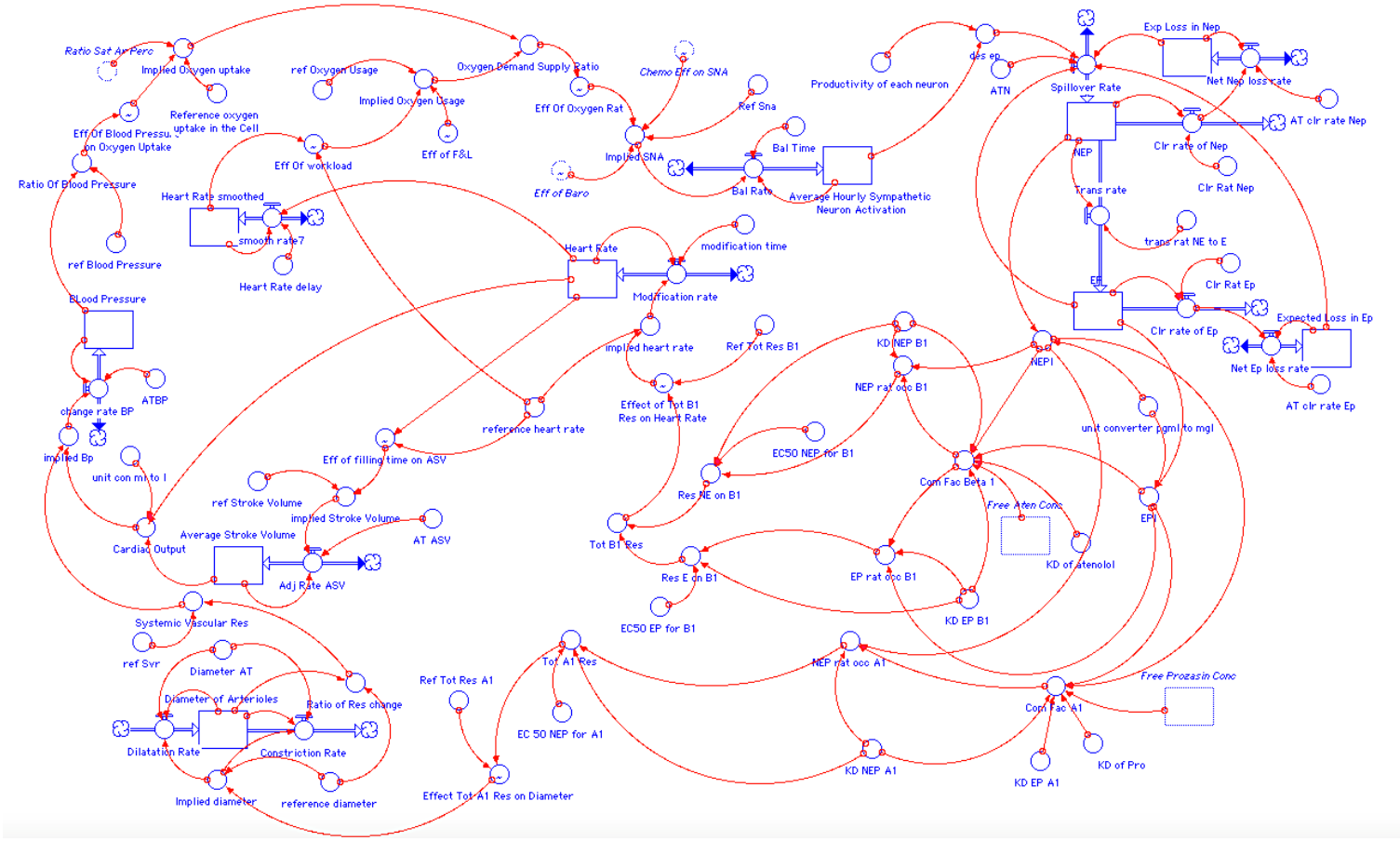

Figure 5.2 Stock-flow diagram of hemodynamic sector.

Des_EP =

*Average_Hourly_Sympathetic_Neuron_Activation*Productivity_of_each_neuron (*5.4)

It was mentioned that the norepinephrine is transformed into epinephrine in the adrenal medulla. Norepinephrine in the blood plasma arrives to the adrenal medulla via circulation after a transportation delay. Thereby, the first order material delay is used to represent the transportation delay. Secondly, the expected losses for epinephrine and norepinephrine should be added to the inflow of norepinephrine stock. Otherwise, the concentration of epinephrine never reaches the desired epinephrine concentration dictated by SNA. The amounts of expected losses of epinephrine and norepinephrine are determined by first order information delay.

Norepinephrine stock "*NEP"* has one inflow and two different outflows. The inflow of norepinephrine stock is *"spillover rate".*

Spillover_Rate = ((Des_EP-EP)/ATN)+Expected_Loss_in_Ep+Exp_Loss_in_Nep (5.5)

The equation above is the formula for the inflow of norepinephrine stock. The *adjustment time* is a measure of how fast epinephrine reaches to desired level. *Exp loss in Ep* and *Exp loss in Nep* are the expected amounts of hormones in the urine. The outflows of norepinephrine stock are transformation rate and clearance rate, represented as *"Trans rate" and "Clr rate of Nep".*

*Trans_Rate = NEP*Trans_Rat_NE_to_E* (5.6)

*Clr_rate_of_Nep = NEP*Clr_Rat_Nep* (5.7)

Equations 5.6 and 5.7 imply that each outflow of norepinephrine is controlled by itself. It was assumed that the total norepinephrine concentration in the blood plasma is transformed into epinephrine in the adrenal medulla within an hour.

The units of *NEP* and *EP* are picogram/milliliter. They are converted to milligram/liter in order to be used in calculations for receptor occupation.

$$EPI = unit\_converter\_pgml\_to\_mgl*(EP) \tag{5.8}$$

$$NEPI = unit\_converter\_pgml\_to\_mgl*(NEP) \tag{5.9}$$

NEPI and *EPI* are the amounts of hormones in the blood plasma in terms of mg/l. The dissociation constants (K_d) of norepinephrine and epinephrine represent the amount of adrenergic hormones to occupy half of the specific receptors when there are no other competitors to occupy these receptors. However, beta1 and alpha1 receptors can create complex with epinephrine and norepinephrine, so there is competition for the receptor occupation among them.

$$Com\_Fac\_A1 = 1/(1+(EPI/KD\_EP\_A1)+(NEPI/KD\_NEP\_A1) +(Free\_Prozasin\_Conc/KD\_of\_Pro)) \tag{5.10}$$

$$NEP\_rat\_occ\_B1 = (NEPI/KD\_NEP\_B1)*Com\_Fac\_Beta\_1 \tag{5.11}$$

$$EP\_rat\_occ\_B1 = (EPI/KD\_EP\_B1)*Com\_Fac\_Beta\_1 \tag{5.12}$$

Equations 5.10, 5.11 and 5.12 give idea about how the competition among hormones will affect the beta1 receptor occupancy. *NEP rat occ B1* and *EP rat Occ B1* denote percentages of beta 1 receptors occupied by norepinephrine and epinephrine, respectively. Let's assume the concentration of epinephrine is zero. Then, the formula turns into:

$$NEP\ rat\ occ\ B1 = NEPI / (K_d\ NEP\ B1 + NEPI) \quad (5.13)$$

If norepinephrine concentration is equal to its dissociation constant (K_d), then norepinephrine will occupy half of the beta1 receptors. When the norepinephrine and epinephrine values are equal to their association constants, then, one third of the beta1-receptors are occupied by epinephrine and one third of the beta1-receptors are occupied by norepinephrine. So, in this scenario, the competition between epinephrine and norepinephrine decreases the percentage of beta1 receptors occupied by norepinephrine from half of the receptors to one third of the receptors.

$$Res\_NE\_on\_B1 = (KD\_NEP\_B1/EC50\_NEP\_for\_B1)*NEP\_rat\_occ\_B1 \quad (5.14)$$

$$Res\_E\_on\_B1 = (KD\_EP\_B1/EC50\_EP\_for\_B1)*EP\_rat\_occ\_B1 \quad (5.15)$$

$$Tot\_B1\_Res = (Res\_E\_on\_B1+Res\_NE\_on\_B1) \quad (5.16)$$

In Equations 5.14 and 5.15, EC_{50} values give us the concentrations of norepinephrine and epinephrine that stimulate the beta 1 receptor to produce half maximal heart rate response. It was assumed that the ratio of K_d to EC_{50} (norepinephrine or epinephrine - beta1 receptor complex) gives us the heart rate response to unit percentage of the receptors occupied by that hormone. This ratio is multiplied with the percentage of the receptor occupied by the hormone gives us individual heart rate response to the hormone-receptor complex. Equation 5.16 is used to calculate total response.

*implied_heart_rate = reference_heart_rate*Effect_of_Tot_B1_Res_on_Heart_Rate* (5.17)

Effect_of_Tot_B1_Res_on_Heart_Rate= GRAPH(Tot_B1_Res/Ref_Tot_B1_Res) (5.18)

where *GRAPH(Tot_B1_Res/Ref_Tot_B1_Res)* is shown in Figure 5.3.

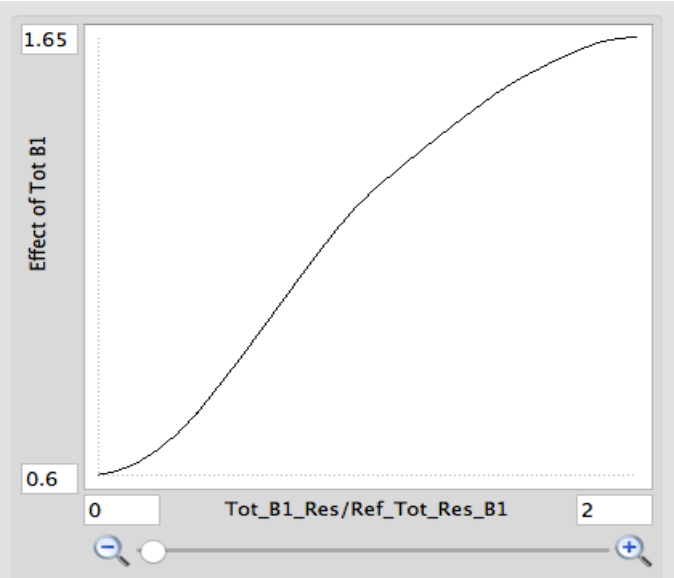

Figure 5.3. Graphical function for the effect of total Beta1 Response on Implied Heart Rate.

The input to the graphical function in Figure 5.3 is the ratio of total beta1 receptor occupancy by hormones to the reference beta1 receptor occupancy by hormones. Experimentation with different ratios of beta1 receptor occupancy by hormones shows that effect function of the beta1 receptor occupancy on the heart rate should be S-shaped (Holtzman *et al.*, 1986). The output is the coefficient to be multiplied with the reference heart rate to determine the implied heart rate. Katzung & Trevor (2015) and Clark *et al.* (2012) stated that the increase in the amount of receptor/hormone complex doesn't increase heart rate after beta1 receptor occupancy is twice as much as the reference level. It was

aforementioned that each receptor has special occupancy ratio to produce maximum response. According to the graph, when total beta1 receptor occupancy by hormones is far below from the reference value, the implied heart rate is still higher than zero. Guyton & Hall (2006) suggests that without any stimulation, heart can beat 45 times per minute with its own intrinsic rhythm.

Heart Rate is a stock, fed by a bi-flow; modification rate. The implied heart rate is a target for actual heart rate to reach. The modification time is a measure how fast heart rate reaches to implied heart rate. Thereby, the formula for the bi-flow: modification rate is:

$$Modification\_rate = (implied\_heart\_rate - Heart\_Rate)/modification\_time \quad (5.19)$$

Also, adrenergic hormones can bind to alpha1 receptor to form a complex. Norepinephrine and epinephrine competitively occupy alpha 1 receptor, but the complex between epinephrine and alpha1 receptor protein doesn't produce a response whereas complex between norepinephrine and alpha 1 receptor protein does.

$$Com\_Fac\_A1 = 1/(1+(EPI/KD\_EP\_A1)+(NEPI/KD\_NEP\_A1) +(Free\_Prozasin\_Conc/KD\_of\_Pro)) \quad (5.20)$$

$$NEP\_rat\_occ\_A1 = NEPI*Com\_Fac\_A1/KD\_NEP\_A1 \quad (5.21)$$

Equations 5.20 and 5.21 are used to calculate the percentage of alpha1 receptor occupied by norepinephrine. It is assumed that the complex between epinephrine and alpha1 receptor protein doesn't produce a response (it actually produces response, but insignificant compared to norepinephrine), Equation 5.22 represents the response related with total alpha1 receptor stimulation.

*Tot_A1_Res = (NEP_rat_occ_A1*KD_NEP_A1/EC_50_NEP_for_A1)* (5.22)

Implied diameter sets a target value for *diameter of arterioles*. Equations 5.23 and 5.24 are used to calculate the value of implied diameter.

*Implied_diameter = Effect_Tot_A1_Res_on_diameter*reference_diameter* (5.23)

Effect_Tot_A1_Res_on_Diameter=GRAPH(Tot_A1_Res/Ref_Tot_A1_Res) (5.24)

where *GRAPH(Tot_A1_Res/Ref_Tot_A1_Res*)is shown in Figure 5.4.

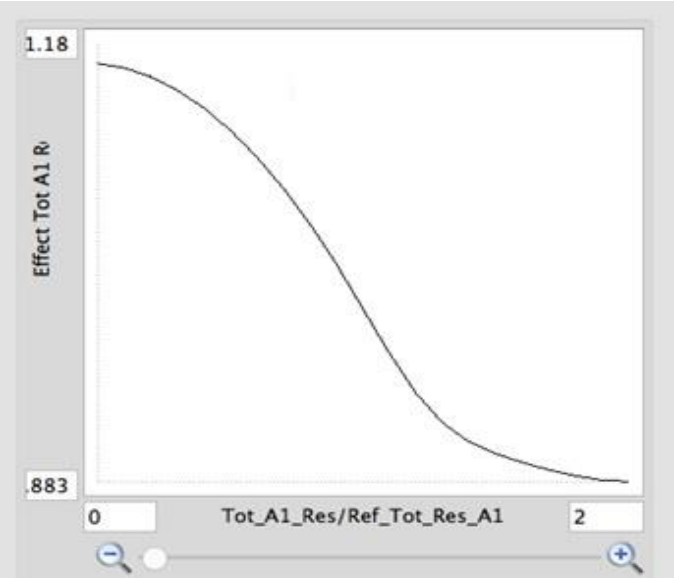

Figure 5.4. Graphical function for the effect of total A1 Response on Implied Diameter.

The input to the graphical function in Figure 5.4 is the ratio of alpha1 occupancy to the reference occupancy. The output is the coefficient to be multiplied with reference diameter to determine the implied diameter of arterioles. The plot of different ratios of receptor occupancy against diameter of arterioles is s-shaped (Ruffolo, 2012). The alpha 1

receptor occupancy by hormones leads to vasoconstriction (decrease in the diameter of vessels). Even with zero receptor occupancy, there is an upper limit for the diameter of arterioles. Increase in the level of alpha1 receptor occupancy by hormones up to the reference level decreases the diameter of arterioles exponentially. After that point, the decrease amount in the diameter of arterioles for unit increase in the alpha1 receptor occupancy gradually decreases. After the point that the receptor occupancy becomes twice as much as the reference level, the diameters cannot decrease because they reached their lower limit. The maximum and minimum response to the alpha1 receptor occupancy level is obtained from the research of Ruffolo (2012).

Brunton et al (2011) and Meibohm (2006) showed that the diameter has minimum and maximum values. These values determine the maximum dilation and constriction of the arterioles. Figure 5.4 shows that when total alpha1 response is far below from the reference value, the implied diameter still is wider than zero. Also, it should be noted that norepinephrine has vasoconstrictor effect on diameters.

Diameter of Arterioles is a stock, fed by one inflow and one outflow: *dilatation rate* and *constriction rate*, respectively. *The implied diameter* is sets a target for actual *Diameter of Arterioles* to reach. *Diameter AT*, which denotes diameter adjustment time, is a measure of the time it takes for *Diameter of Arterioles* to reach *the implied diameter*. Thereby, the formula for the flows are shown in Equations 5.25 and 5.26:

Dilatation_Rate = (Implied_diameter-Diameter_of_arterioles)/(Diameter_AT) (5.25)

Constriction_Rate = (Diameter_of_arterioles-Implied_diameter)/Diameter_AT (5.26)

The resistance is inversely proportional to the fourth power of arterioles diameter, which is represented in Equation 5.27 (Guyton & Hall, 2006).

Ratio_of_Resis_Change = (reference_diameter/Diameter_of_arterioles)^4 (5.27)

$$Systemic\_Vascular\_Resis = Ratio\_of\_Resis\_Change*ref\_Svr \quad (5.28)$$

The Cardiac cycle is divided into two separate periods: diastole and systole. Heart muscles relax and the chambers of heart are filled with blood during diastole period. Heart muscle contraction pumps the blood all over the body. An increase in the heart rate leads to a shorter diastolic filling time. The amount of blood accumulated in the chambers of heart (end-diastolic volume) is decreased due to a shorter diastolic filling time (Guyton & Hall, 2006). Thereby, the volume of blood pumped from left ventricle (Stroke Volume) is decreased. Figure 5.5 shows the effect of filling time on Stroke Volume.

$$Eff\_of\_filling\_time\_on\_ASV = GRAPH(Heart\_Rate/reference\_heart\_rate\ ) \quad (5.29)$$

$$Implied\_Stroke\_Volume = ref\_Stroke\_Volume*Eff\_of\_filling\_time\_on\_ASV \quad (5.30)$$

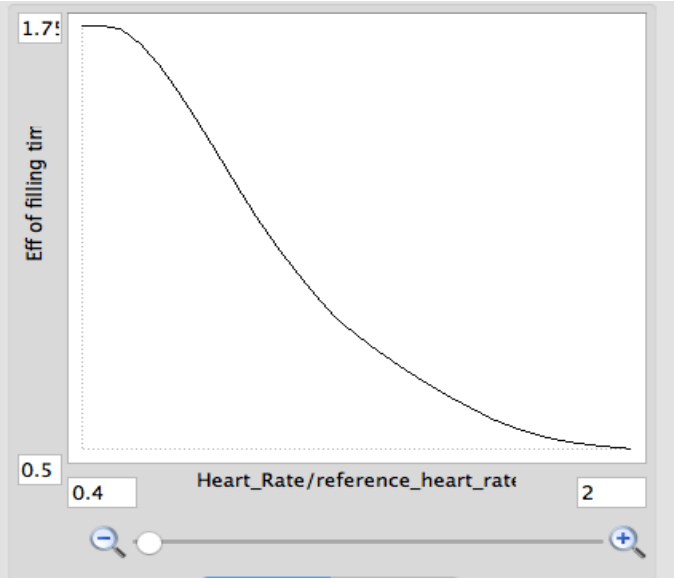

Figure 5.5. Graphical function for the effect of Heart Rate on Stroke Volume.

The input to the graphical function in Figure 5.5 is the ratio of Heart Rate divided by reference Heart Rate. The output is effect of filling time on Stroke Volume. Stroke volume is between 60 and 100 ml/beat for a healthy person (Lidco, 2011). Its initial and reference values are taken as 80 ml/beat. Guyton and Hall (2006) suggest that their minimum and maximum values are respectively 40 and 140 ml/min under extreme conditions. So, minimum and maximum values are determined as 0.5 and 1.75 in Figure 5.5. The period of contraction while the heart pumps blood into circulation is called systole. The period of relaxation while heart chambers fill with blood is called diastole. Guyton and Hall (2006) stated that an increase in heart rate leads to a decrease in the amount of blood that normally fills the heart, because the time interval between two consecutive heartbeats is decreased. So, decrease in the duration of diastole leads to a decrease in stroke volume. Thus, the heart rate and stroke volume is inversely proportional. This information is used to build the effect function in Figure 5.5.

$$Adj\_Rate\_ASV = (implied\_Stroke\_Volume - Average\_Stroke\_Volume)/(AT\_ASV) \quad (5.31)$$

Average Stroke Volume is a stock only fed by a bi-flow named as Adj. Rate ASV. Equation 5.30 implies that the *Implied Stroke Volume* sets a target for the actual *Average Stroke Volume*. The adjustment time of Average Stroke Volume is denoted as "*AT ASV".*

$$Cardiac\_Output = Average\_Stroke\_Volume * Heart\_Rate * unit\_con\_ml\_to\_l \quad (5.32)$$

$$Implied\_Bp = Systemic\_Vascular\_Resis * Cardiac\_Output \quad (5.33)$$

$$Change\_Rate\_BP = (implied\_Bp - BLood\_Pressure)/ATBP \quad (5.34)$$

Cardiac output is equal to the multiplication of Average Stroke Volume and Heart Rate, which can be seen in Equation 5.32. The unit of cardiac output is liter/min. *"Unit con ml to l" is* used to convert milliliter to liter.

The multiplication of systemic vascular resistance and cardiac output is equal to *Implied Blood Pressure* that sets a target for the actual *Blood pressure. Blood Pressure is a stock* fed by only a bi-flow: *Change rate BP* that is calculated in Equation 5.34. Adjustment time of blood pressure is denoted as *ATBP*. ATBP is a measure of how fast *Blood Pressure* converges to *Implied Blood Pressure*.

The rate of oxygen delivery to the tissues is affected by two factors. One of them is the ratio of blood pressure to reference blood pressure, which can be seen in Equations 5.35 and 5.36. The other factor is the arterial oxygen saturation. The arterial oxygen saturation can only be changed by sleep apnea that will be explained in Section 5.5. Apnea Sector. Equation 5.37 is used to find *Implied oxygen uptake rate* of the tissues.

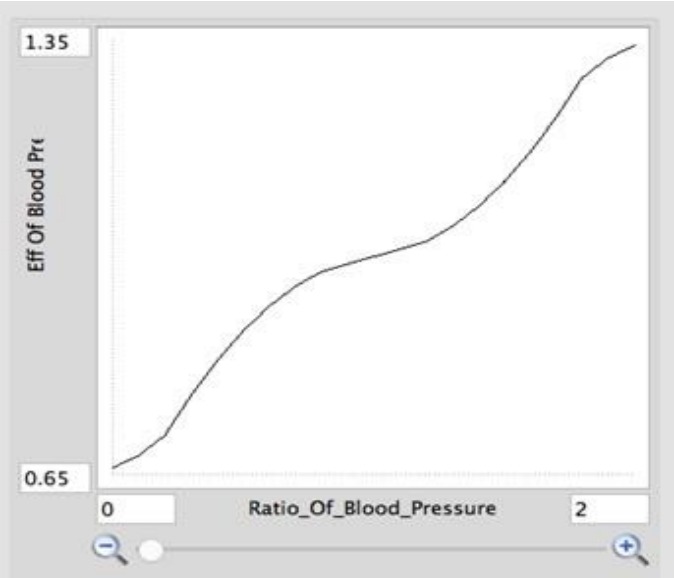

Figure 5.6. Graphical function for the effect of Blood Pressure on Oxygen delivery.

$$Ratio\_Of\_Blood\_Pressure = (BLood\_Pressure/ref\_blood\_Pressure) \quad (5.35)$$

$$Eff\_Of\_Blood\_Pressure\_on\_O2\_Uptake = GRAPH(Ratio\_Of\_Blood\_Pressure) \quad (5.36)$$

The input to the graphical function in Figure 5.6 is the ratio of blood pressure to reference blood pressure. The output is the coefficient to be multiplied with reference oxygen delivery to tissues amount to determine the total oxygen delivery. The shape of effect function in the Figure 5.6 may not be intuitive at first. But, the cells in a way accommodate themselves to changes in diffusion rate after some time. Cells do not opt for diffusion rate adjustments in case that transient blood pressure shifts from the baseline (Pittman 2012). It is assumed that there should be also a lower and an upper limit for the level of oxygen delivery amount.

$$Implied\_Oxygen\_uptake = Ref\_O2\_uptake * Eff\_Of\_Blood\_Pressure\_on\_O2\_Uptake * Ar\_Sat \quad (5.37)$$

It is known that the tissues use oxygen for their daily metabolic needs. The total oxygen usage rate of tissues is calculated in Equation 5.38. We assumed that workload of the heart is dictated by heart rate in the model. Myocardial oxygen demand is related with the workload of the heart. The *effect of workload* of the heart rate on oxygen consumption rate is shown in Figure 5.7. The input to graphical function in Figure 5.7 is the ratio of daily smoothed heart rate to reference Heart Rate that is shown in Equation 5.39.

$$Implied\_Oxygen\_Usage = Eff\_Of\_workload * ref\_Oxygen\_Usage * (Eff\_of\_F\&L) \quad (5.38)$$

$$Eff\_Of\_Workload = GRAPH(Heart\_Rate\_smoothed/reference\_heart\_rate) \quad (5.39)$$

$$Eff\_of\_F\&L = GRAPH(time\ mod\ 24) \quad (5.40)$$

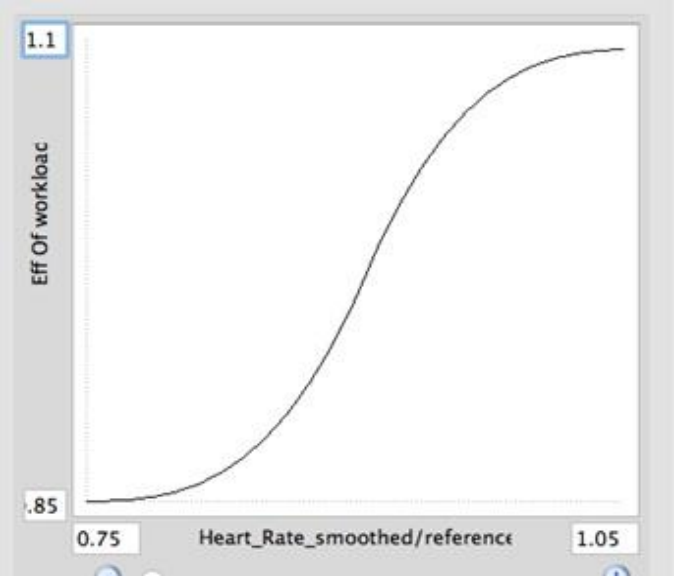

Figure 5.7. Graphical function for the effect of Smoothed Heart Rate on Oxygen consumption.

The graphical function in Figure 5.8 is *Food & Light effect*. The external *Food & Light effect* is to represent the circadian rhythm in the model. Hourly total oxygen consumption rate of tissues is provided by the *Food and light effect* function. The input to this graphical function is the remainder value of simulation time divided by 24. The output to the graphical function is the second coefficient to be multiplied with *reference total oxygen consumption of tissues* and *the effect of workload of heart* to find *implied total oxygen consumption* of tissues. The effect curve implies that total oxygen consumption of tissues is low during nocturnal period, since there are less energy requirements compared to diurnal period. It is not possible to measure oxygen consumption of the whole body throughout a day. We simply assumed in Figure 5.8 that oxygen consumption level should decrease during the sleep period, whereas it should increase during the daily period. Also, the medical literature suggests that the minimum total oxygen consumption of tissues happens at 03:00 AM, whereas the maximum happens at 15:00 PM (Rodela & Wright, 2006). Even though we don't have the exact measurement of the oxygen consumption of the body throughout a day, the research of Rodela & Wright (2006*)* includes the rate of oxygen consumption for fish *"mangrove rivulus".* The shape of this function is constructed in a similar manner.

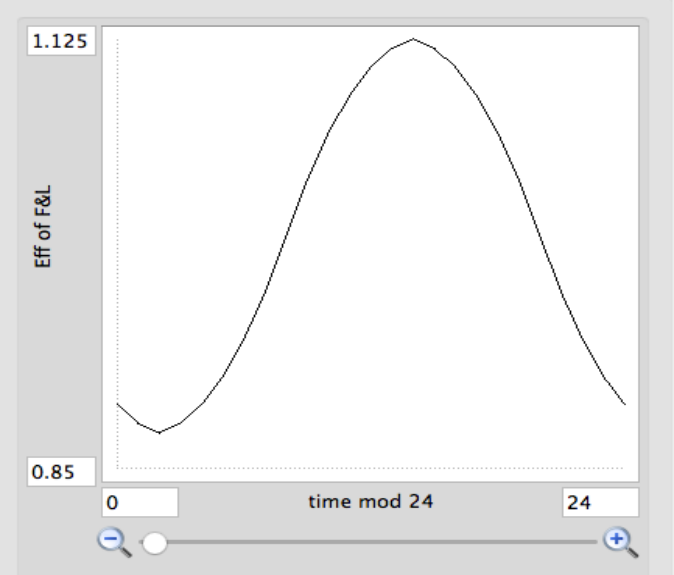

Figure 5.8. Graphical function for the effect of Food and Light (Circadian clock) on Oxygen consumption.

The related ratio of *Implied Oxygen Uptake rate* to *Implied Oxygen Usage rate* of the tissues gives us *Oxygen Demand/Supply ratio* of the tissues in Equation 5.41. *Oxygen Demand/Supply ratio* is one of the factors to determine sympathetic neuron activation. The graphical function in Figure 5.9 shows how the sympathetic neuron activation is affected by that ratio.

Oxygen_Demand_Supply_Ratio = Implied_Oxygen_uptake/Implied_Oxygen_Usage (5.41)

Eff_Of_Oxygen_Rat = GRAPH(Oxygen_Demand_Supply_Ratio) (5.42)

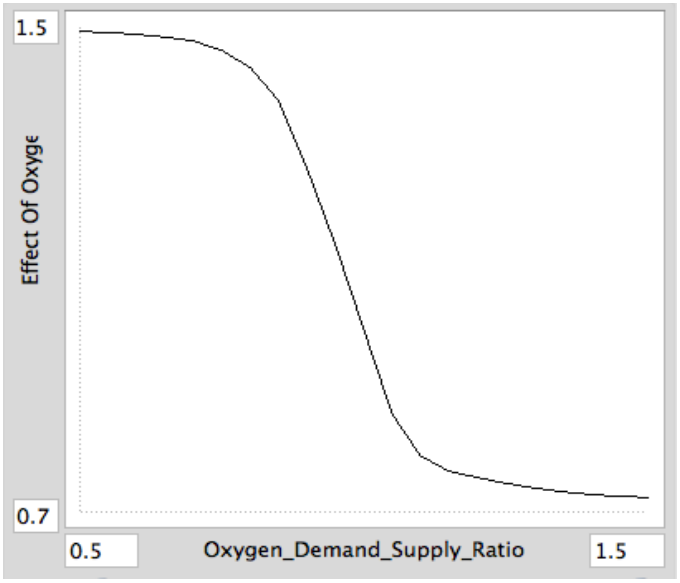

Figure 5.9. Graphical function for the effect of Oxygen Demand Supply Ratio on sympathetic activation.

Main goal of sympathetic activation is to balance the oxygen supply and demand of the tissues. Figure 5.9 implies that if the oxygen consumption of tissues is higher than the delivered oxygen, sympathetic activation increases to prevent oxygen deficiencies in the tissues via increasing the blood pressure. The input to the graphical function in Figure 5.9 is the oxygen demand/supply ratio. The output is the coefficient to be multiplied with reference sympathetic neuron activation to determine the implied sympathetic neuron activation. First, it is ensured that the graphical function for the effect of oxygen demand supply ratio on implied sympathetic neuron activation does not become zero, but yields a minimum sympathetic neuron activation level when oxygen demand/supply ratio is considerably high. It also yields maximum sympathetic neuron activation level when it is zero because sympathetic neuron activation has a maximum capacity constraint. Sympathetic neuron activation level decreases exponentially when oxygen demand/supply ratio goes from 0.5 to 1. After that point, sympathetic neuron activation decreases with goal seeking behavior. The reviewed studies show that oxygen demand/supply ratio and sympathetic neuron activation is inversely proportional. Reference sympathetic neuron activation level is 40 bursts per hour. (Guyton & Hall, 2006)

*Implied_SNA = Ref_Sna*Eff_of_Baro*Eff_Of_Oxygen_Rat*Chemo_Eff_on_SNA* (5.43)

Bal_Rate =

(Implied_SNA-Average_Hourly_Sympathetic_Neuron_Activation)/Bal_Time (5.44)

In Equation 5.43, there are three effects that determine implied sympathetic neuron activation: effects of baroreceptor, oxygen ratio and chemoreceptor. The effects of baroreceptor and chemoreceptor will be explained in their own sections. *Average Hourly Sympathetic Neuron Activation* is a stock only fed by a bi-flow named as Bal. Rate. *Average Hourly Sympathetic Neuron Activation* tries to reach the target value determined by implied sympathetic neuron activation over a balance time, which is shown in Equation 5.44.

5.2. Chemoreceptor Sector

5.2.1. Medical Fundamentals and Assumptions

Chemoreceptor system plays an important role for the regulation of sympathetic neuron activation. Chemoreceptors produce signals dependent to chemical substances in the blood. The chemical substances that stimulate chemoreceptors are mainly oxygen, carbon dioxide and hydrogen ions. Chemoreceptors are mostly located in carotid and aortic body cells. (Guyton & Hall, 2006) Carotid body and aortic body cells are the best location to sense chemical substances in the blood because these places intimately contact with the blood circulation in the body. Chemoreceptors produce signals to warn autonomous nervous system to maintain oxygen homeostasis in tissues via sympathetic neuron activation.

In section 5.1, it was explained that blood pressure controls oxygen delivery to tissues. Hypoxia of tissue is common under the sleep apnea disorder. Hypoxia means that the tissues are deprived of adequate oxygen supply to provide energy. Hypoxia causes

sympathetically mediated vasoconstriction and an increase in heart rate to redistribute blood flow to provide enough oxygen to vital organs (Abboud & Kumar, 2014). Interestingly, hypoxia occurs in tissues during nocturnal period under the sleep apnea disease, but increase in sympathetic neuron activation (SNA) can also be seen during nocturnal and diurnal period. The reason behind this increase throughout the day is quite controversial. Actually, some researches support sympathetic neuron over activation is mostly associated with special byproducts (ROS) during energy production in mitochondria under hypoxia condition (Maher & Schubert, 2000; Dharmansky & Widlansky, 2010; Prabhakar *et al.*, 2012). Mitochondria are responsible for energy production in the tissues that basically convert oxygen and nutrients to energy and byproducts. Reactive oxygen species (ROS) are one type of the byproducts. The examples of ROS are superoxide, peroxide, hydroxyl radical and singlet oxygen. In case of oxygen deficiencies, the amounts of reactive oxygen species produced by tissues are increased (Schieber & Chandler, 2014). Some researchers claim that these reactive oxygen species affect carotid chemo-reflex sensitivity (Narkiewicz *et al.*1999; Magosso & Ursino, 2001; Dopp *et al.*, 2007; Lopez-Barneo *et al.*, 2009), whereas others claim that they lead to increase in chemoreceptor concentration (Cutler *et al.*, 2002;Lahiri *et al.*, 2013;Mansukhani *et al.*, 2014). The common point in the scientific literature is that sympathetic neuron over activation is associated with the problems in the chemoreceptor system.

Murphy (2009) suggests that the balance between oxygen supply and demand mainly determines the extent of reactive oxygen species (ROS) production. The extent of ROS production dictates the concentration of chemoreceptor in the body (Campese *et al.*, 2004; Csordas & Hajnoczky, 2009; Gorlach *et al.*, 2015). It was assumed in the model that the balance between oxygen supply and demand regulates the total concentration of chemoreceptors via excluding intra cellular interaction between ROS and the variables mentioned above.

Chemoreceptors are protein structured like all other receptors. Chemoreceptor production and destruction take hours. Campese *et al.*, (2004) suggests that the half-lives of chemoreceptors are in between 12 and 15 hours. Thereby, it was assumed that the reference

production and destruction ratios of chemoreceptors are 0.05 according to Equation 5.1. It was assumed that the average level of *oxygen supply/demand ratio* leads to changes in the destruction ratio of chemoreceptors. Also, the level of chemoreceptor concentration limits the production ratio of chemoreceptor.

5.2.2. Description of the Chemoreceptor Structure

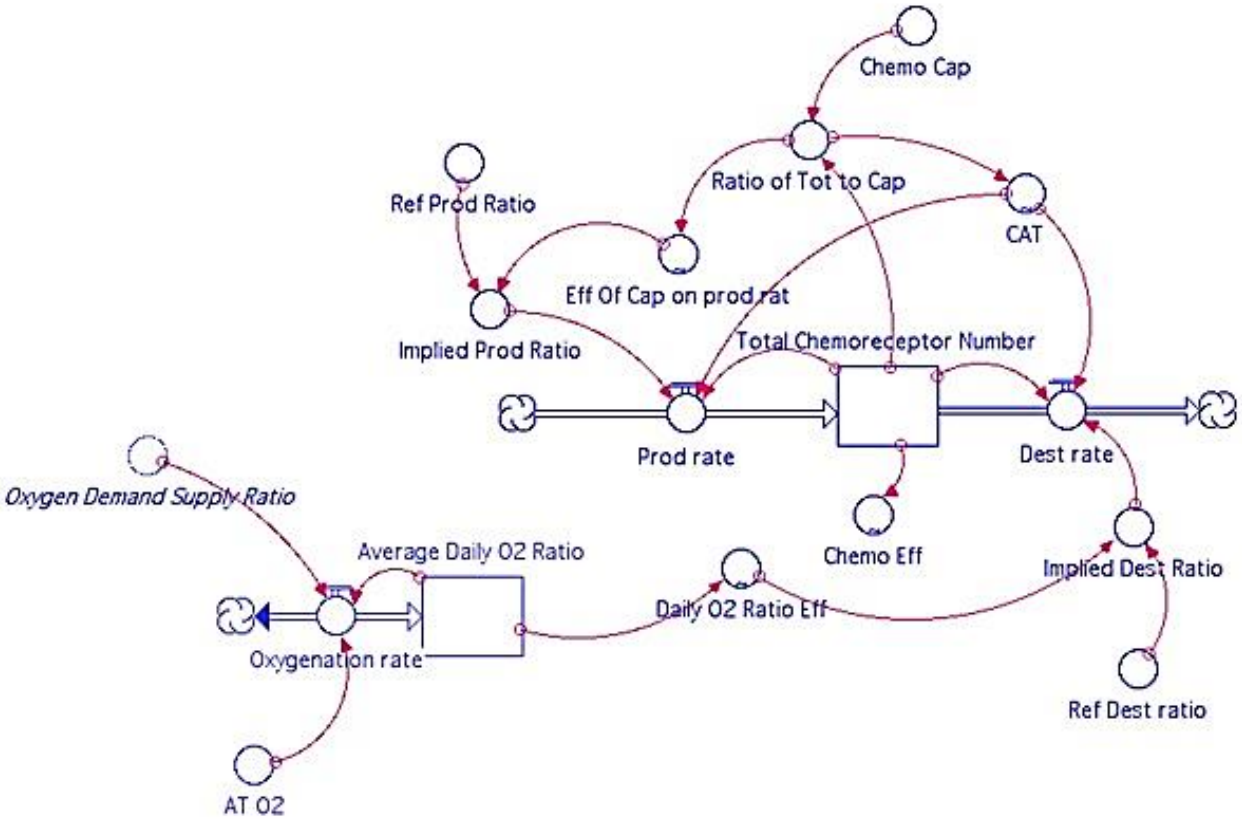

Figure 5.10. Stock-flow diagram of chemoreceptor sector.

The structure constructed in this sector aims to depict the regulation of total chemoreceptor concentration. Figure 5.10 is the representation of stock-flow diagram of chemoreceptor sector. Average oxygen supply/demand ratio is represented as *Average Daily O2 ratio*. Average Daily O2 ratio is a stock. It has only one bi-flow: oxygenation rate. The adjustment time (*AT 02*) is 24 hours. In Figure 5.11 and 5.12, we will show the effects of oxygen supply/demand ratio on chemoreceptor destruction ratio and the effects of chemoreceptor concentration on chemoreceptor production ratio. Chemoreceptor concentration will quickly increase with the decrease in chemoreceptor destruction ratio, whereas it will slowly decrease with the decrease in chemoreceptor production ratio.

Oxygenation_rate =

(Oxygen_Demand_Supply_Ratio-Average_Daily_O2_Ratio)/AT_O2 (5.45)

The oxygen deficiencies in tissues due to the sleep apnea lead to decrease in *average daily oxygen ratio*. When the *average daily oxygen ratio* is smaller than one, *destruction ratio* of chemoreceptor is decreased. *"Implied Dest Ratio"* is determined by the *average daily oxygen ratio* (see Equation 5.47).

Daily_O2_Ratio_Eff = GRAPH(Average_Daily_O2_Ratio) (5.46)

*Implied_Dest_Ratio = Daily_O2_Ratio_Eff*Ref_Dest_ratio* (5.47)

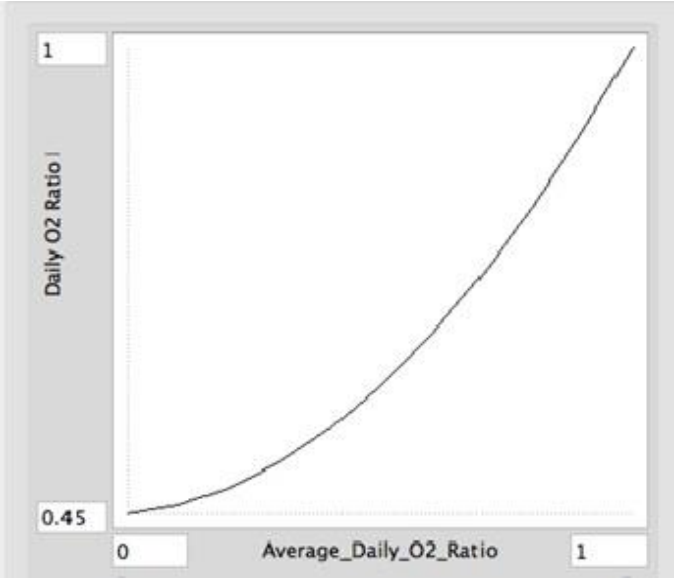

Figure 5.11. Graphical function for the effect of Average Daily Oxygen Ratio on destruction ratio of Chemoreceptor.

The input to the graphical function in Figure 5.11 is the smoothed oxygen demand/supply ratio. The output is the coefficient to be multiplied with *reference destruction ratio* to determine the *implied destruction ratio* of chemoreceptor. It was assumed that the

amount of enzymes determines the destruction rate of the chemoreceptor cells. An initial decrease in oxygen supply demand ratio from normal level, leads to a sharp decrease in chemoreceptor destruction ratio. A further decrease gradually decreases chemoreceptor destruction ratio less and less because the possible maximum amount of enzymes is limited. The graphical function depicting this effect is shown in Figure 5.11.

$$Eff\_of\_Chem\_on\_flows = GRAPH(Ratio\_of\_Tot\_to\_ref) \quad (5.48)$$

$$Implied\_Prod\_Ratio = Eff\_Of\_Chem\_on\_prod\_rat*Ref\_Prod\_Ratio \quad (5.49)$$

The input to the graphical function in Figure 5.12 is the ratio of the *chemoreceptor concentration* to the *reference chemoreceptor concentration*. The output is the coefficient to be multiplied with *reference destruction ratio* to determine the *implied destruction ratio* of chemoreceptor. It was explained that a decrease in oxygen supply/demand ratio leads to an increase in chemoreceptor concentration by decreasing its destruction ratio. Chemoreceptor concentration starts to increase after a time and blood pressure will be increased through the effects of chemoreceptor on sympathetic system. Then, oxygen supply will be greater than or equal to the oxygen demand. It was assumed that there should be a capacity constraint for the chemoreceptor concentration. So, an increase in chemoreceptor concentration leads to a decrease in its own production ratio. If the ratio of total to reference chemoreceptor concentration is higher than 1.1, production ratio will decrease only by 10 percent. It was also assumed that increase in the level of chemoreceptor concentration up to 5 percent increase, decreases the production ratio of chemoreceptors exponentially. After that point, chemoreceptor production ratio decreases with goal seeking behavior.

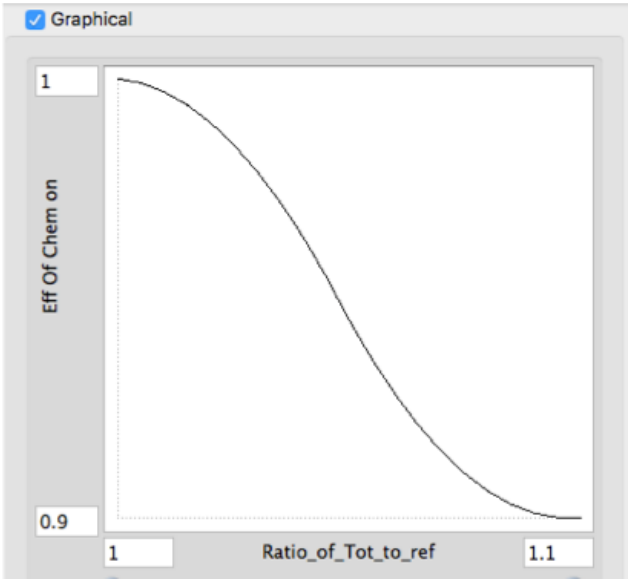

Figure 5.12. Graphical function for the effect of ratio of Total chemoreceptor concentration to reference chemoreceptor concentration on production ratio of Chemoreceptor.

$$Eff\_of\_Chem\_on\_flows = GRAPH(Ratio\_of\_Tot\_to\_ref) \quad (5.50)$$

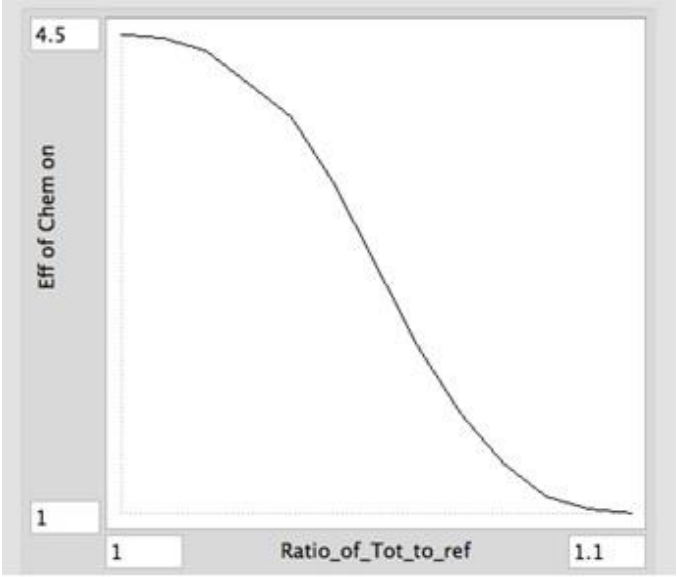

Figure 5.13. Graphical function for the effect of ratio of Total chemoreceptor concentration to reference chemoreceptor concentration inflow and outflow of Chemoreceptor.

If actual chemoreceptor concentration is relatively high to reference concentration, then it should take more time to reach desired chemoreceptor concentration. F(*Ratio of Tot to ref)* is a measure of convergence speed (see Figure 5.13).

Prod_rate =

*Implied_Prod_Ratio*Total_Chemoreceptor_Concentration*Eff_of_Chem_on_flows* (5.51)

Dest_rate =

*Total_Chemoreceptor_Concentration*Implied_Dest_Ratio*Eff_of_Chem_on_flows* (5.52)

Chemoreceptor concentration is one of the factors that regulate the level of sympathetic activation. The input to graphical function in Figure 5.14 is ratio of actual concentration to the reference concentration. The output is to be one of the coefficients to determine the implied level of sympathetic neuron activation.

Chemo_Eff_on_SNA = GRAPH(Ratio_of_Tot_to_ref) (5.53)

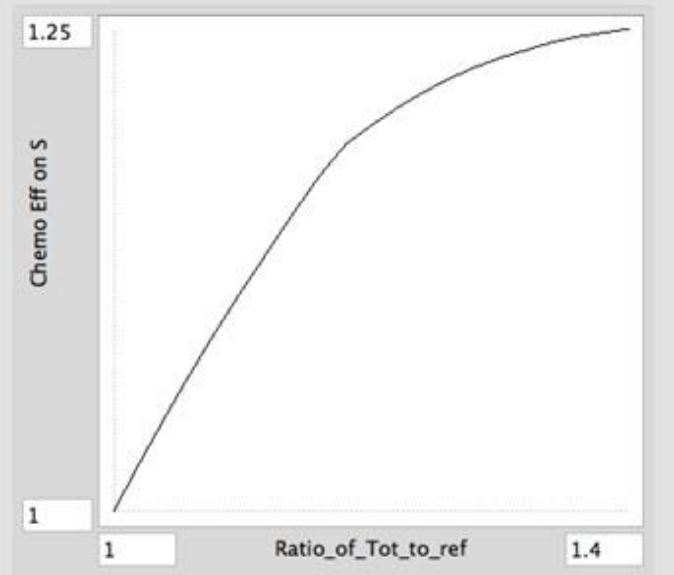

Figure 5.14. Graphical function for the effect of ratio of Total chemoreceptor concentration to reference chemoreceptor concentration on sympathetic neuron activation

As a summary, chemoreceptor concentration has three different effects. Two of them are related with flows of chemoreceptor, and one of them is related with implied sympathetic activation. The ratio effect on implied sympathetic activation leads to change in basal sympathetic activation in order to set daily average oxygen supply/demand ratio to one.

5.3. Baroreceptor Sector

5.3.1. Medical Fundamentals and Assumptions

Baroreceptor system is one of the most important mechanisms for controlling blood pressure. Level of stimulation is determined by stretch amount on the vessel wall due to blood pressure. Baroreceptors, which sense the length of stretch, are located in the walls of carotid sinus and aortic arch (Guyton & Hall, 2006).

The baroreceptors transmit signals to autonomous nervous system in response to the changes in blood pressure. These signals inhibit or promote sympathetic stimulation. As a result, sympathetic neuron activation dictates mean arterial blood pressure.

Graphical representation in Figure 5.15 is used to show the mechanism of baroreceptor activation in response to the changes in the mean arterial blood pressure. The x-axis denotes the level of mean arterial blood pressure, whereas y-axis denotes the number of signal produced by baroreceptors to inhibit sympathetic neuron activation.

The arterial baroreceptors regulate mean arterial blood pressure around the baroreceptor operation point. Initially, the baroreceptor operation point is equal to established mean arterial blood pressure at value P1. It was assumed in Figure 5.15 (a), there is a sudden increase in mean arterial blood pressure (from P1 to P2). The number of inhibitory signals produced by baroreceptors is increased from “A” to “B”. Figure 5.15 (b) and (c) show how the number of inhibitory signals is decreased from “B” to “C” and from “C” to “D” if the mean arterial blood pressure is persistent to stay at “P2” level.

This phenomenon is called *baroreceptor resetting* in the medical literature (Chapleau *et al.*, 1989). The *baroreceptor resetting* means that when the arterial baroreceptor signals cannot decrease mean arterial blood pressure via inhibiting sympathetic neuron activation, baroreceptor operation point should be reset to the level of mean arterial blood pressure.

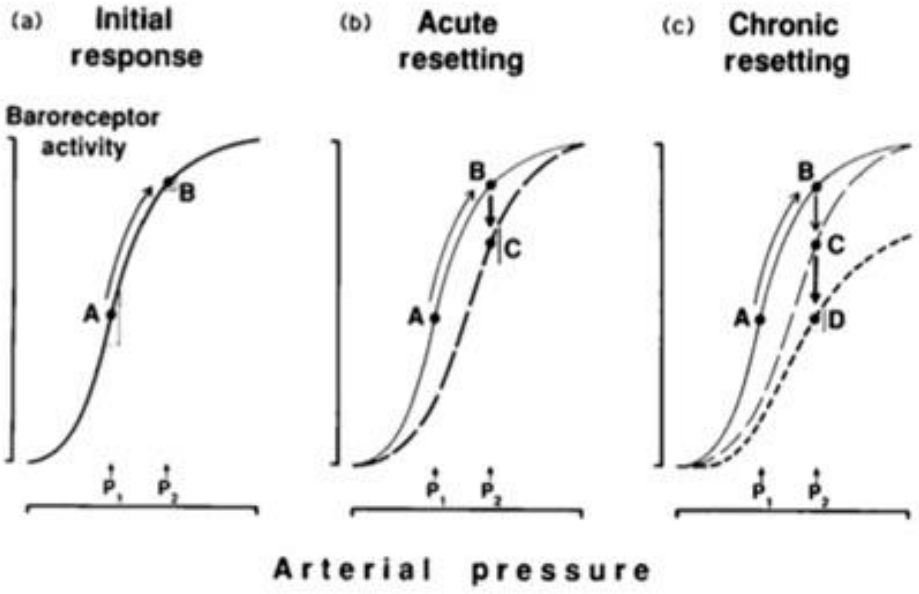

Figure 5.15. The graphical representation of arterial baroreceptor resetting in response to elevated blood pressure (reproduced from Chapleau *et al.*, 1989).

Guyton & Hall (2006) suggest that *"baroreceptor resetting"* is completed in 1 day. In our model, third order delay formulation is used to represent *baroreceptor resetting*.

5.3.2. Description of Baroreceptor Structure

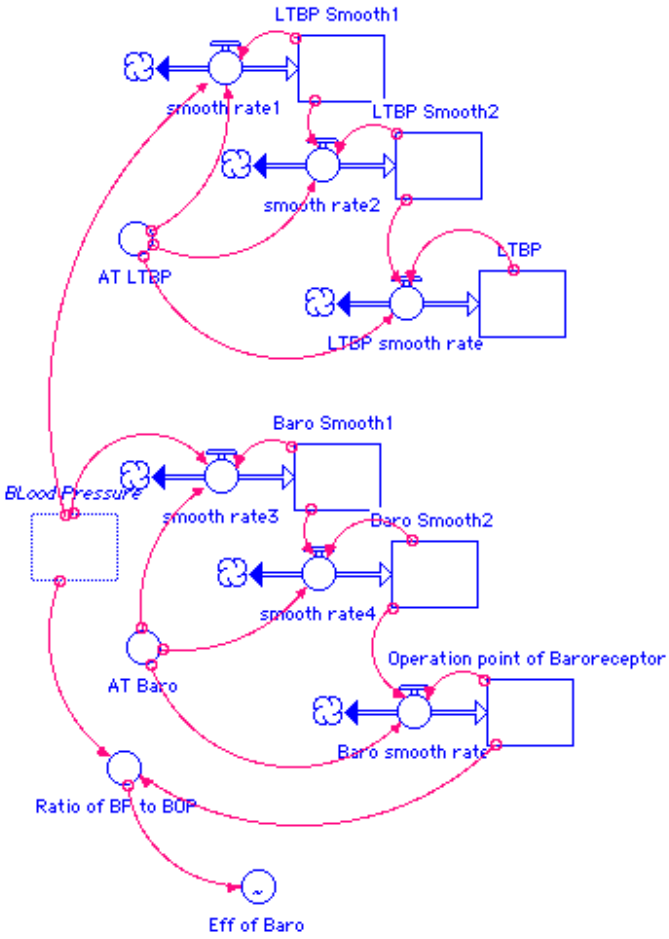

Figure 5.16. Stock-flow diagram of baroreceptor sector.

The stock-flow diagram of the sector is represented in Figure 5.16. It includes one main stock, which is the operation point of baroreceptor. The first characteristic of baroreceptor is that the operation point can be reset when there is persistent change in blood pressure.

It was assumed that baroreceptor operation point is regulated by mean arterial blood pressure. The stocks involved in the process are: *Baro Smooth1*, *Baro Smooth2* and

Operation point of baroreceptor. All stocks are fed by a bi-flow; *smooth rate3, smooth rate4, and Baro smooth* rate. *Operation point of baroreceptor* adapts itself to the level of *blood pressure* after third order delay, which can be seen in Equations 5.54, 5.55 and 5.56.

$$smooth\_rate3 = (BLood\_Pressure - Baro\_Smooth1)/AT\_Baro \quad (5.54)$$

$$smooth\_rate4 = (Baro\_Smooth1 - Baro\_Smooth2)/AT\_Baro \quad (5.55)$$

$$Baro\_smooth\_rate = (Baro\_Smooth2 - Operation\_point\_of\_Baroreceptor)/AT\_Baro \quad (5.56)$$

The magnitude of signals produced by baroreceptor is one of the factors to regulate sympathetic neuron activation. It was assumed that the related ratio of blood pressure to baroreceptor operation point is an indicator of the magnitude of signals produced by baroreceptor.

$$Ratio\_of\_BP\_to\_BOP = BLood\_Pressure/Operation\_point\_of\_Baroreceptor \quad (5.57)$$

$$Eff\_of\_Baro = GRAPH(Ratio\_of\_BP\_to\_BOP) \quad (5.58)$$

where *GRAPH(Ratio_of_BP_to_BOP)* is shown in Figure 5.17

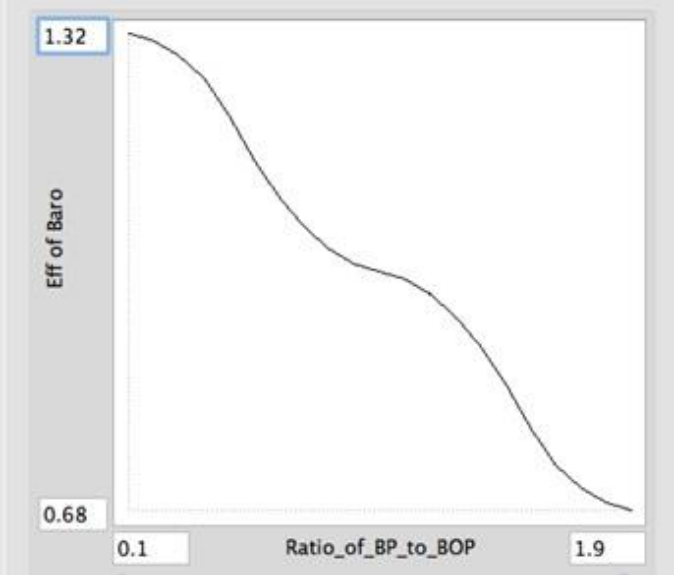

Figure 5.17. Graphical function for the effect of ratio of Blood Pressure to Baroreceptor Operation point on Average Hourly Sympathetic Neuron Activation.

The input to the graphical function in Figure 5.17 is the ratio of Blood pressure to Baroreceptor Operation point. The output is a coefficient to be multiplied with other coefficients and *reference sympathetic neuron activation* to determine *implied sympathetic neuron activation.*

5.4. Medication Sector

5.4.1. Medical Fundamentals and Assumptions

This sector explains pharmacokinetic and pharmacodynamics characteristics of the blocker drugs. Pharmacokinetics shows what body does to drug, while pharmacodynamics shows what drug does to body. In the model, Prozasin and Atenolol are selected as beta1 and alpha1 receptor blockers. Prozasin and Atenolol tablet is administrated orally. These drugs need to be absorbed in blood plasma to block adrenergic receptors in the body.

Some portion of the blocker drug undergoes structural change before the absorption. “Bioavailability” term denotes the fraction of administrated dose of unchanged drug that is absorbed into blood plasma. Once the drug is absorbed into the blood plasma, the drug simultaneously distributed in the body. *Volume distribution* of a drug represents the amount of volume that the drug is distributed in the body. Next, some portion of free drug concentration is able to bound to plasma proteins. The concentration accumulated in plasma proteins cannot be eliminated from the body. The molecular structure of the drug is very important concept that determines the plasma protein-binding ratio of blocker drugs. Also, pharmaceutical industry tries to optimize plasma-binding ratio in order to prolong or shorten duration of drug effect (Brunton *et al.*, 2011).

Trevor & Katzung (2015) presents the values of pharmacokinetic parameters for adrenergic receptor blockers that are shown in Table 5.4.

Table 5.4. Pharmacokinetic parameters for adrenergic receptor blockers.

Drug	Dose	Bioavailability	Plasma Protein Binding Ratio	Volume Distribution	Usage Frequency
Atenolol	50 mg	.56 Unitless	0.05 Unitless	67 liters	Once in a day
Prozasin	0.5 mg	.68 Unitless	0.95 Unitless	42 liters	Once in a day

Every drug has their absorption constant which determines their absorption rate. 14.11 percent of non-absorbed atenolol turns into free atenolol concentration per hour, whereas percentage of non-absorbed prozasin is 39.43 (Clark *et al.*, 2012).

When absorption rate of the drug is higher than elimination rate of free drug concentration, free drug will continue to be stored in plasma proteins (Meibohm, 2006). When elimination rate of free drug concentration is higher than absorption rate, some concentration bound to plasma protein will be released back into the blood. Free concentration of drug dictates desired level of drug concentration bound to plasma proteins.

Difference between *desired level of concentration bound to plasma proteins* and *actual concentration bound to plasma protein* determines the direction of flow.

Elimination ratio is defined as the ratio of free drug cleared from the body per hour. The two parameters determine *elimination ratio* of free drug: *clearance* and *volume of distribution*. Clearance denotes the volume of plasma from which a substance is completely removed per unit time. It was already mentioned that *volume of distribution* represents the available space to contain the drug in terms of liter. Their relative ratio gives us the *elimination ratio* of the drug per hour. Clearances of atenolol and prozasin are given as 10.2 and 12.6 liters per hour, correspondingly (Brunton *et al.*, 2011).

Free concentrations of the atenolol and prozasin can bind to beta1 and alpha1 receptors, correspondingly. Firstly, the complexes between adrenergic receptors and the blockers don't produce responses to affect related organs. Yet, the presence of blockers at receptor sites decreases the ratio of the receptors occupied by adrenergic hormones.

Dissociation constant (K_D) represents the concentration resulting half-maximal binding with related receptor. There is more than one ligand that can bind to receptors. For example, alpha-receptor can create complexes with the molecules of norepinephrine, epinephrine and prozasin (ligands). There is competition between ligands to produce complex with specific receptor, which was explained in the section 5.1.1. Dissociation constants of Atenolol (for beta 1 receptor) and Prozasin (for alpha 1 receptor) are taken 388.00 (Hoffman *et al.*, 2004) and 10.2 (Vicentic *et al.*, 2002) in terms of molarity, correspondingly. Molarity unit is converted to mg/l in the model.

5.4.2. Description of Medication Structure

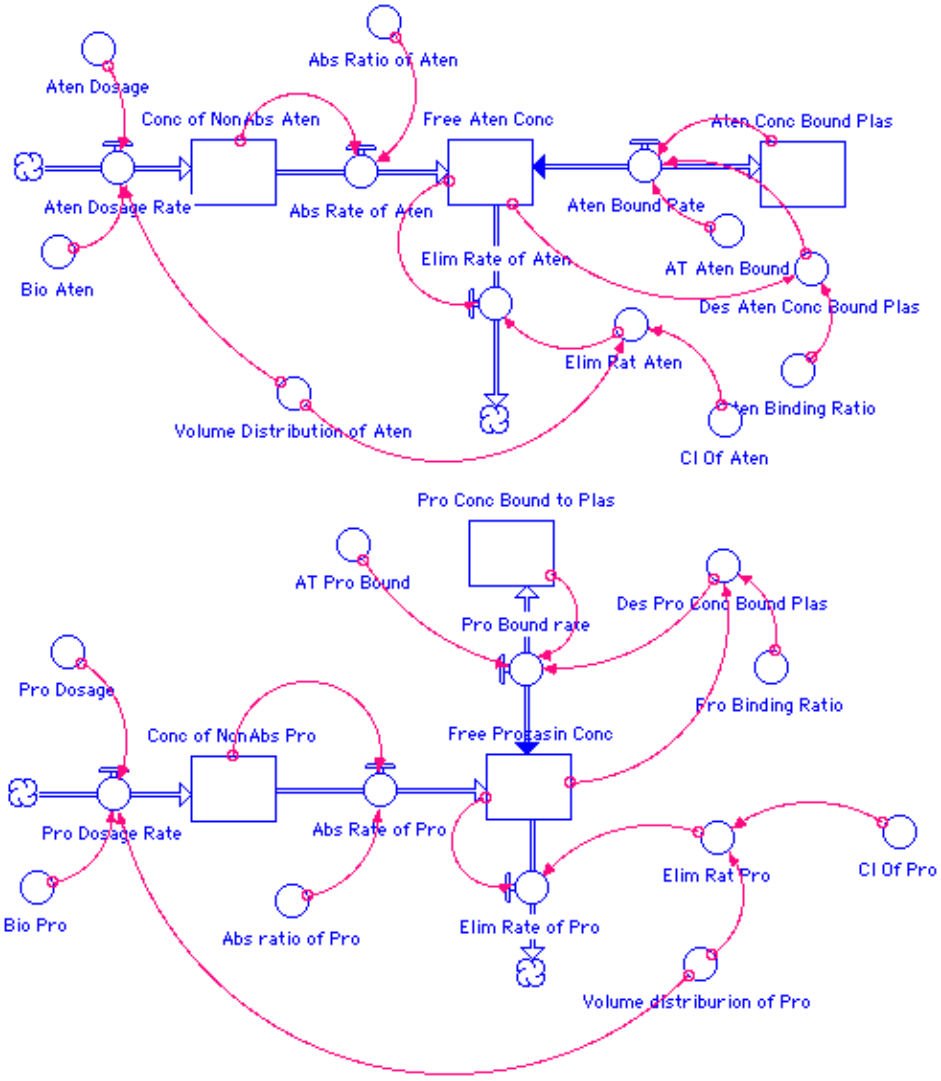

Figure 5.18. Stock-flow diagram of medication sector.

The structure constructed in this sector aims to investigate the effectiveness of selective alpha1 and beta1 blocker medications on hypertension under the sleep apnea disease. In the medical literature, the sympathetic over activation under the sleep apnea condition is a well-known concept. Sympathetic over activation causes over secretion of adrenergic hormones and consequently over stimulation of adrenergic receptors. An

adrenergic receptor blocker administration aims to decrease the percentage of the adrenergic receptor occupied by adrenergic hormones in order to prevent increase in blood pressure associated with adrenergic receptor overstimulation.

Conc of NonAbs Aten and *Conc of NonAbs Pro* represent the concentrations of blockers that wait to be absorbed in digestive system. Each of them has an inflow and an outflow: *dosage rate* and *absorption rate*.

Pro_Dosage_Rate =

Pulse(Pro_Dosage Bio_Pro / Volume_distriburion_of_Pro,6000,24)* (5.59)

Aten_Dosage_Rate =

PULSE(Aten_Dosage Bio_Aten/Volume_Distribution_of_Aten,6000,24)* (5.60)

Pulse function is used to represent the instantaneous and repetitive usage of drugs in Equations 5.59 and 5.60. When the blocker drugs are taken through mouth, the blocker drugs enter the body and wait to be absorbed. Prozasin and Atenolol are used once every day. The first parameter used in the pulse function is to determine the concentration of a drug waits to be absorbed. The second parameter is used to represent the time of first usage of blocker drug. The third parameter is used to represent the time interval between successive drug usages.

Non-absorbed Atenolol and *Prozasin* are absorbed into blood with constant ratios. *Abs Ratio of aten* and *pro* denotes the absorption ratios. The non-absorbed concentrations of blocker drugs are multiplied by the corresponding absorption ratios to determine absorption rate in Equations 5.61 and 5.62.

*Abs_Rate_of_Aten = Abs_Ratio_of_aten*Conc_of_NonAbs_Aten* (5.61)

$$Abs\_Rate\_of\_Pro = Conc\_of\_NonAbs\_Pro*Abs\_ratio\_of\_Pro \quad (5.62)$$

The concentrations absorbed into the blood are represented as Free *Atenolol and Prozasin Concentration.* Free *Atenolol and Prozasin Concentration* stocks have one inflow (see Equations 5.61 and 5.62), one outflow and one bi-flow. The outflows of the stocks are *elimination rates* represent the concentration that are excreted and metabolized per hour. *Elim Cons Pro* and *Aten* denote elimination ratios of blocker drugs. Elimination ratios of Prozasin and Atenolol are equal to the ratio of *clearance* to *volume distribution*.

$$Elim\_Rat\_Pro = Cl\_of\_Pro/Volume\_distriburion\_of\_Pro \quad (5.63)$$

$$Elim\_Rat\_Aten = Cl\_Of\_Aten/Volume\_Distribution\_of\_Aten \quad (5.64)$$

$$Elim\_Rate\_of\_Pro = Free\_Prozasin\_Conc*Elim\_Rat\_Pro \quad (5.65)$$

$$Elim\_Rate\_of\_Aten = Free\_Aten\_Conc*Elim\_Rat\_Aten \quad (5.66)$$

Blocker drugs can bind to blood plasma protein. The desired concentration of blocker drug bound to plasma proteins is regulated by free drug concentration in the blood. Free drug concentration is multiplied by plasma protein binding ratio of blocker drug to calculate the desired concentration of blocker drug bound to plasma proteins that can be seen in Equations 5.67 and 5.68.

$$Des\_Aten\_Conc\_Bound\_Plas = Free\_Aten\_Conc*Aten\_Binding\_Ratio \quad (5.67)$$

$$Des\_Pro\_Conc\_Bound\_Plas = Free\_Prozasin\_Conc*Pro\_Binding\_Ratio \quad (5.68)$$

The bi-flow, which connects *Free Drug Concentration* and *Drug concentration bound to plasma protein, are Drug Bound Rate.* Equations 5.69 and 5.70 implies that the *desired concentration of blocker drugs bound to plasma proteins* sets a target for the *actual concentration of blocker drugs bound to plasma protein*. The adjustment time (*AT Bound Aten and Pro*) denotes the required time for the actual concentration to reach the desired concentration.

Aten_Bound_Rate =

(Des_Aten_Conc_Bound_Plas-Aten_Conc_Bound_Plas)/AT_Aten_Bound (5.69)

Pro_Bound_rate =

(Des_Pro_Conc_Bound_Plas-Pro_Conc_Bound_to_Plas)/AT_Pro_Bound (5.70)

5.5. Sleep Apnea Sector

5.5.1. Medical Fundamentals and Assumptions

The main aim of blood pressure regulation is to deliver required substances to the cell and to clear byproducts of energy production process. Oxygen delivery from arterial blood to tissues is controlled by different factors like blood oxygen saturation and blood pressure (Pittman 2011;Koeners *et al.*, 2016). Breathing cessations during the sleep period due to apnea, lead to decrease in arterial oxygen saturation. Arterial oxygen saturation in the blood denotes the ratio of the hemoglobin concentration that carries oxygen to total hemoglobin concentration. The decrease in hemoglobin saturation due to apneas disrupts the regulation of blood pressure to maintain enough oxygen delivery to the tissues.

The severity of the sleep apnea disorder is measured in terms of average hypopnea-apnea index (AHI). AHI is the average number of breathing cessation per hour during a sleep

period. Karunejeewa *et al.* (2006) suggest that the apnea-hypopnea index isn't satisfactory in the researches of sleep apnea related disorders. Author assumed that new measurement standards should be accepted rather than Apnea-hypopnea index.

The proposed measurement standard is Apnea-hypopnea Index Time Series. The histogram results show that the patients may have different apnea distributions during the sleep period (Karunejeewa, 2006). In the model, it was assumed that the apnea numbers have normal distribution. The center point of distribution is the middle of the sleep (03:00 AM).

Oxygen saturation has a standard unit: "percentage". Duration of breathing cessation is between 10 and 20 seconds in the medical literature, which was assumed 10 seconds in our model. Thereby, duration of breathing cessation is found 1/120 per 20 minutes. Adjustment time of oxygen blood saturation is taken as an hour.

Guyton & Hall (2006) suggest that oxygen saturation should be taken as 97 percent under the normal conditions. This percentage is our reference oxygen saturation. Even it might appear to be erroneous at first sight to take oxygen saturation as a constant number, it is rational because the oxygen saturation doesn't vary much under the normal conditions.

5.5.2. Description of Apnea Structure

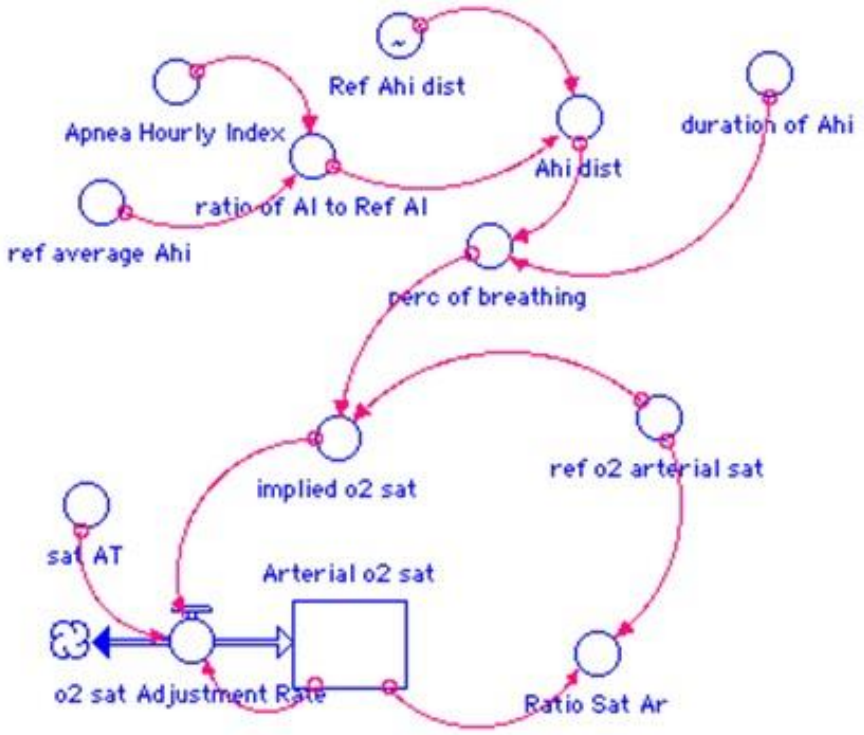

Figure 5.19. Stock-flow diagram of apnea sector.

The structure constructed in this sector shows the interaction between sleep apnea disorder and blood pressure regulation. *Ref AHI distribution* is the external variable to represent the distribution of apneas during sleep period. It was assumed that the apneas start at 00:00 AM and finish at 06:00 AM. The apnea numbers reach peak at the middle of the sleep period at 03:00 AM, since the apnea numbers are normally distributed, which can be seen in Figure 5.20. In the research of Emdin *et al.* (2017), 525 people with heart failure underwent 24 hour cardiorespiratory polygraphic recording for monitoring apnea occurrences throughout a day. The research showed that 77 patients have obstructive sleep apnea disorder, and their obstructive apnea index is normally distributed (Emdin *et al.*, 2017).

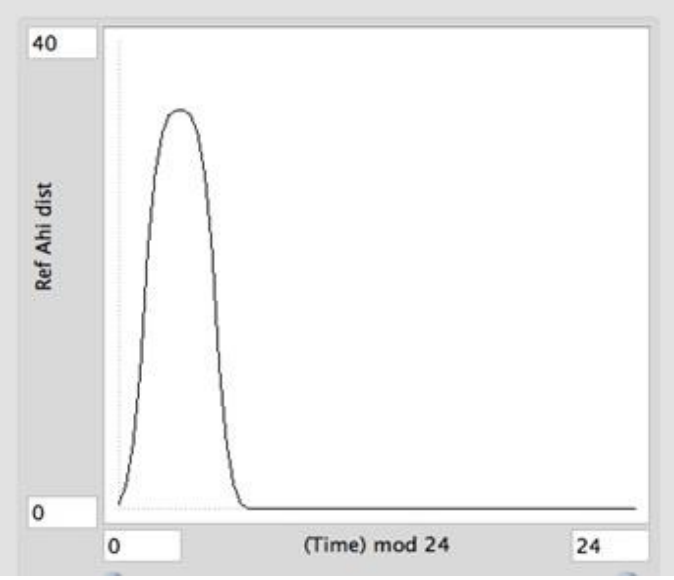

Figure 5.20. Graphical function for Sleep Apnea and its effect on AHI distribution.

The input to the graphical function in Figure 5.20 is the remainder value of simulation time divided by 24 to represent a pseudo clock. The output represents reference apnea-hypopnea distribution. In our model, it was assumed that people sleep between 11:00 PM and 07:00 AM. Thereby, the sum of the apnea numbers between 11:00 PM and 07:00 AM is divided to total number of intervals between 11:00 PM and 07:00 AM to find apnea-hypopnea index for reference AHI distribution. Apnea-hypopnea index for reference AHI distribution is denoted as *ref AHI* in our model.

$$ratio\_of\_AHI\_to\_Ref\_AHI = Apnea\_Hypopnea\_Index/Ref\_Ahi \quad (5.71)$$

Apnea Hypopnea Index denotes the average number of apneas during the sleep period. It is divided to *ref average AHI* in Equation 5.71 to find ratio of actual AHI to AHI of reference distribution.

$$Ahi\_dist = Ref\_Ahi\_dist*ratio\_of\_AHI\_to\_Ref\_AHI \quad (5.72)$$

The ratio found in Equation 5.71 is multiplied by *reference distribution of AHI* (*Ref Ahi dist*) to make normal distribution with the given *AHI* in Equation 5.72.

$$Perc\_of\_Breathing = (1\text{-}duration\_of\_Ahi*Ahi\_dist) \quad (5.73)$$

It is known that sleep apnea condition leads to breath cessations during the sleep period. The variable *percentage of breathing* shows the percentage of time without breathing cessations throughout a sleep in Equation 5.73.

$$Implied\_o2\_sat = perc\_of\_breathing*ref\_o2\_arterial\_sat \quad (5.74)$$

Arterial O2 saturation is a stock, which represents actual O2 saturation in the arterial blood. *Arterial O2 saturation* is fed by only a bi-flow: O2 saturation Adjustment Rate. Equation 5.74 means that Implied O2 saturation sets a target for the actual arterial O2 saturation.

$$o2\_Sat\_Adjustment\_Rate = (implied\_o2\_sat\text{-}Arterial\_o2\_sat)/sat\_AT \quad (5.75)$$

The ratio of Arterial O2 saturation to reference o2 arterial saturation is a factor that regulates the amount of oxygen delivery to tissues. (See Equation 5.76)

$$Ar\_Sat = Arterial\_o2\_sat/ref\_o2\_arterial\_sat \quad (5.76)$$

Finally, the decrease in the oxygen delivery during the sleep period leads to imbalances between oxygen supply and demand. These imbalances may lead to problems in blood pressure regulation and consequently hypertension.

6. VALIDATION

The validation of dynamic system modeling mainly concentrates on the internal structure of the model, and behavior validation is not tested until there is enough confidence in the underlying structure. Hence, a formal validation process is followed in order to detect structural flaws of the model (Barlas, 2002).

The expectation is that the structure is able to reflect the relationships among variables in the real system. When there is enough confidence in the underlying structure, the behavior validity test is applied. The dynamic behaviors produced by the model should reflect the dynamics of the blood pressure regulation system.

In this chapter, structural validation has been accomplished during the process of model construction. The validation of the model is basically demonstrated by performing "structure-oriented behavior tests" proposed in literature, such as extreme condition and behavior sensitivity tests. The structure in the model and the dynamic behaviors are verified by the information found in the medical literature.

The aim of this chapter is to demonstrate the simulation results under extreme conditions to test the validity of the model described in the previous chapters. The model is simulated in Stella Software and the simulation time unit is hours. Time step for the simulation is 1/16 hour that is tested to be sufficiently small. The time horizon is kept as 1440 hours in order to see the behaviors in the long run.

6.1. Equilibrium Behavior

In this section, the basic dynamic behaviors of important variables, produced by the model are outlined. In real life, circadian clock is found in every person. However, in this section, we made simulations for a person without a circadian clock to show steady state behavior. For "A person without a circadian clock" the amount of oxygen delivered to tissues and the amount of consumption are equal at any interval during the day.

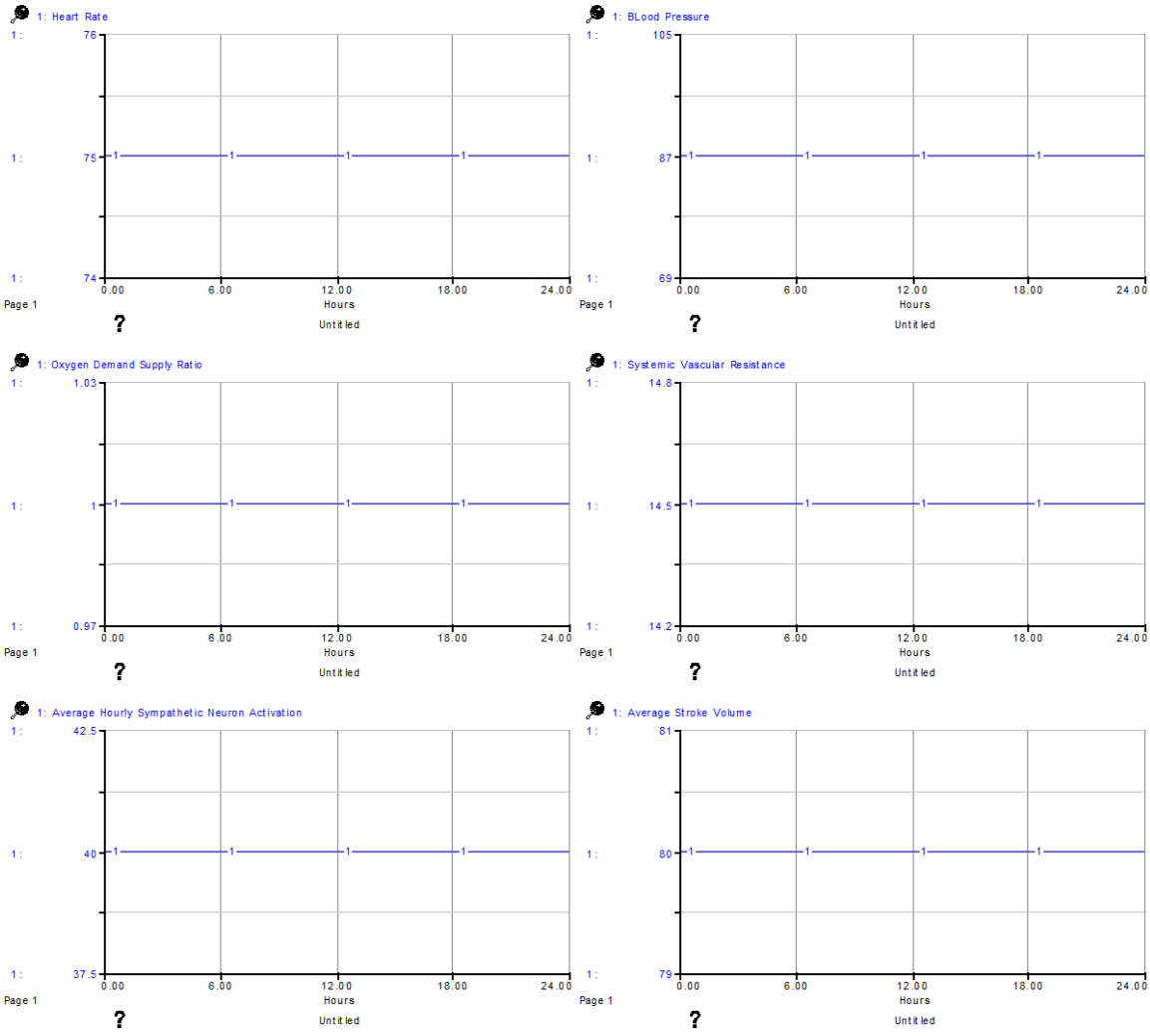

Figure 6.1. Heart Rate (left top), Blood Pressure (right top), Oxygen Demand Supply Ratio (left mid), Systemic Vascular Resistance (right mid), Sympathetic Activation (left bottom), Stroke Volume (right bottom), at equilibrium conditions.

The variables in the model have been set to their equilibrium values. The model shows a steady state behavior when the variables are initialized with their equilibrium values.

6.2. Base Runs

In the base runs, only a single variable is not initialized at equilibrium level. All other stocks are initialized at their equilibrium values. The aim of these runs is to show that the aforementioned negative feedback loops are active. Thus, the feedback loops bring variables to their equilibrium values within hours. Again, the dynamics in base runs are conducted for a person without the circadian clock. It means the amount of oxygen delivered to tissues and the amount of consumption are equal at any interval. The equilibrium values of the important variables are shown in Table 6.1.

Table 6.1. Equilibrium Values Of Important Variables

Variable Name	Equilibrium Value	Unit
Heart Rate	75	Beats/min
Systemic Vascular Resistance	14.5	mmHg*min/liter
Blood Pressure	87	mmHg
Sympathetic Neuron Activation	40	burst/min

6.2.1. Change in the Initial Value of Heart Rate

Initial values of all the variables, other than heart rate, are at their equilibrium level. The dynamic behaviors of the important variables are examined when the heart rate is initialized at 60 beats/min and 90 beats/min, correspondingly in Figure 6.2.

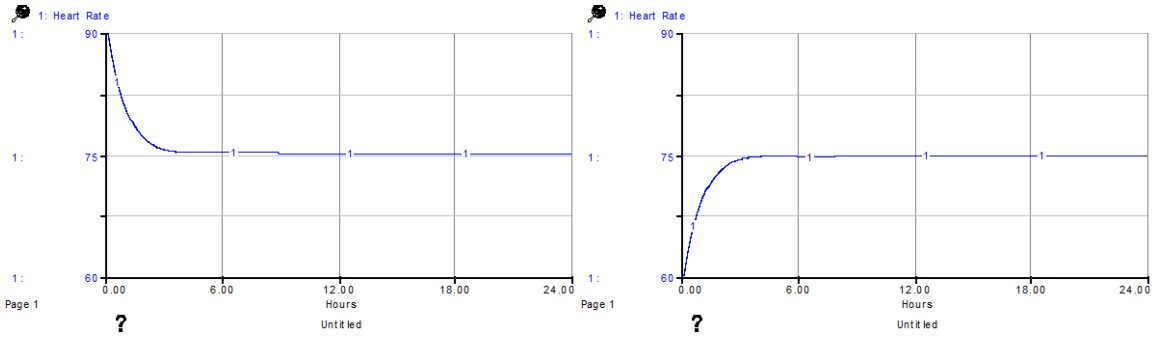

Figure 6.2. Dynamics of Heart Rate when initial value of heart rate 60 (left) and initial value of heart rate 90 (right).

The heart rate gradually moves toward its equilibrium and stabilizes there. It takes several hours to reach its equilibrium level, since the model includes adjustment delays.

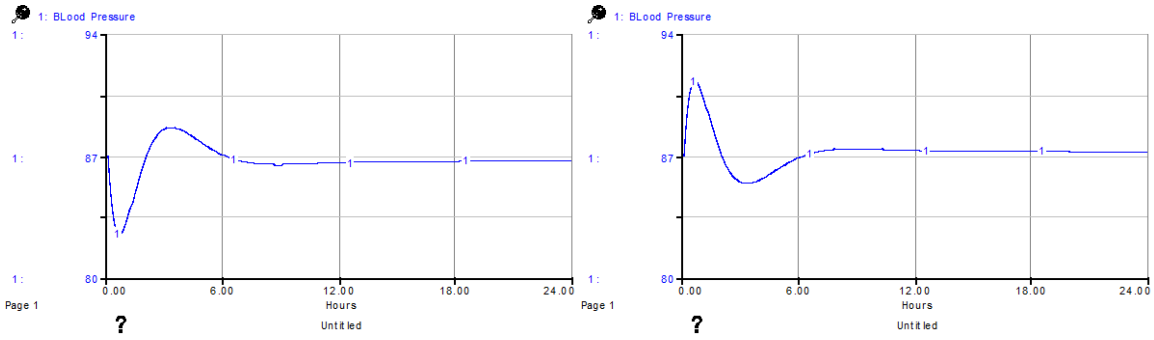

Figure 6.3. Dynamics of blood pressure when initial heart rate 60 (left) and initial heart rate 90 (right).

Heart rate is one of the multipliers to determine blood pressure, so the blood pressure is affected by initial heart rate change proportionally. As hemodynamic variables converge to the equilibrium, blood pressure restores its normal level. Delays in the blood pressure regulation cause to overshoot behavior.

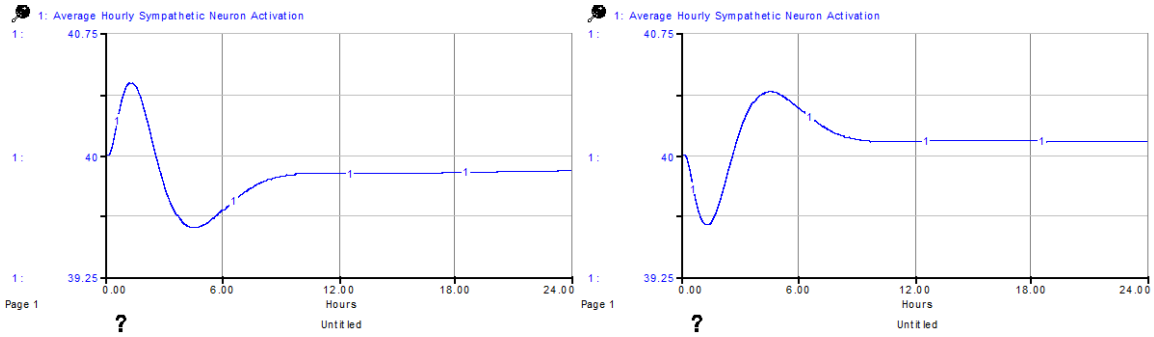

Figure 6.4. Dynamics of sympathetic stimulation when initial heart rate 60 (left) and initial heart rate 90 (right).

The negative effect of blood pressure on the average hourly sympathetic neuron activation leads to change in the average hourly SNA in reverse direction. Thereby, average hourly SNA regulates heart rate, systemic vascular resistance and stroke volume to make blood pressure restore its normal level. The example of SNA effect on systemic vascular resistance can be seen in Figure 6.5.

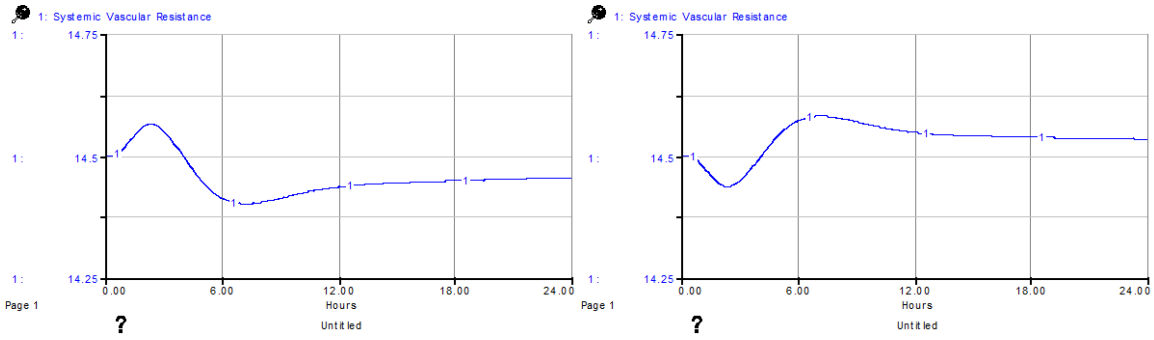

Figure 6.5. Dynamics of vascular resistances initial heart rate 60 (left) and initial heart rate 90 (right).

It may take a few days for some variables to reach their equilibrium values due to delay formulations in our model. Long-term dynamics of important variables in Figure 6.6 show that the variables converge to their equilibrium values.

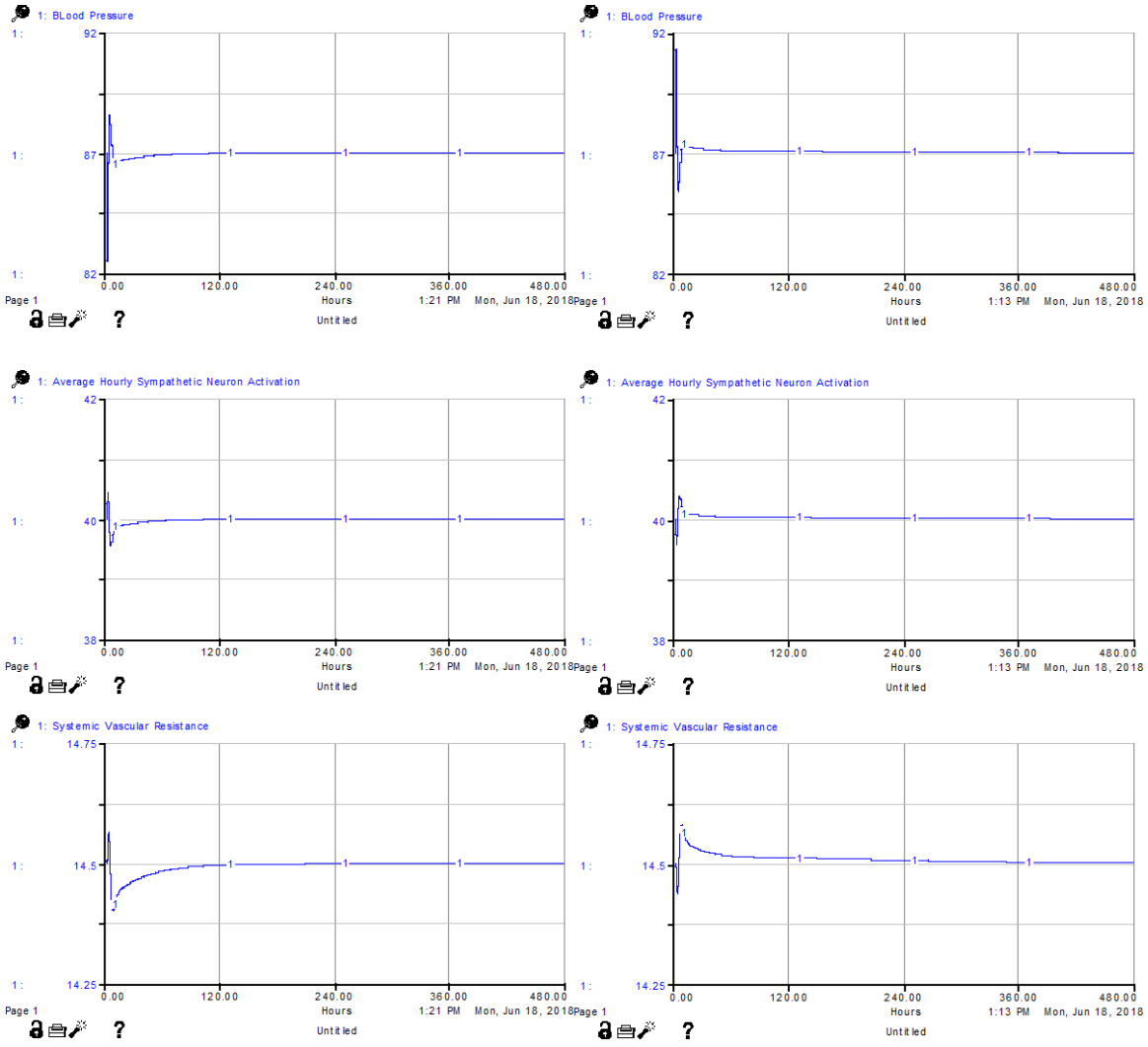

Figure 6.6. Long-term Dynamics of Blood Pressure (left top), Blood Pressure (right top), Oxygen Demand Supply Ratio (second left), Oxygen Demand Supply Ratio (second right), Sympathetic Activation (third left), Sympathetic Activation (third right), Resistance (bottom left), Resistance (bottom right) with initial heart rate 60 (left) and 90 (right)

6.2.2. Change in the Initial Value of Vascular Diameter

In this base run, the dynamics of important variables are shown when the initial value of the diameter changes. A decrease in the initial value of diameter means higher systemic vascular resistance, because they are inversely proportional. The systemic vascular resistance is another multiplier to determine the blood pressure like the heart rate. The negative feedback loops ensure that the important variables converge to the equilibrium.

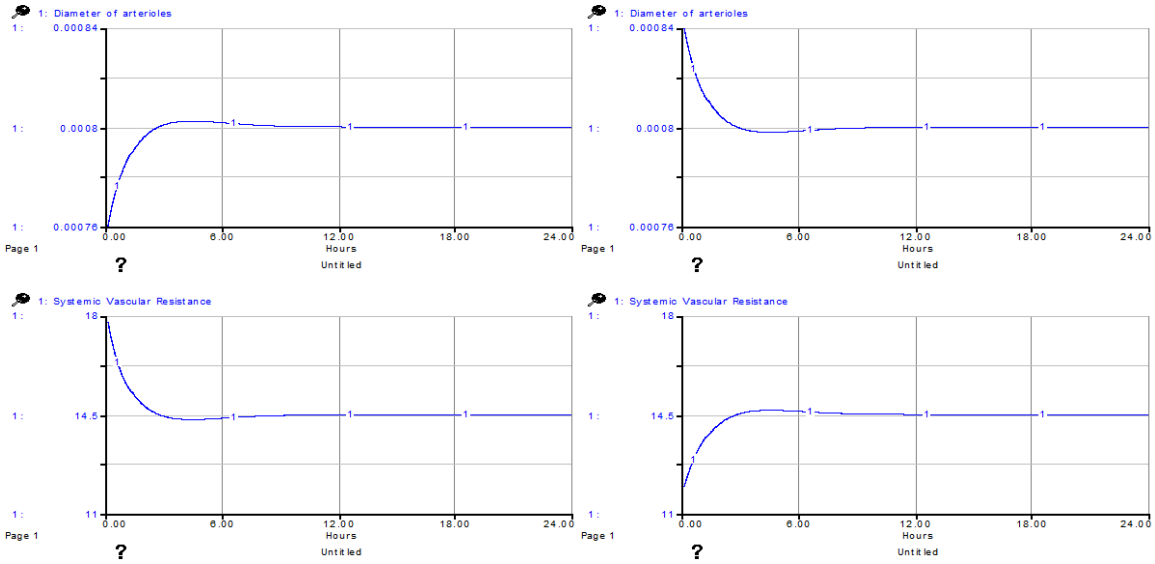

Figure 6.7. Dynamics of diameter (top) and vascular resistance (bottom) when initial diameter 7.6 * 10^-4 cm (left) and 8.4 * 10^-4 cm (right).

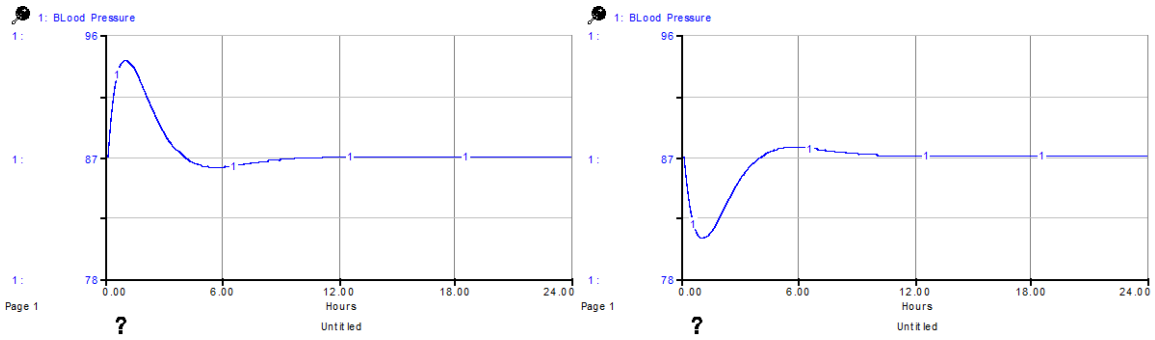

Figure 6.8. Dynamics of blood pressure when initial diameter 7.6 * 10^-4 cm (left) and 8.4 * 10^-4 cm (right).

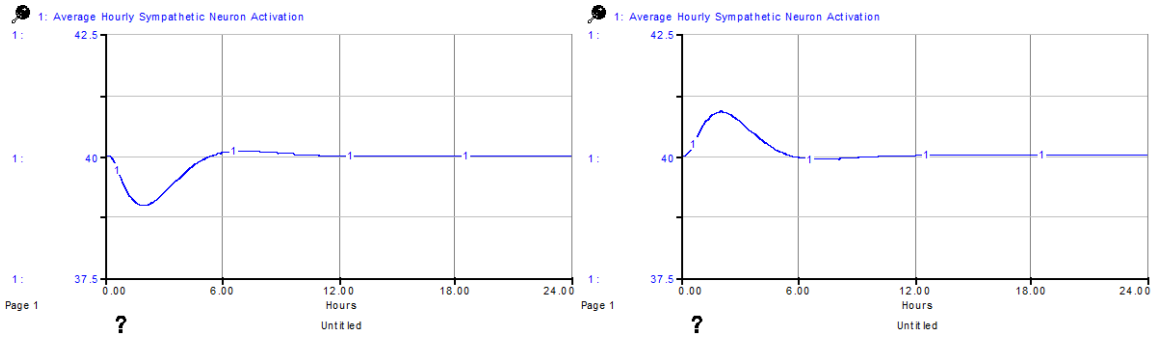

Figure 6.9. Dynamics of sympathetic activation when initial diameter 7.6 * 10^-4 cm (left) and 8.4 * 10^-4 cm (right).

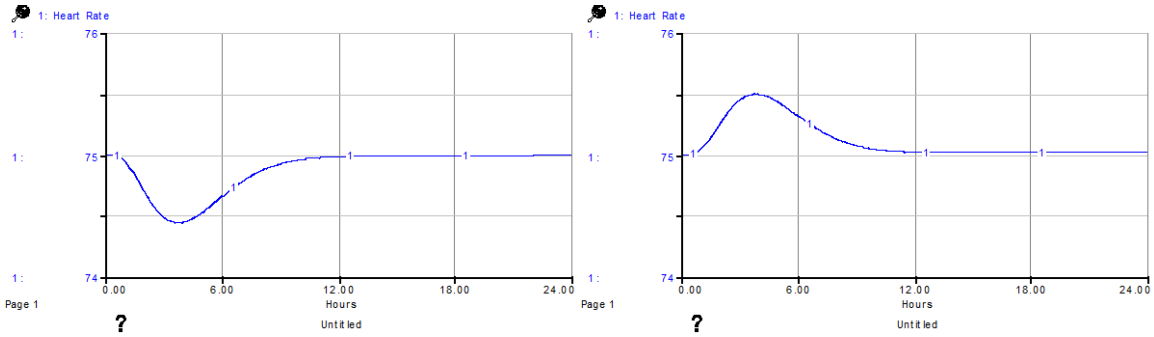

Figure 6.10. Dynamics of heart rate when initial diameter 7.6 *10^-4 cm (left) and 8.4 *10^-4 cm (right).

6.3. One-Fold Initial Increase in Sympathetic Neuron Activation for An Hour

It was assumed that all variables are at their equilibrium value, but there is one fold increase in sympathetic neuron activation for first hour.

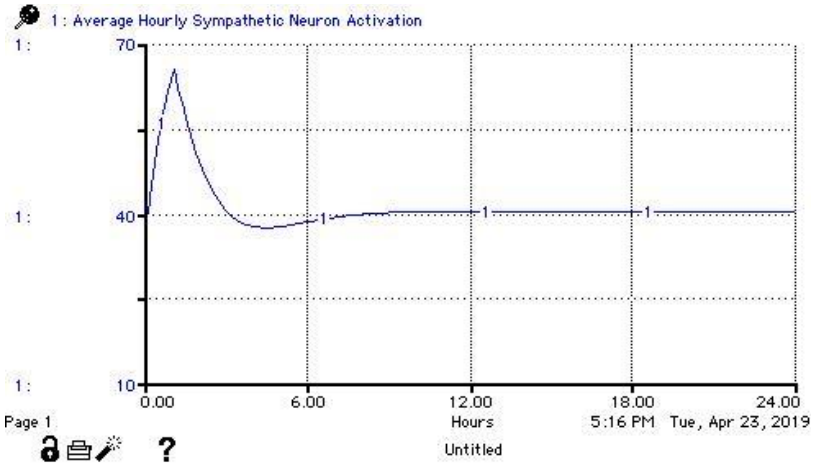

Figure 6.11. Sympathetic neuron activation when sympathetic stimulation is increased one fold for one hour.

In this scenario, *the implied sympathetic neuron activation* level is increased one fold for the first hour. So, the *Average Hourly SNA* increases during the first hour. After the first hour, the level of sympathetic neuron activation reaches its equilibrium value with overshoot

behavior within hours (see the Figure 6.11). Moreover, hemodynamic variables are affected by this change in sympathetic neuron activation. It can be seen in Figures 6.12,6.13 and 6.14.

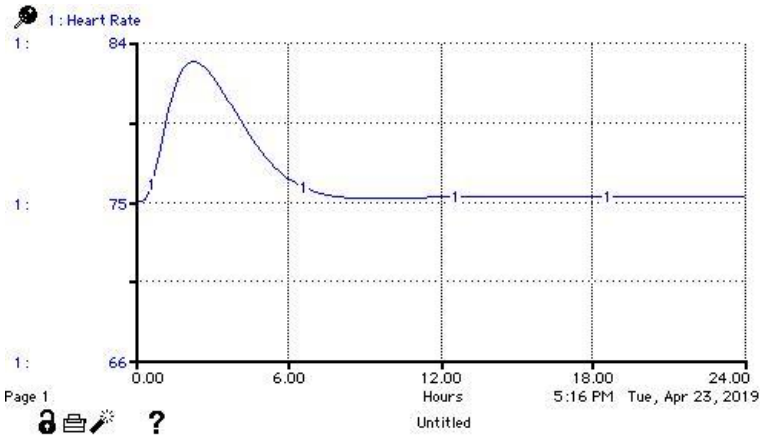

Figure 6.12. Heart Rate when sympathetic stimulation is increased one fold for one hour.

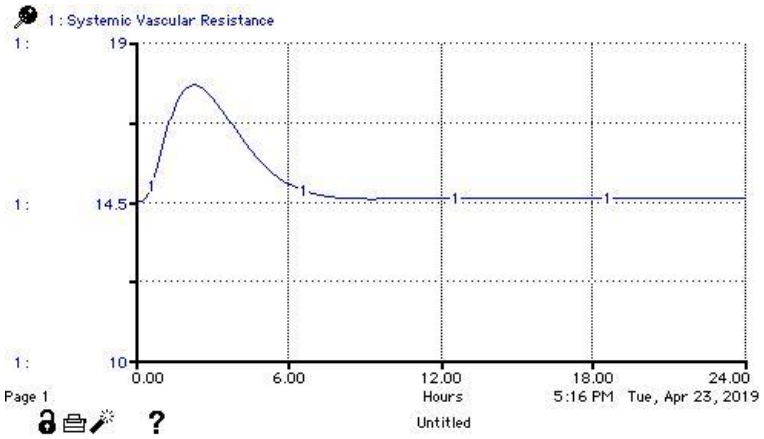

Figure 6.13. Resistance when sympathetic stimulation is increased one fold for one hour.

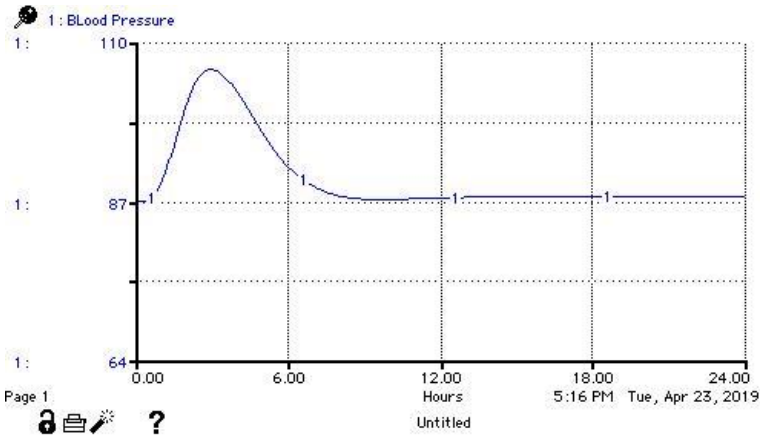

Figure 6.14. Blood Pressure when sympathetic stimulation is increased one fold for one hour.

6.4. Zero Initial Sympathetic Neuron Activation for An Hour

Zero sympathetic neuron activation for the first hour leads to decrease in sympathetic activation. All variables reach their equilibrium values at the end of twenty-four hours, as can be seen in Figures 6.15,6.16,6.17 and 6.18. In Figure 6.15, since sympathetic stimulation is decreased to zero for one hour, the Average Hourly SNA decreases to lower level for the first hour.

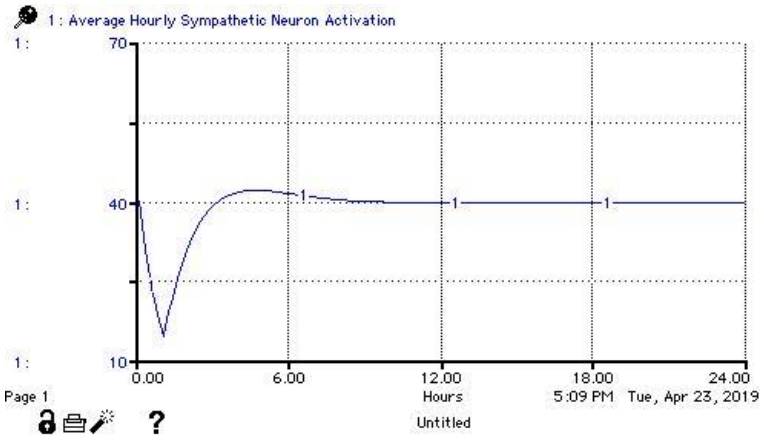

Figure 6.15. Sympathetic neuron activation when stimulation is zero for one hour.

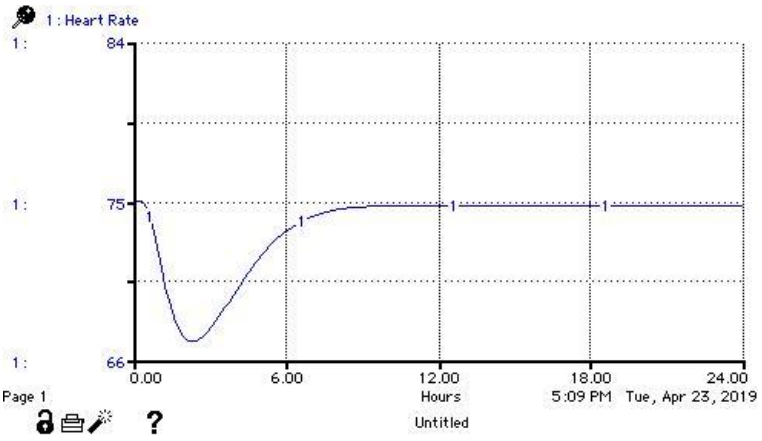

Figure 6.16. Heart rate when stimulation is zero for one hour.

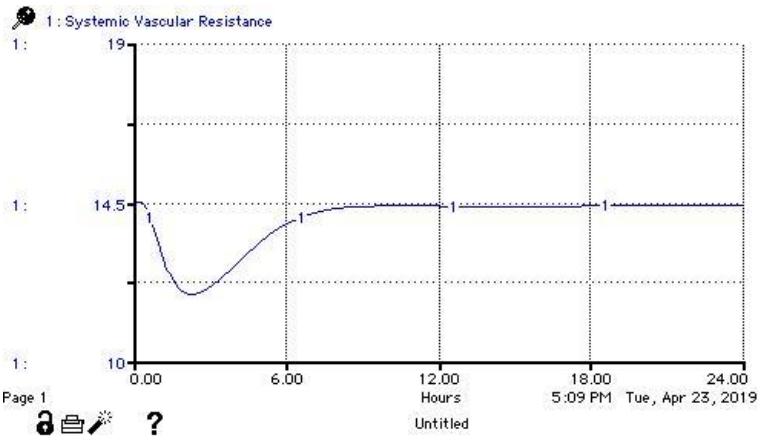

Figure 6.17. Resistance when stimulation is zero for one hour.

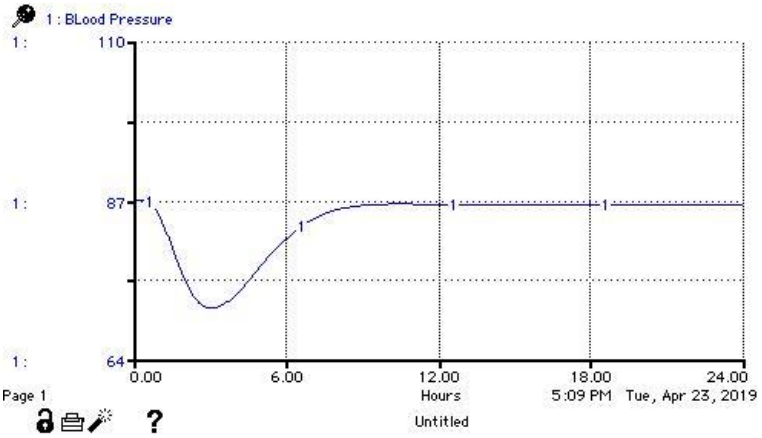

Figure 6.18. Blood Pressure when stimulation is zero for one hour.

6.5. Healthy “Circadian” Case

Circadian rhythm predetermines activity level of a person during twenty-four-hour cycles. It is one of the most important factors for people to adapt their own lifestyles according to their circadian cycles. In real life, circadian clock is one of the factors that determine tissues’ total oxygen consumption to provide required energy for the activities. In this section, the dynamic behaviors of hormonal, neural and hemodynamic variables produced by the circadian version of our model are compared with the dynamic behaviors of these variables in medical literature.

6.5.1. Long-Term Dynamics for Healthy Circadian Person

Firstly, we will look at long-term changes, and then their short-term changes. The circadian clock effect on tissues’ total oxygen consumption is represented in Figure 6.19.

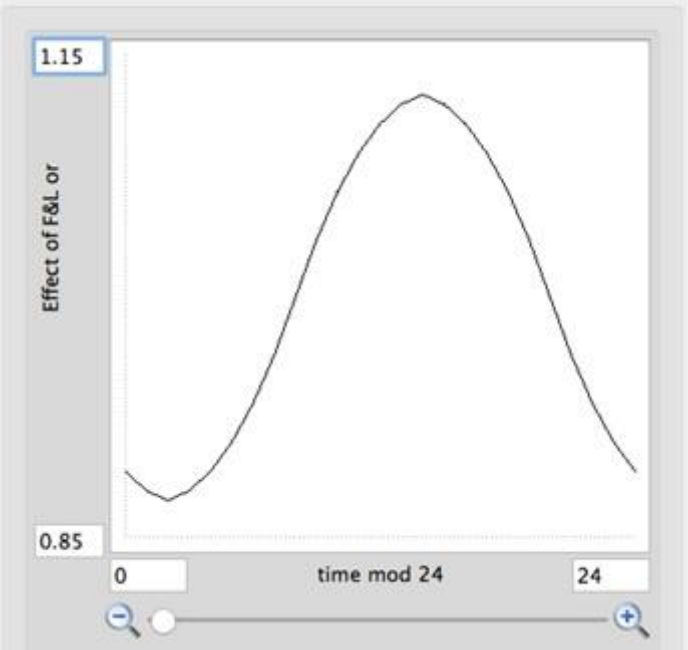

Figure 6.19. Circadian clock effect.

It was assumed that the total oxygen consumption in the body reaches its minimum and maximum levels at 03:00 AM and 15:00 PM respectively in the model.

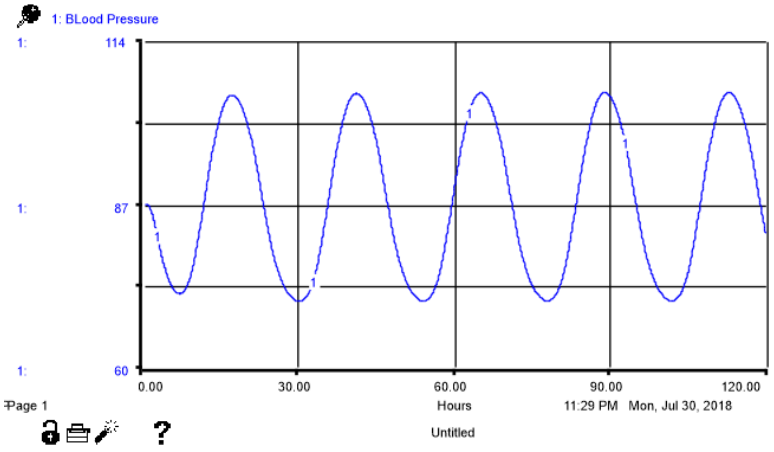

Figure 6.20. Simulated dynamics of Blood Pressure of a healthy person for the first five days.

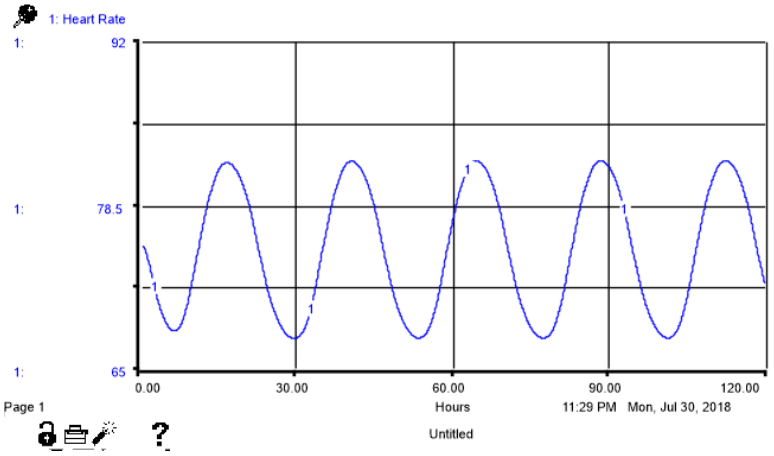

Figure 6.21. Simulated dynamics of Heart Rate of a healthy person for the first five days.

Figure 6.22. Simulated dynamics of Resistance of a healthy person for the first five days.

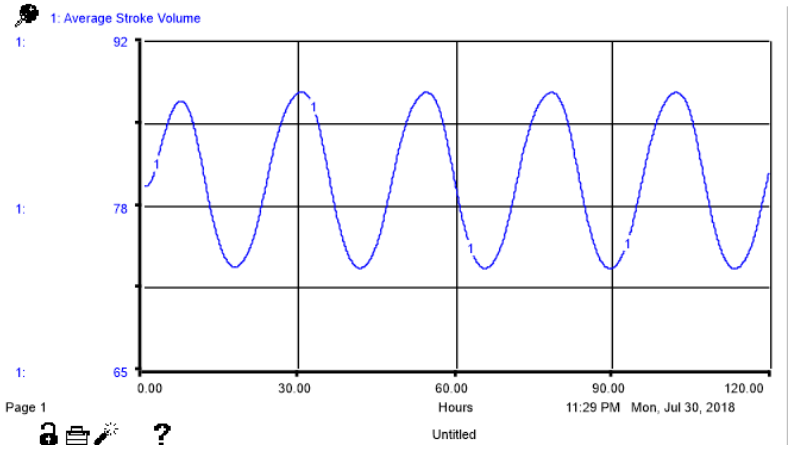

Figure 6.23. Simulated dynamics of Stroke Volume of a healthy person for the first five days.

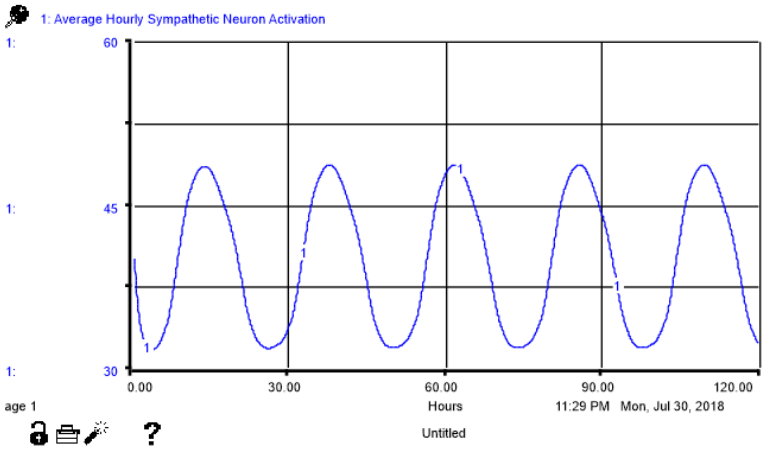

Figure 6.24. Simulated dynamics of Sympathetic activation of a healthy person for the first five days.

The aim of this section is to show that the internal structure of the model produces stabilized 24-hour dynamics of the important variables in the long run.

6.5.2. Short-Term Dynamics for Healthy Circadian Person

Since the circadian clock is one of the factors that affect the tissues' total oxygen consumption, it affects the oxygen demand/supply ratio throughout the day. The changes in the oxygen demand supply ratio affect sympathetic neuron activation (burst) after an hour.

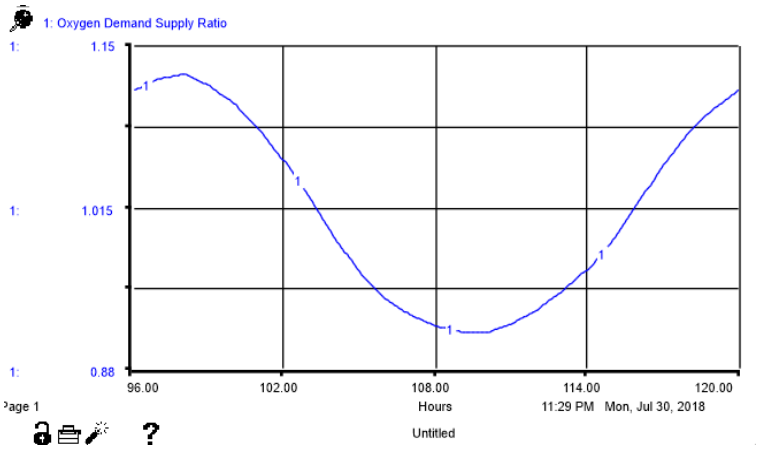

Figure 6.25. Simulated dynamics of Oxygen Ratio of a healthy person for 24 hours.

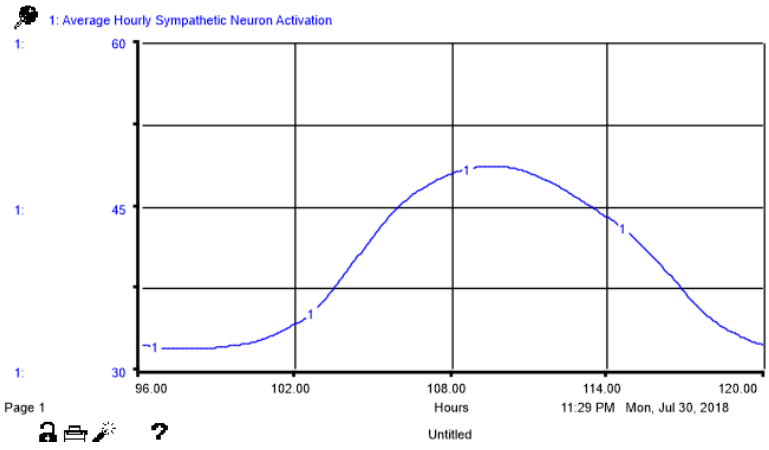

Figure 6.26. Simulated dynamics of Average Hourly SNA of a healthy person for 24 hours.

The work conducted by Linsell *et al.* (1985) investigates the effects of circadian clock on adrenergic hormones throughout the day. The authors claim that daily epinephrine level varies between 25 pg/ml and 55 pg/ml. It should be noted that *Average Hourly sympathetic neuron activation* is the only determinant of *epinephrine* level in our model.

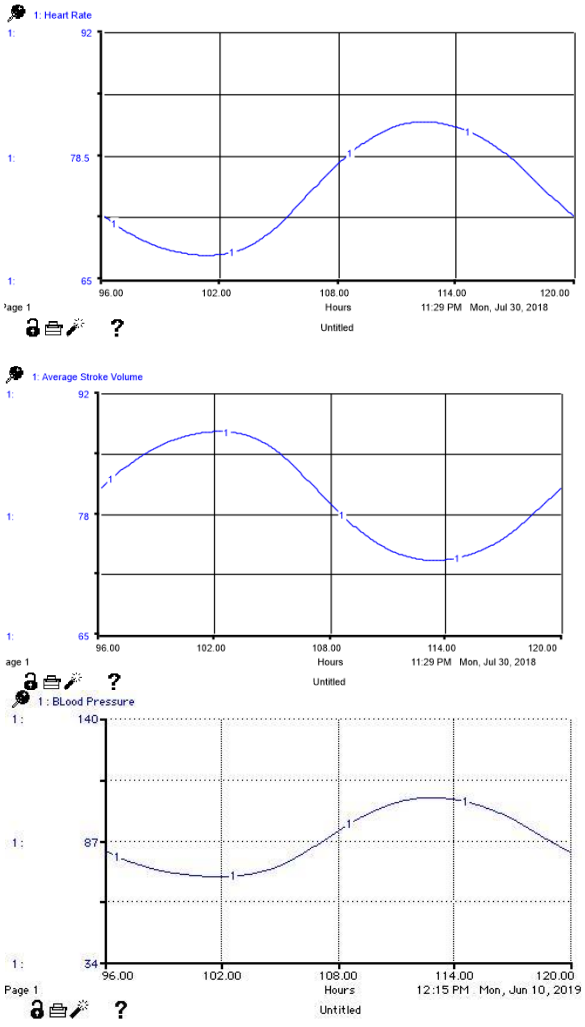

Figure 6.27. Model-generated Dynamics for; Heart Rate (First Graph), Average Stroke Volume (Second Graph), Blood Pressure (Last graph)

Heart rate, stroke volume and systemic vascular resistance are affected by sympathetically regulated hormonal changes to match oxygen supply to demand with the changes in blood pressure. The dynamics of heart rate, stroke volume and blood pressure

that are presented in Figure 6.27. It is important to note that circadian clock is the main determinant of 24-hour patterns of these variables.

7. SCENARIO ANALYSIS

Chapter 6 aims to show the behavior validity of our model. Once, the model is structurally and behaviorally valid, the simulation experiments are used to analyze the model. It is well known factor that sleep apnea condition leads to high blood pressure in the medical literature. The first aim in this chapter is to understand what extent the interactions between circadian clock and sleep apnea can make blood pressure dynamics worse. Firstly, without a circadian clock, the individual effect of frequency or intensity of sleep apnea on blood pressure regulation will be investigated. Secondly, the dynamic behaviors of the variables in blood pressure regulation system will be examined under different apnea distributions with the existence of circadian rhythm. Thirdly, the hypertension cases due to the interactions between circadian clock and sleep apnea will be simulated and possible treatment methods will be suggested. There are two possible treatment methods in the model, usage of alpha-blocker or beta-blocker. Finally, different usage times of blockers will be compared and effectiveness of medication will be discussed.

7.1. Sleep Apnea

Sleep apnea is a common disorder that is related with the interruption of the breathing during sleep periods. It affects nearly 16 million people in USA that is approximately 7 percent of total USA population. Muscular changes and additional thickened tissue in the respiratory airway, even changes in the brain related neurological function might lead to sleep apnea disorder. People, who have sleep apnea disease, inadequately deliver oxygen to tissues during sleep period. The inadequate oxygen delivery produces neurological impulses to increase sympathetic stimulation immediately. Interestingly, the episodes of apnea raise the level of sympathetic stimulation not only during nocturnal period, but also during the diurnal period in the long-term. Effects of the sleep apnea on arterial receptor systems (chemoreceptor and baroreceptor system) lead to an increase in sympathetic neuron activation throughout a day. In each nocturnal episode of sleep apnea, the chemoreceptor concentration increases progressively, which sets daily sympathetic neuron activation and

blood pressure to higher level in the long term. This adaptation mechanism protects tissues from oxygen deficiencies during sleep period in exchange for higher daily blood pressure.

The term *sympathetic overstimulation* means excessive level of sympathetic activation throughout a day. The level of sympathetic neuron activation is the main determinant of related norepinephrine and epinephrine hormones. Vardhan & Shanmuganandan (2012) claims that sympathetic overstimulation can be measured with the concentrations of adrenergic hormones in the blood.

Baroreceptor system has two important features. The first one, transient changes in blood pressure is suppressed via affecting sympathetic stimulation. The second one, baroreceptor operation point resets itself to new blood pressure level under persistent changes in blood pressure level.

7.1.1. 30-AHI-Sleep apnea without Circadian Clock

In sleep apnea disease, *Apnea Hypopnea Index* (AHI) is used to assess the severity of the disease. AHI number denotes average number of apneas per hour during nocturnal period. In the related research papers, AHI is classified in four different groups that can be seen in Table 7.1

Table 7.1. Apnea Classifications.

Normal	AHI<5
Mild sleep apnea	5≤AHI<15
Moderate sleep apnea	15≤AHI<30
Severe sleep apnea	AHI≥30

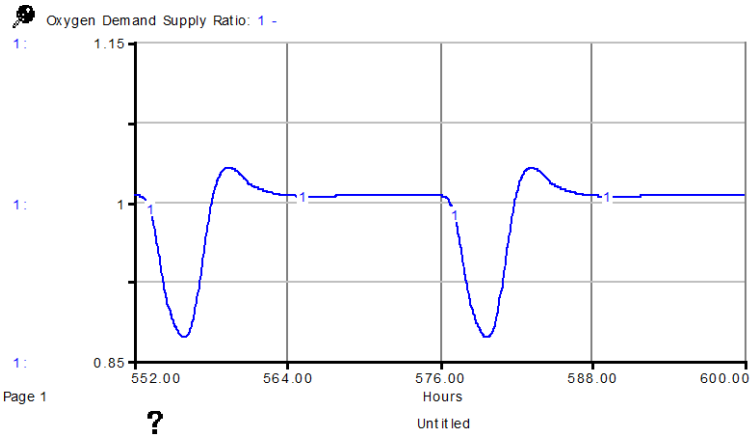

Figure 7.1. 30-AHI Sleep Apnea without Circadian clock case; Oxygen Demand Supply Ratios between 23th - 25th days.

In this case, it was assumed that a patient without the circadian clock continues his/her life with 30-AHI between 11:00 PM – 08:00 AM (Sleep period). The ratio of oxygen delivery to consumption is decreased to approximately 87 percent during sleep period in Figure 7.1. In the model "Oxygen Demand Supply Ratio" name is used as a substitute for "Oxygen Delivery Consumption Ratio". Negative feedback loop tries to increase blood pressure in order to supply enough oxygen to tissues. Delay formulations in our model are the cause of the overshoot behavior that is observed in Figure 7.2.

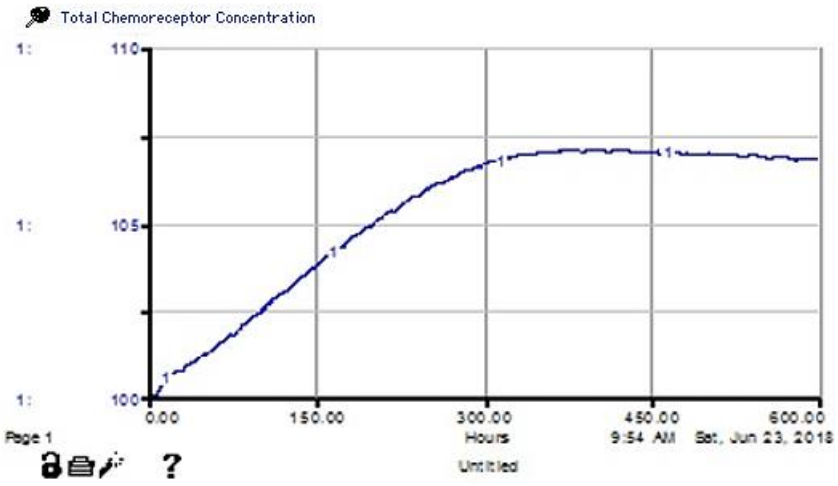

Figure 7.2. 30-AHI Sleep Apnea without Circadian clock case; Total Chemoreceptor Concentration for the long term.

In each apneic episode, the oxygen deficiencies of the tissues lead to progressive increase in the total chemoreceptor concentration. Also note that, the increase in the chemoreceptor concentration is responsible for over sympathetic stimulation. The increase in the chemoreceptor concentration leads to increase in hormonal, neural and hemodynamic variables, not only in nocturnal (night period between 11:00 PM and 09:00 AM) period but also in diurnal (daily period between 09:00 AM and 11:00 PM) period. In Figure 7.2, increase in the chemoreceptor concentration is 6.8 percent.

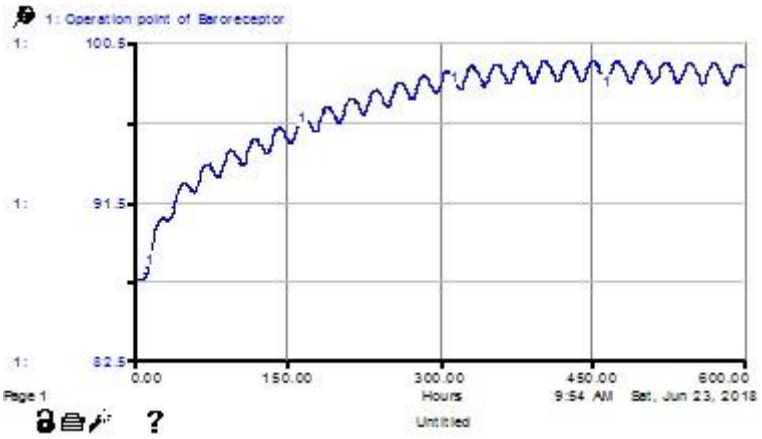

Figure 7.3. 30-AHI Sleep Apnea without Circadian clock case; Dynamics of Baroreceptor Operation point for the long term.

It was mentioned that baroreceptor always tries to keep blood pressure value close to its operation point via affecting the sympathetic neuron activation. Yet, in Figure 7.3, the long-term persistent increase in blood pressure due to sleep apnea disorder shifts operation point of baroreceptor to higher level.

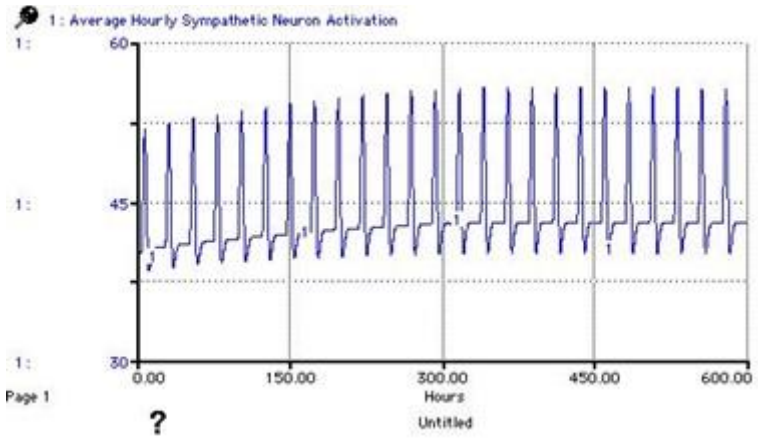

Figure 7.4. 30-AHI Sleep Apnea without Circadian clock case; Dynamics of Average Hourly Sympathetic Neuron Activation.

There is a difference between acute and chronic effects. In Figure 7.4, the increase in SNA level throughout sleep is related to the effect of oxygen supply/demand ratio on sympathetic neuron activation. This increase in the SNA level is needed to provide enough oxygen to tissues during sleep period. It is an acute effect that is a result of the decrease in oxygen deliverance due to sleep apnea. As the time goes by, the diurnal SNA level is increased due to the increase in chemoreceptor concentration. Chronic effect is related to recurrent episodes of upper airway construction (sleep apnea) over a long period of time. In the research of Goya et al (2016), patients with sleep apnea disorders have nearly %10 - % 15 increase in sympathetic stimulation compared to healthy ones. Also note that, the difference between the peak value and diurnal value is increased due to the increase in baroreceptor operation point (BOP) throughout the simulation.

The increase in BOP attenuates the inhibitory effect of baroreceptor on SNA. Blood pressure changes are related with the change in sympathetic activation, which can be seen in Figure 7.5. The increase in blood pressure during the sleep period is caused by the acute effect of sleep apnea on sympathetic neuron activation. However, the increase in the average level of blood pressure is caused by the chronic effect of sleep apnea on chemoreceptor concentration.

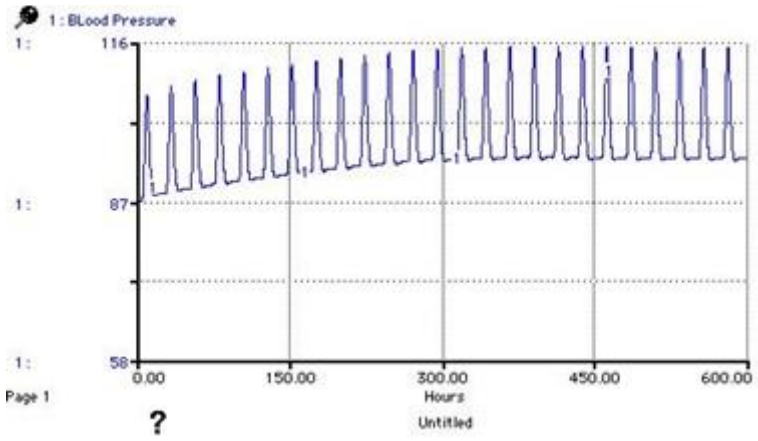

Figure 7.5. 30-AHI Sleep Apnea without Circadian clock case- Blood Pressure.

7.1.1.1. Different Sleep Apnea Frequencies. We already discussed the acute and chronic effects that sleep apnea have on blood pressure. Different sleep apnea frequencies lead to similar level of blood pressure increase during the sleep period. The difference between average blood pressure levels is increased due to chronic effects of sleep apnea in the long run. (See the Figure 7.9). In this scenario, the dynamic behaviors of important variables are compared under different sleep apnea frequencies for a patient without circadian rhythm. This scenario helps us to comprehend the individual effect of different apnea frequencies on blood pressure regulation system. Sleep apnea occurs every day for the first patient. Another one encounters with apneas during the sleep period once in two days. In the scenario, there is no circadian effect to change oxygen consumption hourly. The average apnea-hypopnea index is 30 for each scenario.

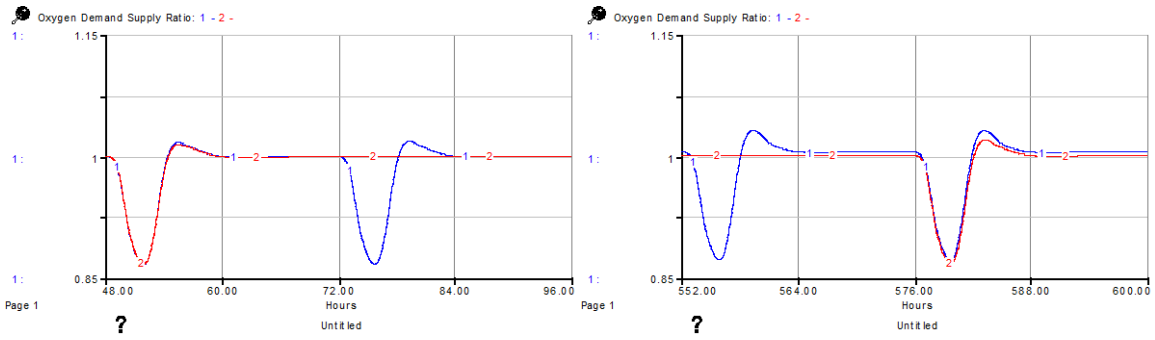

Figure 7.6. Comparative Dynamics of Short Term Oxygen; between 2nd and 4th days (right) and 23th and 25th days (left). Line1: apnea once a day, and Line2: apnea once in two days.

Figure 7.6 shows that the sleep apnea disorder causes to oxygen deficiencies in tissues. However, the increase in frequency leads to further increase in the level of oxygen supply/demand ratio throughout the simulation. It can be said that blood pressure regulation system prepares tissues for expected oxygen deficiencies when apneas occur more frequently.

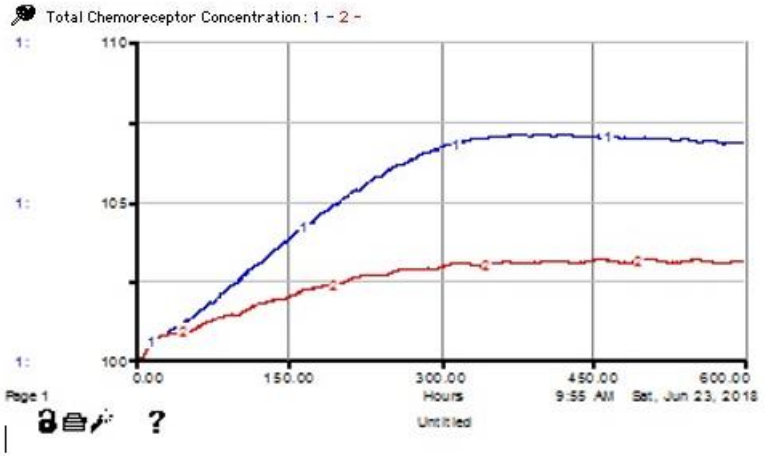

Figure 7.7. Comparative Dynamics of Chemoreceptor Concentration. Line1: 30-AHI Apnea each day, Line2: 30-AHI Apnea once in two days.

Chemoreceptors are stimulated more frequently when the apneas occur every day. The increase in chemoreceptor concentration is nearly two times higher when apneas occur every day.

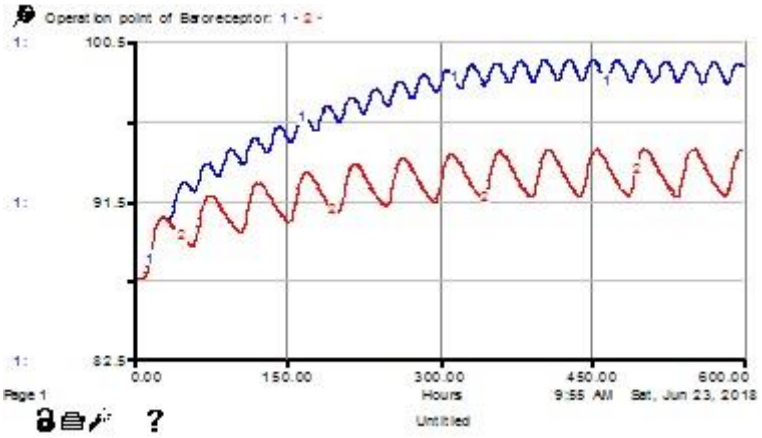

Figure 7.8. Comparative Dynamics of Baroreceptor operation points. Line1: 30-AHI Apnea each day, Line2: 30-AHI Apnea once in two days.

Figure 7.9 demonstrates how the baroreceptor reaction changes for different sleep apnea frequencies. Increase in the sleep apnea frequency causes more persistent increase in the blood pressure that leads higher baroreceptor operation point (92.5 vs. 98.5 mmHg). Then, the baroreceptor operation point cannot inhibit the increase in blood pressure when the apneas occur more frequently.

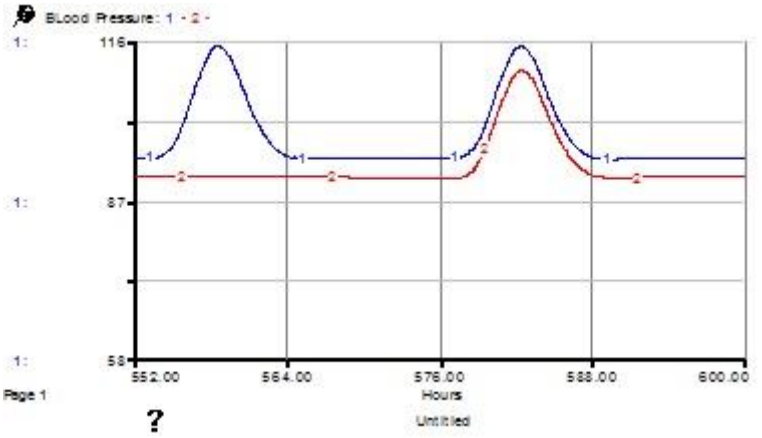

Figure 7.9. Comparative Dynamics of Blood Pressure between 23th and 25th days Line 1: 30-AHI Apnea each day, line 2: 30-AHI Apnea once in two days.

The blood pressure during the diurnal period is 91.1 and 96.9 mmHg for different sleep apnea frequencies. As a result, an increase in the sleep apnea frequency becomes an individual risk factor for hypertension.

7.1.1.2.Different Sleep Apnea Intensities. Different sleep apnea intensities show the acute effects of sleep apnea. The blood pressure level is increased more during the sleep period for the case with the sleep apnea with higher intensity. The blood pressure dynamics produced from the simulation can be seen in the Figure 7.13 (left). Table 7.1 shows the classification of sleep apnea disorder according to its intensities in the related researches. The sleep apnea disorder when apnea-hypopnea index less than 10 is not taken into consideration as a severe disease, since it doesn't have significant effect on blood pressure. In this scenario, the dynamic behaviors of important variables are compared under different the sleep apnea intensities.

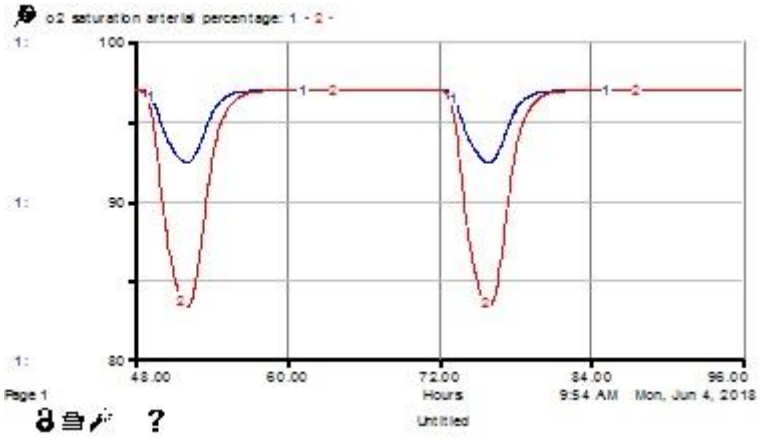

Figure 7.10. Dynamics of Arterial Oxygen Saturation between 2nd and 4th days.

1st line-10-AHI Sleep Apnea, 2nd line 30-AHI Sleep Apnea.

It was mentioned that the oxygen saturation in the blood is only affected by sleep apnea disorder in the model. The effects of different sleep apnea intensities on oxygen saturation can be seen in Figure 7.10. The blood oxygen saturation below %90 is considered

as harmful for a human body. Also, the blood oxygen saturation decreases to 84 percent if the apnea –hypopnea index is 30 as similar to medical literature.

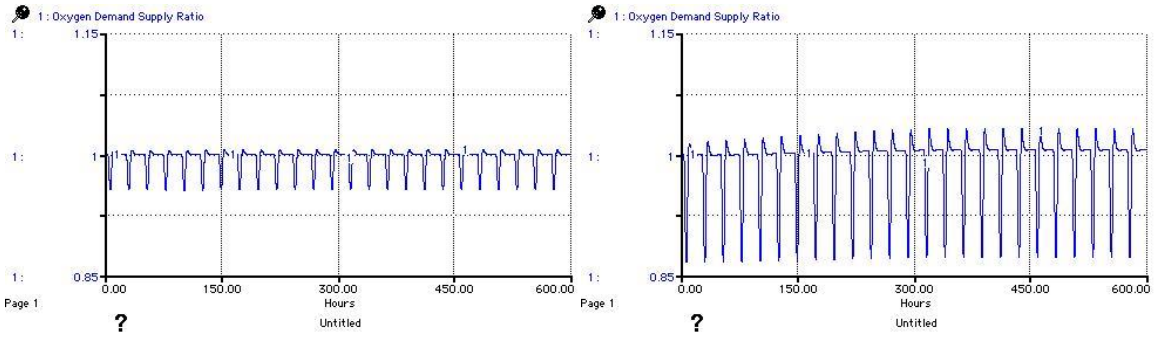

Figure 7.11. Long-term Dynamics of Oxygen supply/demand ratio change for10-AHI (left) and 30-AHI (right)

Figure 7.11 indicates that oxygen supply/demand ratio during sleep period is decreased to 0.96 when apnea-hypopnea index is 10, and 0.86 when apnea-hypopnea index is 30. The increase in the amount of oxygen deficiency causes to progressive increase in baroreceptor operation point, chemoreceptor concentration and consequently blood pressure, as shown in Figures 7.12, 7.13 and 7.14.

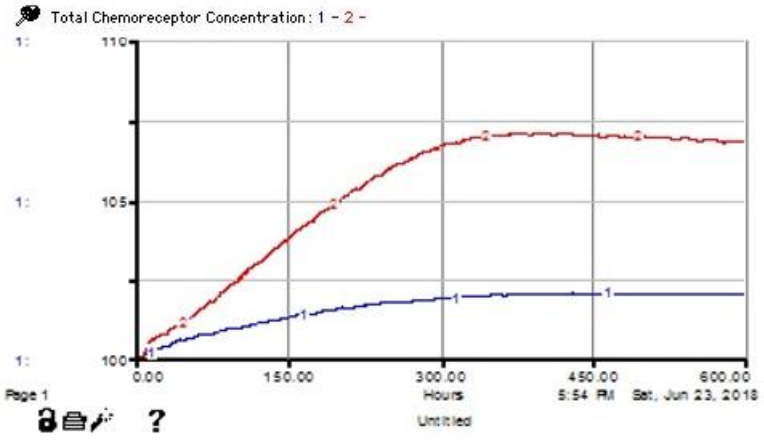

Figure 7.12. Long-term Dynamics of Total Chemoreceptor Concentration 1st line 10-AHI, 2nd line 30-AHI.

The increase in the amount of oxygen deficiency decreases the destruction ratio of chemoreceptor and eventually total chemoreceptor concentration. Under severe sleep apnea, the chemoreceptor concentration is increased 7 percent whereas, under mild sleep apnea, the chemoreceptor concentration is increased nearly 2 percent. (see Figure 7.12)

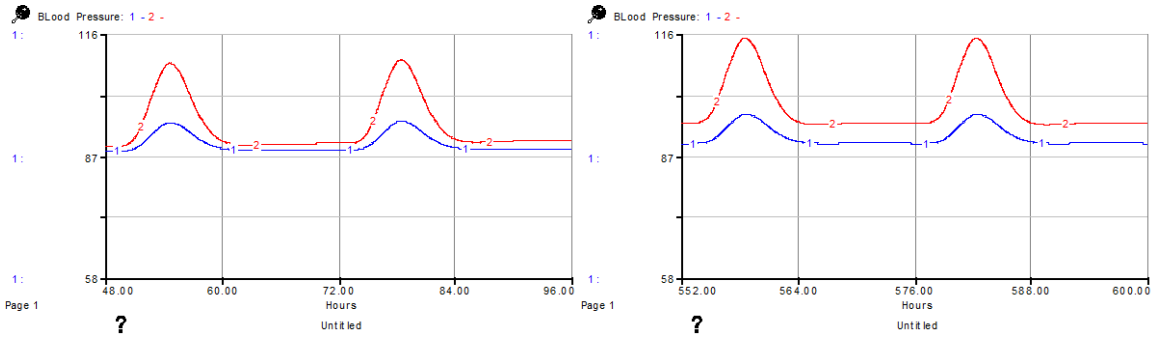

Figure 7.13. Dynamics of Blood Pressure; 1st line-10-AHI, 2nd line 30-AHI; between 2nd and 4th days (left), between 23th and 25th days (right).

In Figure 7.13, the difference between diurnal blood pressure values for different intensities is increased throughout the simulation. The difference is less than 1 mmHg between 2nd and 4th days; whereas, the difference is near to 6 mmHg between 23th and 25th days. Since the chemoreceptor concentration converges to higher values for higher intensities, the gap between diurnal blood pressure values enlarges. Also, the peak points at the left graph are lower than the right ones due to increase in baroreceptor operation point.

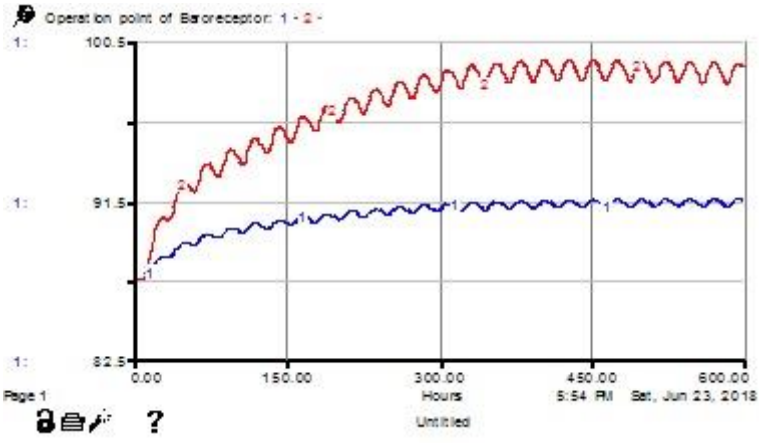

Figure 7.14. Dynamics of Baroreceptor Operation Point; 1st line-10-AHI, 2nd line 30-AHI

Under the mild sleep apnea, the increase in baroreceptor operation point is nearly 3 mmHg in the simulation result. Under the severe sleep apnea, the baroreceptor operation point is increased approximately 11 mmHg.

7.1.2. Sleep Apnea with Circadian Clock

7.1.2.1.Different Distributions of 30-AHI- Sleep Apnea. This scenario is important to show how sleep apnea interferes with the circadian clock. In the model, there is no direct interaction between sleep apnea and circadian clock. Apnea occurrences decrease the percentage of hemoglobin that is saturated with oxygen, whereas circadian clock determines the activity level of cells and oxygen consumption throughout a day. Oxygen supply/demand ratio is affected by both variables. Thus, the dynamic behavior of oxygen supply/demand ratio shows us how sleep apnea interferes with the circadian clock.

The comparison of real life data and simulation results for a healthy person has been analyzed in the Chapter 6.4. As a reminder, apnea-hypopnea index (AHI) denotes average number of breathing cessations during the sleep period (See Table 7.1 for classification of AHI). Even though, the average sleep apnea-hypopnea index during the sleep period is known, the distribution of apneas throughout the sleep isn't known for sure. It was logical to assume that apneas have a near Normal distribution during sleep period. The apnea distribution used in the model can be seen in Figure 7.15. The x-axis indicates time, and y-axis shows the number of apneas occurring at different times.

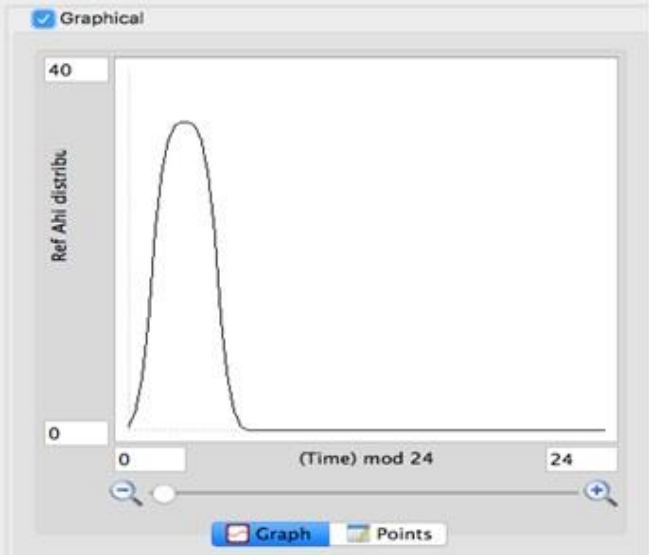

Figure 7.15. Sleep apnea distribution effect graph.

Since there is not only one-way to distribute 30-AHI throughout the sleep, it might be interesting to see what would happen if the apneas are distributed differently. Two different distributions of apneas are examined in this scenario to see how the dynamics of important variables are affected.

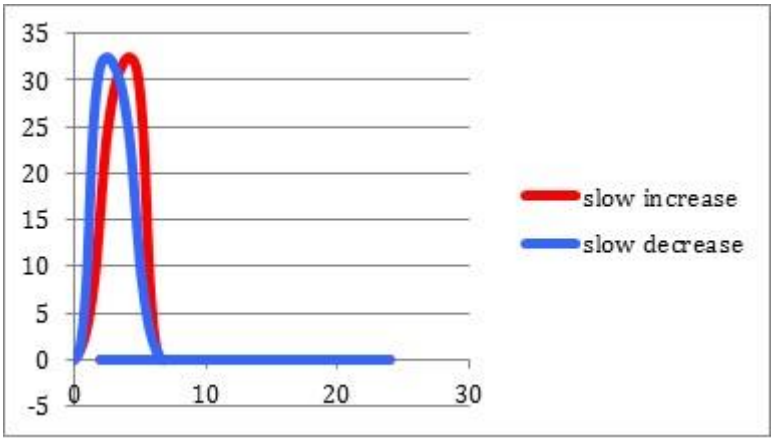

Figure 7.16. Sleep apnea distribution experiments.

It was mentioned that the oxygen saturation of the blood is only affected by the sleep apnea disorder in the model, so the change in the oxygen saturation of the blood is shown in Figure 7.17.

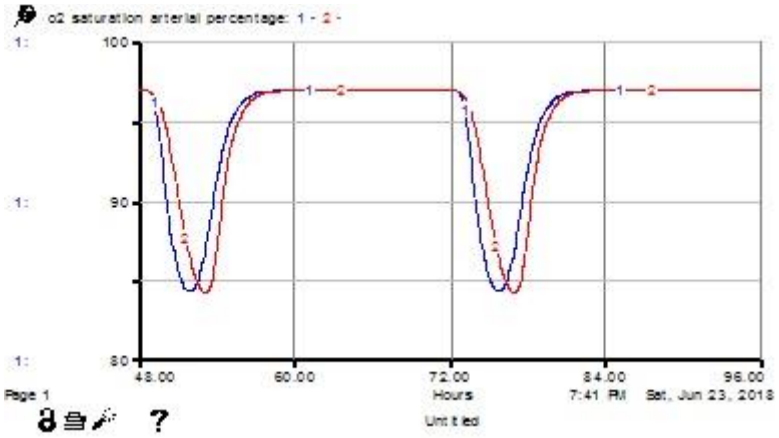

Figure 7.17. Dynamics of O2 saturation in the blood; slow decrease (1st line), slow increase (2nd line).

The minimum oxygen saturation is identical for each scenario that is nearly equal to 84 percent.

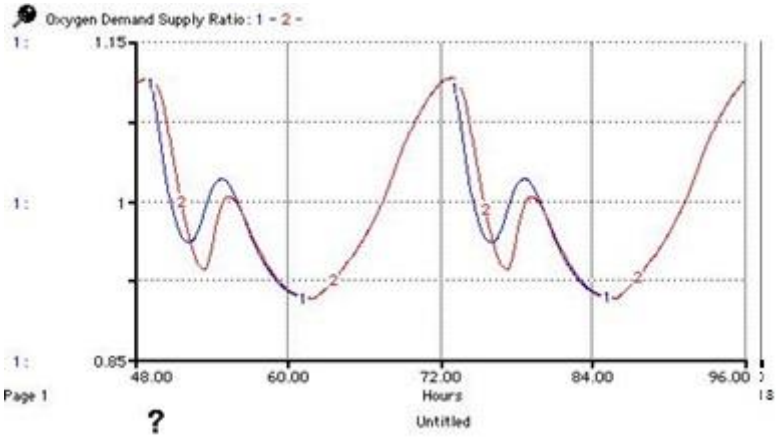

Figure 7.18. Dynamics of O2 supply/demand ratio in the blood; slow decrease (1st line), slow increase (2nd line).

Figure 7.18 shows the effects of different sleep apnea distribution on *Oxygen Demand/Supply ratio* dynamics for a person with the circadian clock. The dynamic behavior is similar for both cases.

The first apnea distribution leads to less oxygen supply/demand ratio from 00:00 AM to 04:00 AM, but the second apnea distribution leads to a decrease in oxygen supply/demand ratio in the related tissues from 04:00 AM to 08:00 AM (see Figure 7.16). The minimum point is 0.90 (the amount of oxygen delivered to tissues is equal to 90 percent of the amount consumed by the tissue) and the maximum point is 1.11 (111 percent).

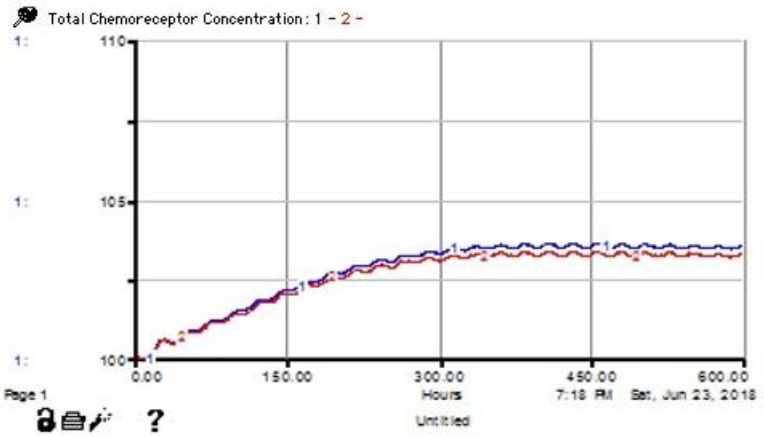

Figure 7.19. Dynamics of Total Chemoreceptor concentration; slow decrease (1st line), slow increase (2nd line)

The decrease in the *oxygen supply/demand ratio* during nocturnal period due to the sleep apnea disorder decreases *chemoreceptor destruction ratio*, which leads *chemoreceptor concentration* to increase. Yet, the effect of chemoreceptor concentration on its own production ratio limits the increase in chemoreceptor concentration. The chemoreceptor concentration converges to 103.43 mg/l for the first distribution, whereas the other one converges to 103.16 mg/l. The chemoreceptor concentration reaches to new equilibrium point at the end of 20th days for each scenario.

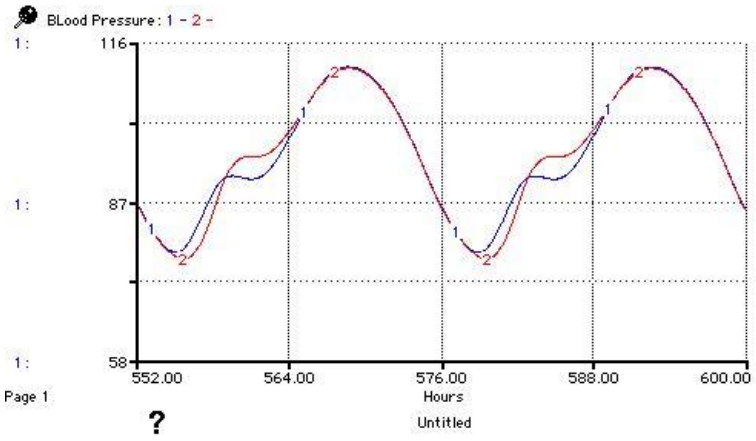

Figure 7.20. Blood Pressure dynamics in last two days; slow decrease (1st line), slow increase (2nd line)

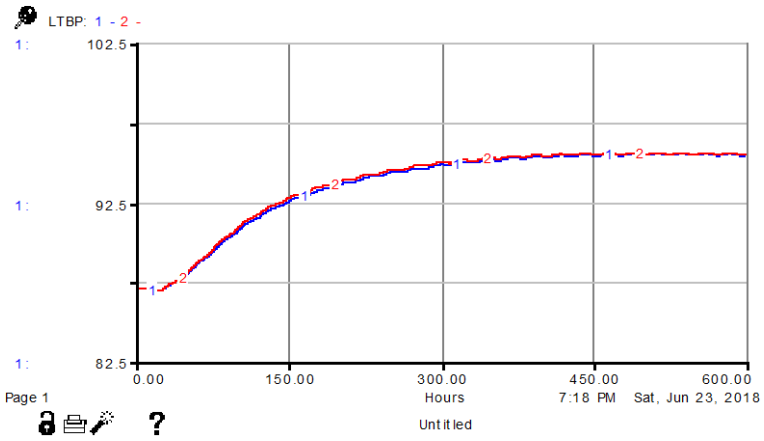

Figure 7.21. Dynamics of Long Term Blood Pressure; slow decrease (1st line), slow increase (2nd line)

Figure 7.20 shows that the changes in the apnea distribution lead to higher level of blood pressure from 00:00 AM to 04:00 AM for the first distribution, whereas the level of blood pressure is higher from 04:00 AM to 08:00 AM for the second distribution. At the end of the simulation run, Figure 7.21 shows that long-term blood pressure converges to 95.15 mmHg for each distribution. Thereby, the changes in the apnea distribution lead to negligible changes in long-term average blood pressure.

7.2. Prehypertension Case and Medication

In the chapter 6.5, it was seen that the daily average blood pressure is found as 87 mmHg for healthy person. The sleep apnea disorder scenario in section 7.1.2 shows that average blood pressure goes up to 95.15 mmHg. The time horizon in the model is not long enough, but increased blood pressure due to sleep apnea disorder may lead to cumulative damage in the arterioles over years. Moreover, the cumulative damage in the arterioles leads to more severe problems in blood pressure regulation. Continuous Positive Airway Pressure (CPAP) masks and oral appliances to prevent apneas during sleep periods are the most effective treatment methods. Yet, patients find sleeping with a CPAP mask difficult. According to the estimation of Iftikhar *et al.* (2014), 55% of the patients quit CPAP treatment after 3 weeks. The other treatment options are the administrations of alpha or beta-blockers to attenuate the effect of the sleep apnea disorder on blood pressure. In this section, alpha and beta-blockers are used as a treatment to pre-hypertensive case to normalize the blood pressure. The dynamic behaviors of important variables will be compared under different usage times of beta-blockers and alpha-blockers.

7.2.1. Beta Blocker Atenolol

In section 7.1.2, it was already examined that how the related hemodynamic, neural variables and consequently blood pressure are affected by sleep apnea disorder. The reason behind the high blood pressure under the sleep apnea disorder is over sympathetic stimulation related increase in hormone secretion. The beta-blockers occupy beta-receptors to prevent possible adrenergic hormones occupation. In this way, they decrease the complex between receptors and adrenergic hormones. The complexes between beta-blockers and beta-receptors don't produce any stimulation. In the medical literature, the beta-blockers also classified as reversible or irreversible according to the strength of the bond that they created with beta-receptors. The drugs that are produced by the pharmaceutical companies are mainly reversible. Atenolol is one of the most popular beta-blockers, which is used in the treatments of hypertensive patients. 50 mg atenolol tablets are used to decrease heart rate, which was elevated due to sleep apnea disorder in our model.

Firstly, it should be checked that the daily atenolol usage shouldn't increase free atenolol and atenolol concentration bound to plasma proteins progressively. Also, free atenolol and plasma protein bound atenolol concentrations should decay to zero after some time if atenolol tablet is used only once. It can be seen that these conditions are satisfied. (see the Figure 7.22 and 7.23)

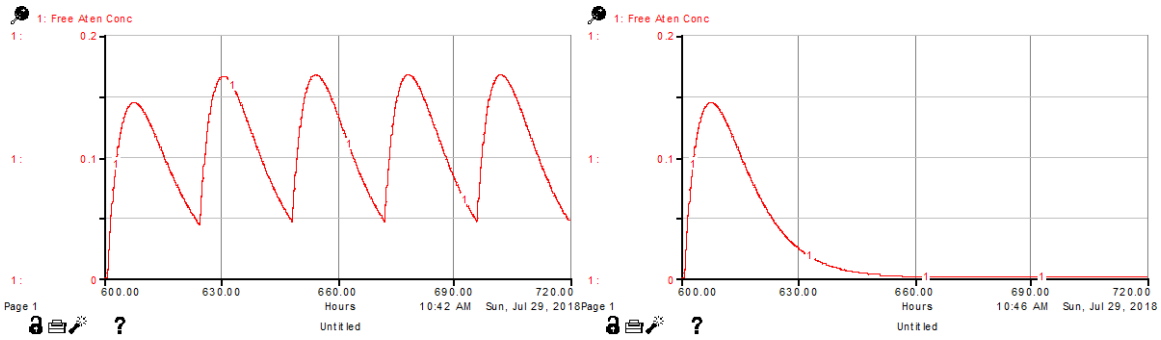

Figure 7.22. Free atenolol concentration: when atenolol tablet is used each day (left), when atenolol tablet is used once (right).

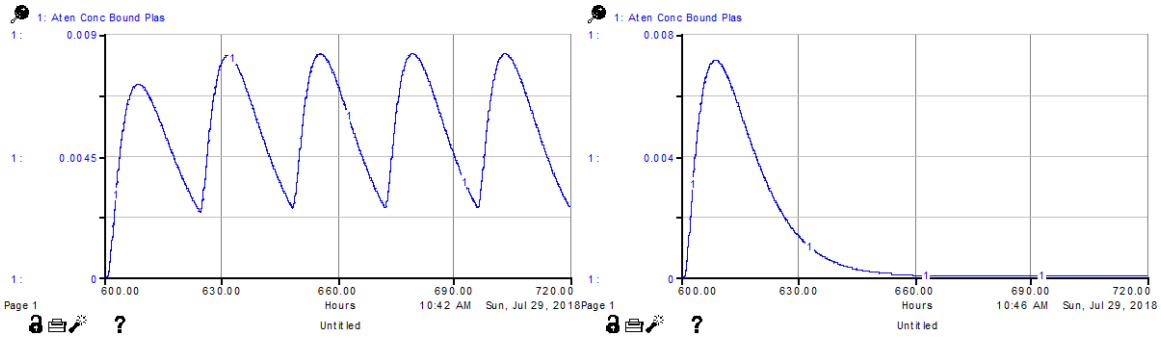

Figure 7.23. Plasma protein bound atenolol concentration: when atenolol tablet is used each day (left), when atenolol tablet is used once (right).

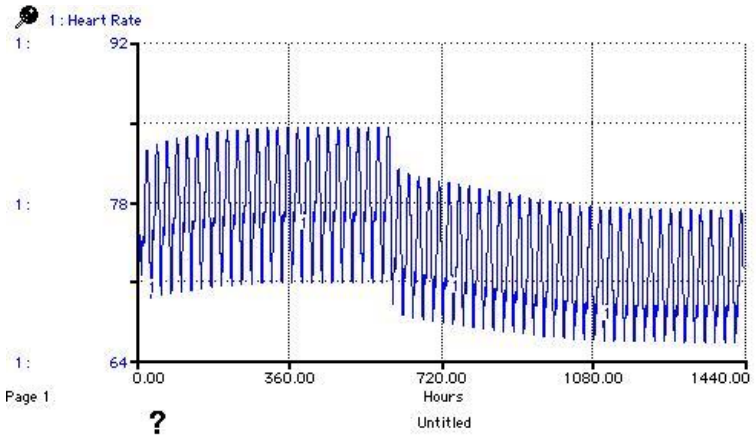

Figure 7.24. Dynamics of Heart Rate with the daily usage of atenolol starting on 25th day at 11:00 pm

The "healthy circadian person" scenario in Chapter 6 (Validation) shows that the heart rate varies between minimum 67.5 and maximum 82.5 beat/min throughout a day. Due to sleep apnea disorder, there is overall 3.2 percent increase in the daily level of heart rate before atenolol administration (see Figure 7.24). After 25th day, the daily usage of the 50 mg atenolol quickly decreases daily average heart rate from 77.4 beats/min to 70.47 beats/min. Holtzman *et al.* (1986) claim that the decrease in the daily average heart rate is 8 beat per minute whereas Viitasalo & Karjalainen (1992) found the decrease in the daily average heart rate 11.2 beat per minute under atenolol administration.

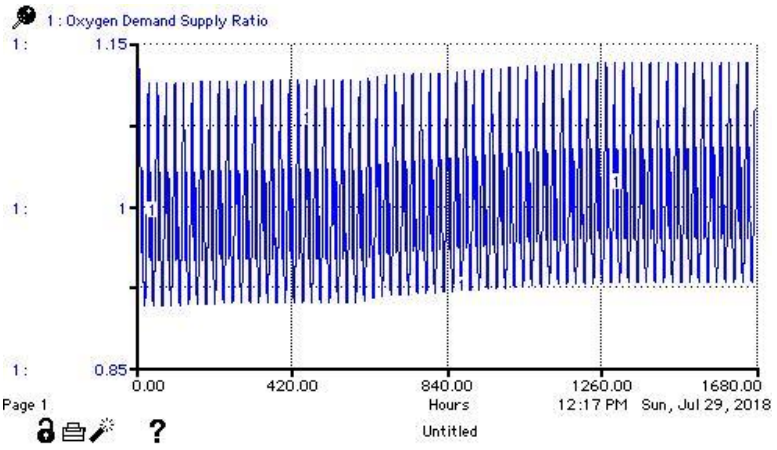

Figure 7.25. Dynamics of Oxygen Supply Demand Ratio with the daily usage of beta-blocker starting on 25th day at 11:00 pm

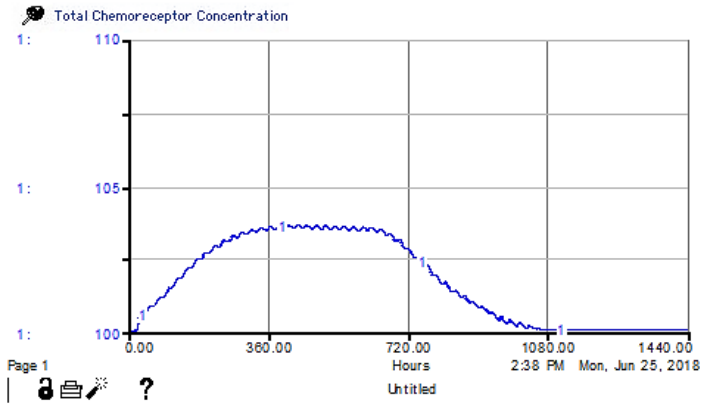

Figure 7.26. Chemoreceptor Concentration with the daily usage of beta-blocker starting on 25th day at 11:00 pm

The chemoreceptor concentration returns to its original level for beta 1 blocker medication in a very short time span (nearly 20 days). Normally the chemoreceptor concentration returns to original level in a longer time. However, in our case, beta-blocker medication starts before the patients have hypertension (meaning arterial blood pressure is lower than 113). In figure 7.24, we showed that heart rate decreases sharply at the beginning of medication, so oxygen supply demand ratio has a sharp increase. As a result, chemoreceptor concentration returns to its original level quickly.

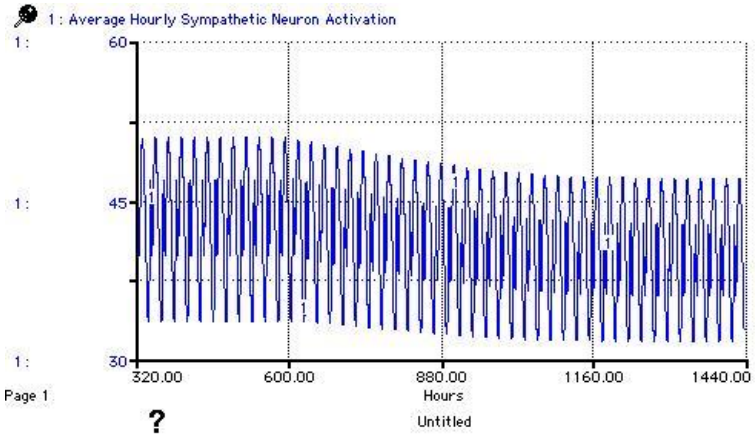

Figure 7.27. Dynamics of Sympathetic stimulation with the daily usage of atenolol starting on 25th day at 11:00 pm

The medical literature suggests that the decrease in the work output of the heart leads to a decrease in total oxygen consumption. Similarly, *the ratio of oxygen supplied to oxygen demanded* is increased that can be seen in Figure 7.25. The decrease in total oxygen consumption helps reducing excessive chemoreceptor concentration shown in Figure 7.26. The decrease in excessive chemoreceptor concentration prevents over sympathetic neuron activation in the long run (Holtzman, 1986; Viitasalo & Karjalainen, 1992). After the 25th day, the daily usage of atenolol decreases sympathetic neuron activation progressively throughout simulation (see Figure 7.27).

The medical literature suggests that the beta-blocker usage leads to a vasodilation of arterioles in the long run. Beta-blocker progressively attenuates over sympathetic stimulation via decreasing work output of heart. Thereby, systemic vascular resistance also decreases over time.

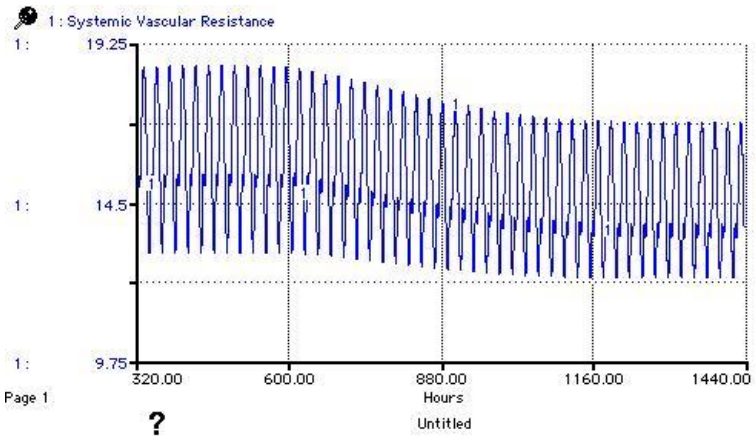

Figure 7.28. Dynamics of systemic vascular resistance with the daily usage of atenolol starting on 25th day at 11:00 pm

In Figure 7.28, the decrease in systemic vascular resistance is progressive. Holtzman *et al.* (1986) investigated another alpha-blocker named as propranolol. In his research, long-term decrease in the systemic vascular resistance is approximately given as 214 dynes.cm/sec, which is equal to 2.675 HRU/Wood. Before the usage of atenolol, the minimum and maximum values of systemic vascular resistance are 13.08 and 18.45, whereas

the usage of atenolol leads to a decrease in corresponding values to 12.04 and 16.88. (see Figure 7.28)

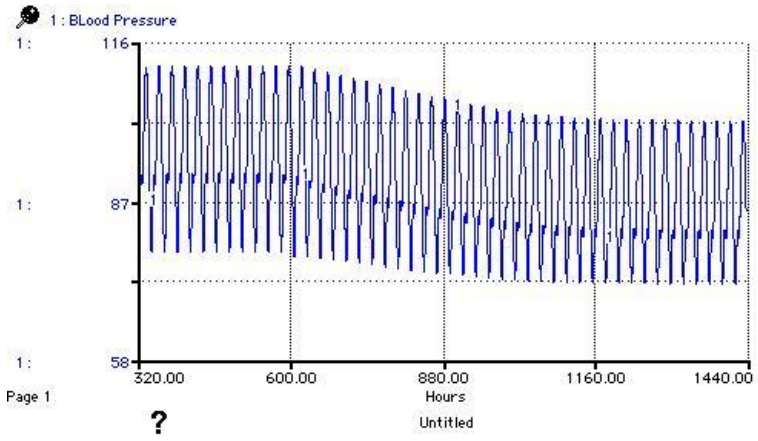

Figure 7.29. Dynamics of Blood Pressure with the daily usage of atenolol starting on 25th day at 11:00 pm

The beta-blocker usage does not produce immediate effect on blood pressure. The decrease in mean arterial blood pressure is slowly provided by the decrease in the chemoreceptor concentration and baroreceptor operation point. Consequently, sympathetic neuron activation returns to original level. The research of Holtzman *et al.* (1986) investigated the effect of daily atenolol administration for hypertensive patients. It was found that the decrease in the blood pressure is 10.2 mmHg (Holtzman *et al.*, 1986), which is 9 mmHg in our simulation.

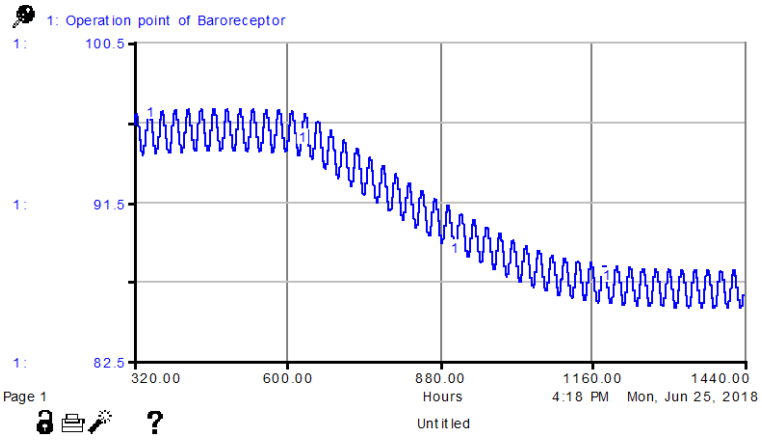

Figure 7.30. Dynamics of Baroreceptor operation point with the daily usage of atenolol starting on 25th day at 11:00 pm.

In Figure 7.30 the decrease in daily mean arterial blood pressure, thanks to atenolol usage, leads to decrease baroreceptor operation from 96 mmHg to 87 mmHg. In turn, the decrease in baroreceptor operation point narrows the range between minimum and maximum values of blood pressure during a day, which can be seen in Figure 7.29.

7.2.1.1.Different Usage Times of Atenolol. Different usage times of atenolol blocker change the effectiveness of blood pressure regulation. Some researchers claim that beta-blocker usage before sleep results better improvement in blood pressure regulation, whereas the others claim the usage when patients wake up. Simulation results show that the latter leads to better treatment of high blood pressure in the long term. It is aroused curiosity about how the usage times of beta-blockers affect the dynamics of related variables. Thereby, two different usage times of atenolol will be compared. The first one will be the atenolol administration at the 11:00 PM before the bedtime, and the other one will be at the 9 AM after a patient wakes up.

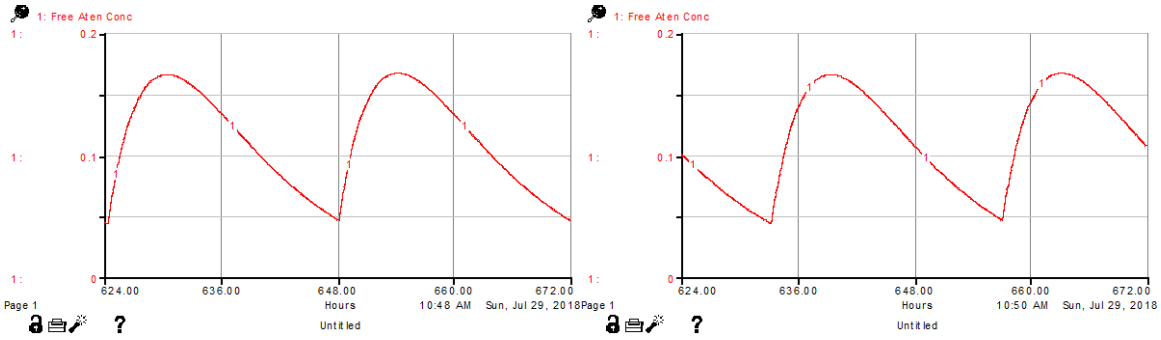

Figure 7.31. Dynamics of Free Atenolol Concentration with the daily usage of atenolol at 11:00 pm (right) or at 09:00 am (left) between 2nd and 4th days after its first usage

Simulation results show that after the usage of oral tablet of atenolol, free atenolol concentration reaches its peak level 0.16 mg/l with 6 hours delay. Similarly, Holtzman *Et al.* (1986) claimed that the peak atenolol concentration is seen 6 hours after atenolol administration.

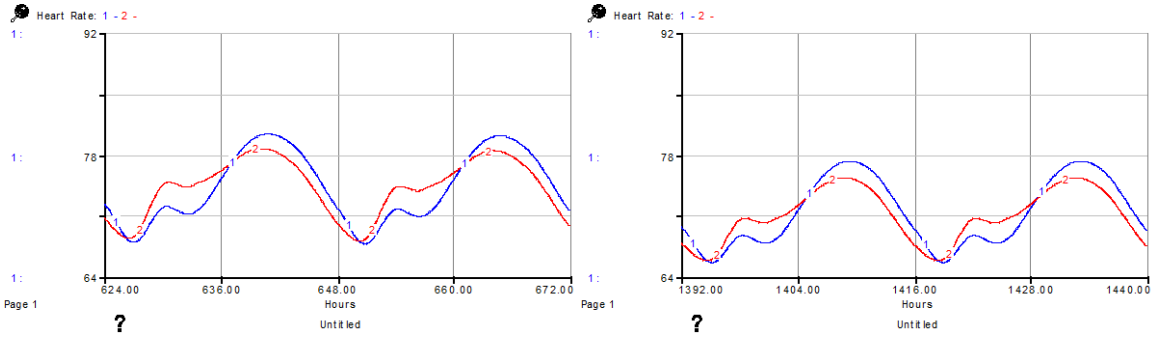

Figure 7.32. Dynamics Heart Rate between 2nd-4th days after its first usage (left), last two days (right). 1st line 11:00 pm usage of atenolol; 2nd line 09:00 am usage of atenolol

First line in Figure 7.32 represents atenolol administration at 11:00 PM, whereas the second line represents the atenolol administration at 09:00 AM. Different free atenolol concentrations throughout a day lead to different heart rate dynamics. The peak atenolol concentration is seen between 03:00 and 07:00 AM when the atenolol is administrated at 11:00 PM. Thereby, the heart rate value is lower between 03:00 and 07:00 AM compared to administration at 09:00 AM. It must be noted that in each scenario, the levels of heart rate are decreased throughout simulation.

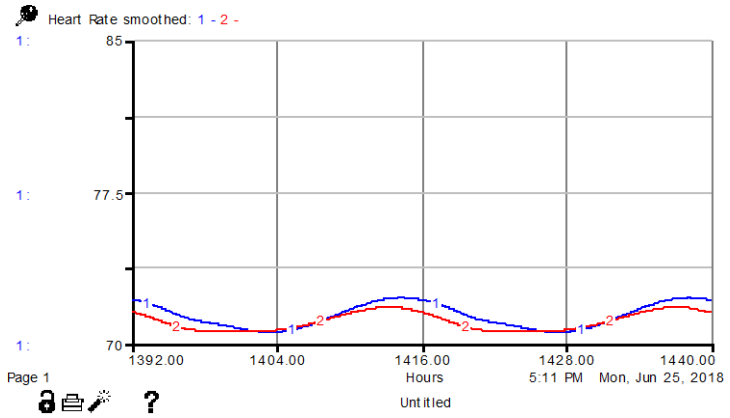

Figure 7.33. Smoothed Heart Rate with the daily usage of atenolol

1st line 11:00 pm usage of atenolol; 2nd line 09:00 am usage of atenolol

Smoothed heart rate is used to represent the daily average of heart rate. In the long run, the smoothed heart rate varies in a narrower range under atenolol administration at 09:00 AM. Also, the level of smoothed heart rate is lower under atenolol administration at 09:00 AM. Thereby, the work output of heart is decreased more with atenolol administration at 09:00 AM.

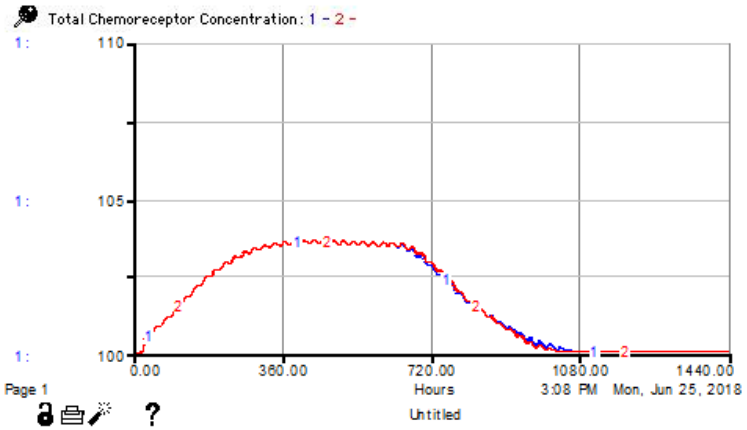

Figure 7.34. Dynamics of Chemoreceptor concentration with the daily usage of atenolol

1st line 11:00 pm usage of atenolol; 2nd line 09:00 am usage of atenolol

The chemoreceptor concentration returns to its original level in either case in a very short time interval (nearly 20 days). It may does not sound intuitive at first, but don't forget that the beta-blocker medication starts before the patients have hypertension (mean arterial blood pressure is lower than 113). In figure 7.32, we showed that heart rate sharply decreased at the start of medication, so oxygen supply demand ratio is increased suddenly. As a result, chemoreceptor concentration returns to original level quickly.

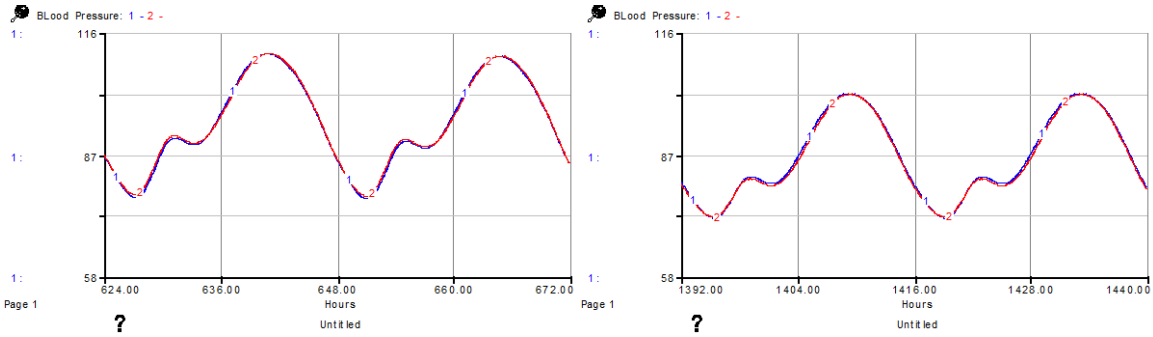

Figure 7.35. Blood Pressure Dynamics with the daily usage of atenolol between 2nd-4th days (left), last two days (right) after its first usage. 1st line 11:00 pm usage of atenolol; 2nd line 09:00 am usage of atenolol

The left graph in Figure 7.35 shows that one administration time does not lead to lower blood pressure compared to the other one throughout a day in short term. Yet, in the long run, atenolol administration at 09:00 AM results lower blood pressure throughout a day, compared to atenolol administration at 11:00 PM.

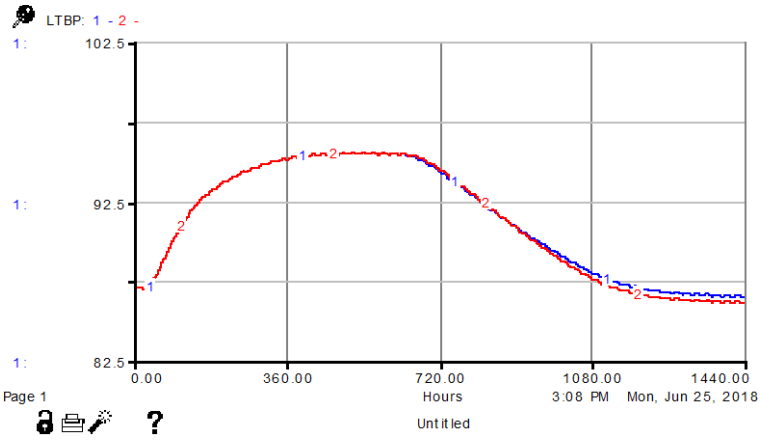

Figure 7.36. Dynamics of Long term blood pressure with the daily usage of atenolol

1st line 11:00 pm usage of atenolol; 2nd line 09:00 am usage of atenolol

Dynamics of daily average blood pressure in Figure 7.36 shows that the better treatment option is daily atenolol usage at the 09:00 AM. Daily usage at the 09:00 AM decreases mean arterial blood pressure to 86.04 mmHg, whereas the usage at the 11:00 PM decreases to 86.45 mmHg. Also, Figure 7.33 shows that the smoothed heart rate is decreased more at 09:00 AM usage. Eventually, the oxygen consumption of tissues becomes lower at 09:00 AM usage. So, the simulation results show that the atenolol administration at 09:00 AM is more effective treatment method compared to atenolol administration at 11:00 PM.

7.2.2. Alpha Blocker Prozasin

The aim of Prozasin administration is to decrease the increased blood pressure due to sleep apnea disorder. Alpha-blockers occupy alpha 1 receptor, which prevents norepinephrine to create possible complex. The prevention way is to competitively occupy alpha 1 receptor. So, alpha-blocker usage decreases the possible number of available alpha-receptors. Thereby, same amount of norepinephrine occupies less receptor due to competitiveness of the alpha-blocker. As a result, less alpha1 receptor occupancy of norepinephrine results in less vasoconstriction of the arterioles. In this way, the blood pressure is decreased.

The researches show that alpha-blocker administration had been pretty popular up to 1980’s compared to beta-blockers. Nowadays, it has been surfaced that alpha-blocker administration might lead to further complications in blood pressure regulation. The short-term risks are dizziness, fatigue and postural hypotension that are related with sudden decrease in blood pressure (Colucci, 1982).

Past research shows that administration time is more crucial for alpha-blocker due to its side effects in terms of hemodynamic variables and blood pressure. One of the side effects is irregular heartbeat that can even lead to tachycardia (heart beats faster than normal). Similarly, Wilson S. Colucci (1982) claimed that the medication might lead to further sympathetic neuron activation. Moreover, antihypertensive treatment effect of prozasin can be attenuated by increase in heart rate and further sympathetic neuron activation.

In this case,0.5 mg Prozasin is daily administrated at 11:00 PM starting on 25th day. Prozasin is selected as an alpha-blocker because of its selective effect on alpha 1 receptor. Also, prozasin is one of the most popular alpha1 blocker in the pharmaceutical industry.

Before scenario analysis, it is necessary to check that the daily prozasin usage shouldn't increase *free prozasin* and *plasma protein bound prozasin concentrat*ions progressively. Also, free prozasin and plasma protein bound prozasin concentrations should reach zero after a time, if prozasin tablet is used once. These conditions are satisfied that can be seen in Figure 7.37 and 7.38.

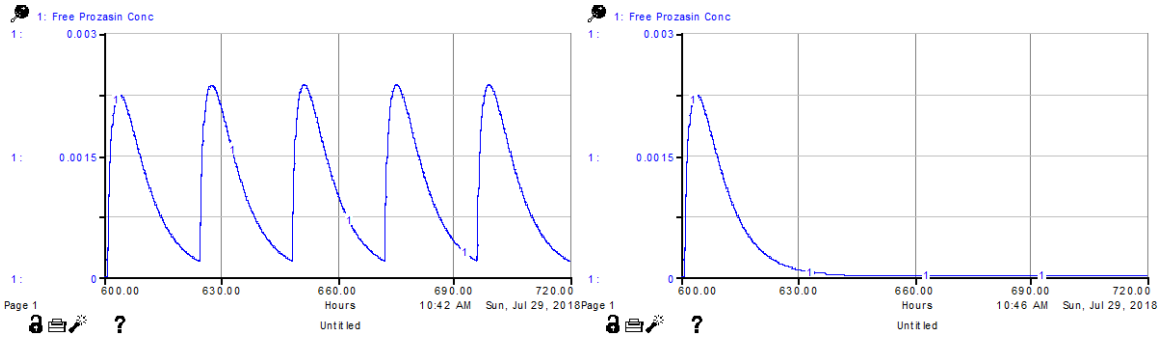

Figure 7.37. Free Prozasin concentration: when Prozasin tablet is used each day (left), when Prozasin tablet is used once (right).

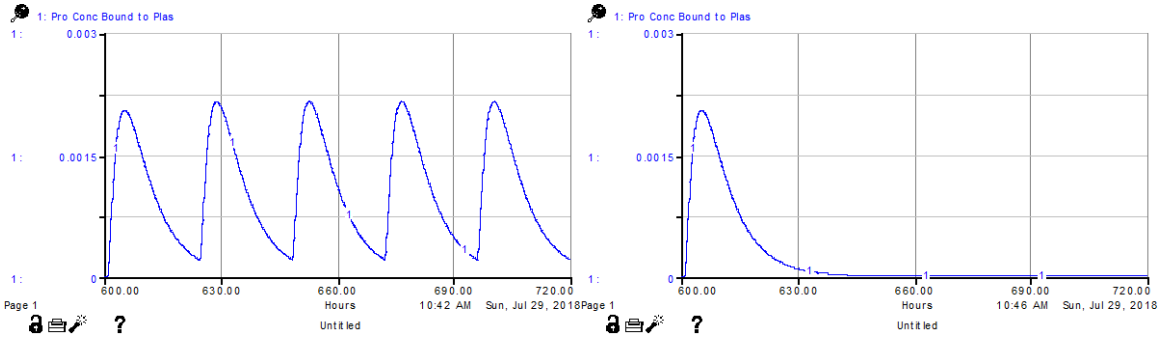

Figure 7.38. Plasma protein bound Prozasin concentration: when Prozasin tablet is used each day (left), when Prozasin tablet is used once (Right)

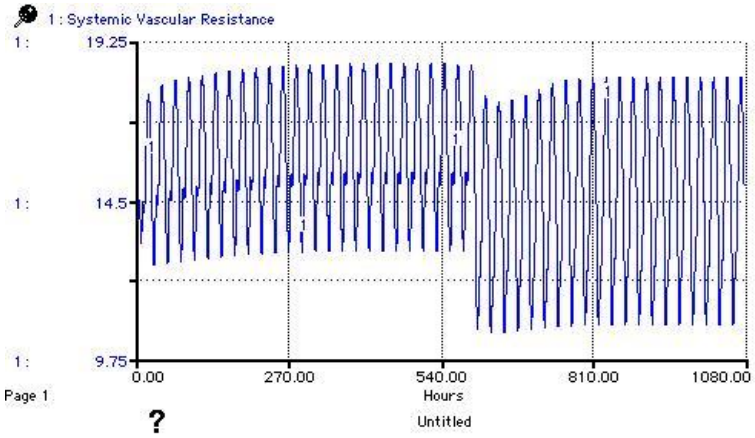

Figure 7.39. Dynamics of Systemic vascular resistance with the daily usage of Prozasin at 11:00 pm starting on 25th day

The daily prozasin administration at 11:00 PM decreases minimum systemic vascular resistance (SVR) from 12.96 to 10.61 HRU/Wood, whereas the maximum SVR is decreased from 18.53 from 18.03 HRU/Wood throughout simulation (see Figure 7.39). The difference between the decrease amounts in the minimum and the maximum points throughout a day is related with Prozasin administration time. Moreover, the administration of Prozasin leads to sudden decrease in systemic vascular resistance. Subsequent to this sudden decrease, the level of systemic vascular resistance is increased (see Figure 7.39).

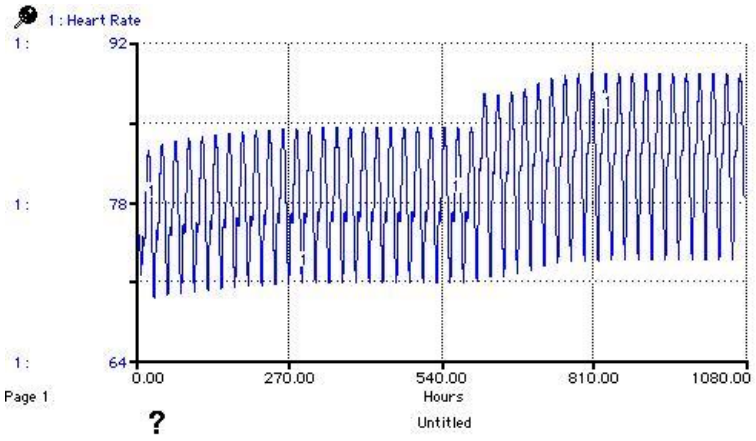

Figure 7.40. Dynamics of Heart Rate with the daily usage of Prozasin at 11:00 pm starting on 25th day

It was expected that the Prozasin administration would lead irregular and increased heartbeat due to its side effects. The daily heartbeat level is increased from 73.9 to 81.08 beats/min after the Prozasin administration. The increase in heart rate causes an increase in work output of the heart. Thereby, oxygen consumption of the heart tissues is increased too. Consequently, over sympathetic neuron activation due to sleep apnea disorder is increased additionally by daily prozasin administration.

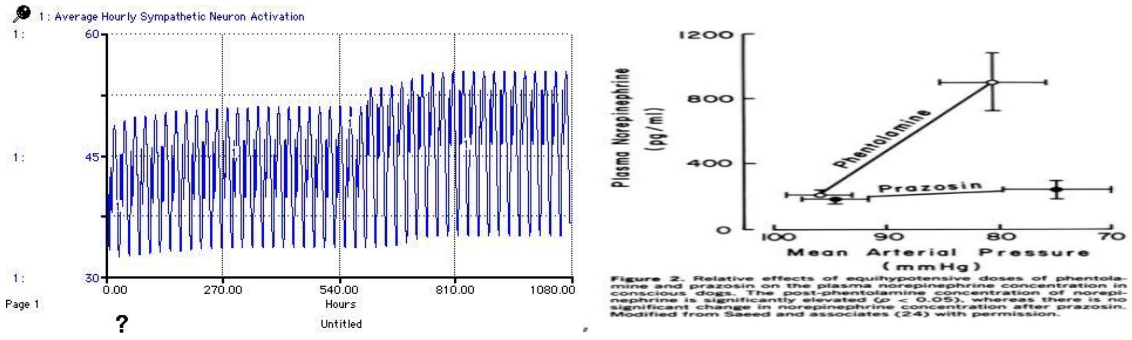

Figure 7.41. Sympathetic Neuron Activation Dynamics with the daily usage of Prozasin at 11:00 pm starting on 25th day (left); Norepinephrine versus Blood pressure data from the experiments made on dogs by Colucci (1982) (right)

Before Prozasin administration daily average sympathetic neuron activation is approximately 42.5 burst/min. Prozasin administration progressively increases daily average SNA to 50 burst/min (see graph at left in Figure 7.41). Graph at right in Figure 7.41 is taken from the research of Colucci (1982). In his experiment made on dogs, the prozasin administration leads to decrease in blood pressure and simultaneously, an increase in the sympathetic stimulation related hormones, consistent with our simulation results.

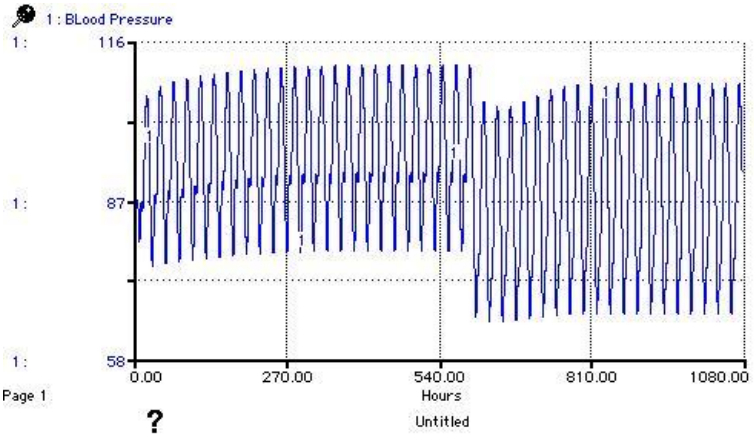

Figure 7.42. Blood Pressure Dynamics with the daily usage of Prozasin at 11:00 pm starting on 25th day

Initially, Prozasin administration decreases the resistance, which is increased due to sleep apnea disorder. Thereby, blood pressure is decreased immediately. Yet, the sudden

decrease in blood pressure is not permanent. Colucci (1982) and Elkayam *et al.* (1979) claimed that the decrease in blood pressure is attenuated by the increase in the sympathetic neuron activation during the treatment. The additional increase in sympathetic neuron activation, which is already excessive, leads to an increase in adrenergic hormone levels. The increase in adrenergic hormone level may attenuate the effect of Prozasin on blood pressure, as shown in Figure 7.42.

7.2.2.1.Different Usage Times of Prozasin. In this subsection, different Prozasin administration times are compared. First line in Figure 7.43 represents Prozasin administration at 11:00 PM, whereas the second line represents the Prozasin administration at 09:00 AM.

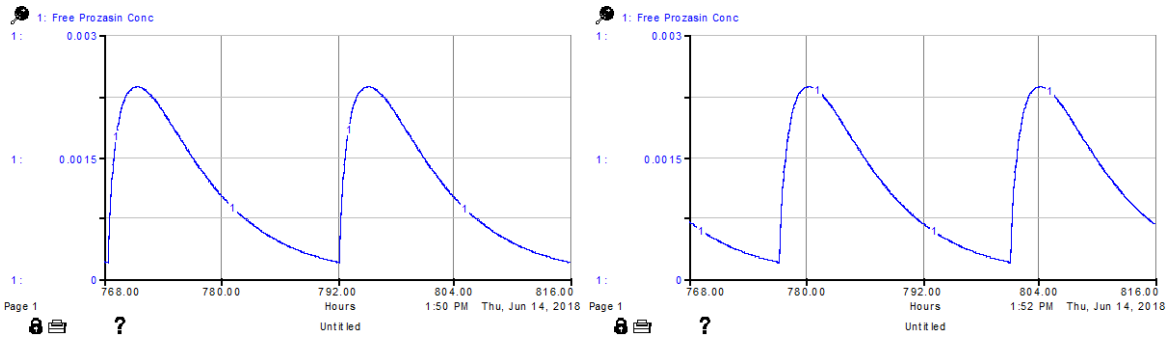

Figure 7.43. Free Prozasin concentration with the daily usage of alpha-blocker at 11:00 pm (right) or at 09:00 am (left)

Simulation results show that after the 0.5 mg tablet prozasin administration, free prozasin concentration reaches its peak level 0.0024 mg/l. Prozasin takes about 3 hours to reach peak level in the blood, whereas atenolol takes about 6 hours.

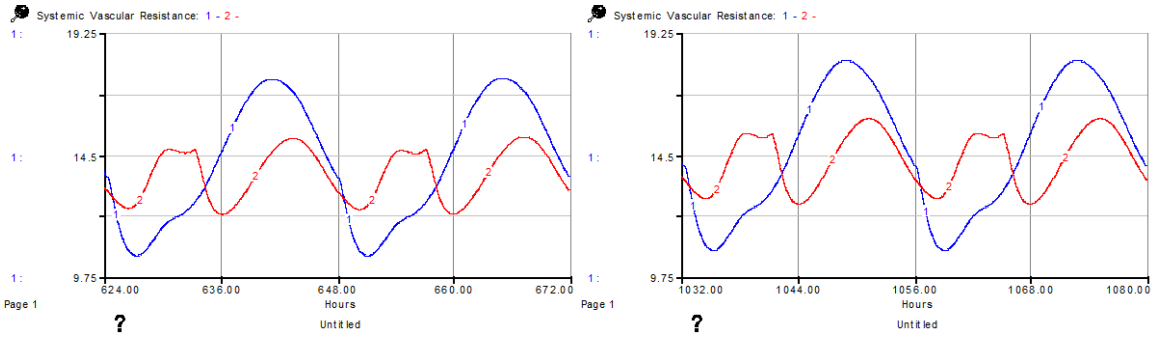

Figure 7.44. Systemic Vascular Resistance with the daily usage of Prozasin between 2nd and 4th days (left), last two days (right) after its first usage (1st line 11:00 pm usage of Prozasin, 2nd line 09:00 am usage of Prozasin)

The different Prozasin administration times may change the dynamic behavior of systemic vascular resistance. The first simulation result (blue line) represents prozasin administration at 11:00 PM in Figure 7.44. Prozasin administration increases the difference between minimum and maximum values of systemic vascular resistance throughout a day, rather than changing the dynamic behavior. The comparison between the left and right graph in Figure 7.44 shows that the decreasing effect of prozasin on systemic vascular resistance is attenuated during the treatment.

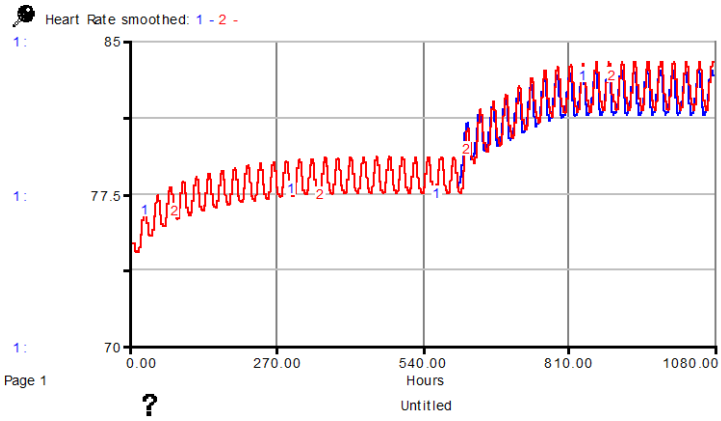

Figure 7.45. Dynamics of Average Heart Rate with the daily usage of Prozasin (1st line 11:00 pm usage of Prozasin, 2nd line 09:00 am usage of Prozasin)

Figure 7.45 shows that smoothed heart rate level is increased during treatment. The Prozasin administration at 09:00 AM leads to slightly higher smoothed heart rate compared to Prozasin administration at 11:00 PM. Poliner *et al.* (1979) found that the increase in the heart rate is 12.56 percent after the prozasin administration, whereas Parmley (1981) found that the increase in the heart rate is 9.47 percent. The simulation results in Figure 7.45 shows that the increase in smoothed heart rate is 5.9 percent (from 78.3 to 82.88 beats/min).

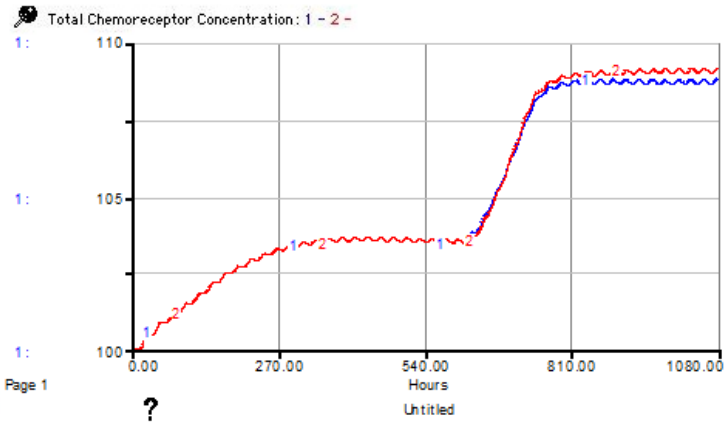

Figure 7.46. Long-Term Dynamics of Total Chemoreceptor concentration with the daily usage of Prozasin starting on 25th day. (1st line 11:00 pm usage of Prozasin, 2nd line 09:00 am usage of Prozasin)

Figure 7.46 shows that total chemoreceptor concentration is increased throughout the simulation for each scenario. The chemoreceptor concentration is increased from 103.53 to 109.03 for the usage at the 09:00 AM and to 108.72 for the usage at 11:00 PM. As a remainder, Prozasin usage decreases blood pressure immediately, but it leads to further increase in the SNA.

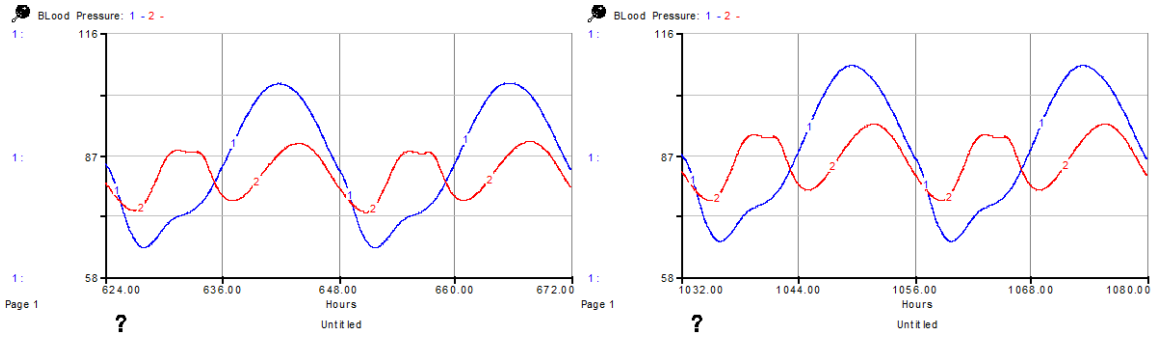

Figure 7.47. Blood Pressure Dynamics with the daily usage of Prozasin first two days (left), last two days (right) after its first usage

(1st line 11:00 pm usage of Prozasin, 2nd line 09:00 am usage of Prozasin)

The graph at right in Figure 7.47 shows that the minimum and maximum blood pressure values throughout a day is 64.67 and 104.07 mmHg respectively when Prozasin is administrated at 11:00 PM. The Prozasin administration at 09:00 AM changes dynamic behavior of blood pressure and leads to hypotension between 12:00 AM and 03:00 PM. The minimum and maximum points are 73.51 and 89.08 mmHg when Prozasin is administrated at 09:00 AM.

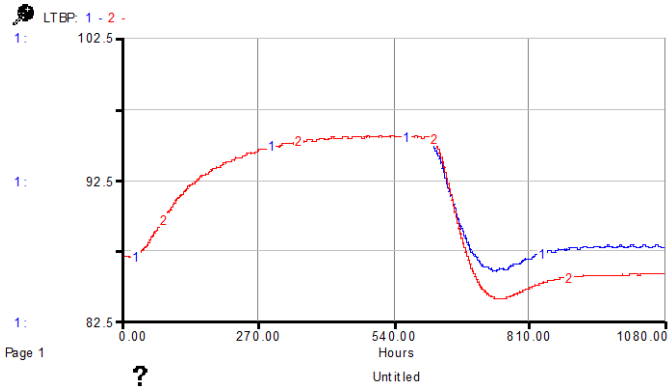

Figure 7.48. Long-term average Blood Pressure with the daily usage of Prozasin starting on 30th day. (1st line 11:00 pm usage of Prozasin, 2nd line 09:00 am usage of Prozasin)

We saw in previous section that atenolol administration leads to progressive decrease in chemoreceptor concentration and SNA. Thereby, the atenolol administration leads to

progressive decrease in the blood pressure. Yet, Prozasin administration leads to an additional increase in total chemoreceptor concentration and SNA, which are already increased by sleep apnea disorder. Figure 7.48 shows that rather than progressive decrease in the blood pressure, prozasin administration leads to sudden decrease in blood pressure. Due to further increase in SNA after prozasin administration, average long-term blood pressure (LTBP) is slightly increased as a result of the sudden decrease in the long run. The average long-term blood pressure is 85.72 mmHg with prozasin administration at the 09:00 AM. The average long-term blood is 87.65 mmHg with prozasin administration at 11:00 PM. Simulation results show that the Prozasin administration at 09:00 AM leads to further decrease in average LTBP compared to 11:00 AM.

8. CONCLUSION

In this study, a model for the blood pressure regulation system is constructed. The blood pressure is the most important factor to transport main nutrients to tissues and to clear waste products of tissues. Hypertension is a common disorder due to problems in blood pressure regulation system. The first aim of the model is to understand and show behaviors of important hemodynamic variables in the blood pressure regulation system. Under pathological circumstances, the model should be able to show unique dynamic behaviors of the important variables in blood pressure regulation system. Thereby, different scenarios can be simulated and analyzed without necessity of human body.

In model validation part, the structural and behavioral tests have been applied. The model is structurally tested with an initial change in the values of some hemodynamic variables. Firstly, the initial values of heart rate and diameter are changed one by one. It was shown that all variables return to their equilibrium values. Secondly, desired sympathetic neuron activation is doubled for an hour. Also, desired sympathetic neuron activation is set to zero for an hour. The tests showed that the values of important variables reached equilibrium values. The dynamic behaviors of important variables produced by model are compared with real life dynamic behaviors of these variables to validate our model. The resulted dynamic behaviors are consistent with the data in related scientific literature.

In the scenario analysis part, the sleep apnea disorder effects on healthy person are examined under different frequencies or intensities or apnea distributions. The increase in the frequencies or intensities of sleep apnea leads to more deterioration in the autonomous nervous signaling system. Similarly, the literature suggests that the extra sympathetic activation is the main reason behind abnormal increase in blood pressure under the sleep apnea disorder. The change in the apnea distribution generated simulated dynamics similar to those suggested by the literature. The last scenario compared the improvement in the regulation of blood pressure, which is disrupted by sleep apnea disorder, under different

blocker drug types and administration times. Beta-blockers progressively prevent the oxygen deficiencies in the tissues caused by the sleep apnea disorder. In this way, the chemoreceptor concentration and sympathetic neuron over-activation is decreased to treat high blood pressure. On the other hand, even though alpha-blockers treat high blood pressure caused by sleep apnea disorder, they lead to more disruption in the autonomous nervous system and further increase in sympathetic neuron activation. The model captures the dynamics of the variables in the blood pressure regulation system under sleep apnea disorder and additionally under the medications, as the literature suggests.

The effects of different blocker administration times (before sleeping or after waking up) are analyzed in our model. Our simulation results indicated that the blocker administration after waking up has better results in terms of daily average blood pressure.

As future direction of study, the high blood pressure-related damage in arteries and its effect on blood pressure regulation might be implemented in the model. Some extensions can also be implemented to analyze other medical interventions. Finally, some of the model parameters can be estimated more precisely with additional quantitative and qualitative real data.

REFERENCES

Abboud, F., & Kumar, R. (2014). Obstructive sleep apnea and insight into mechanisms of sympathetic overactivity. *The Journal of clinical investigation, 124*(4), 1454-1457.

Alarcón, T., Byrne, H. M., & Maini, P. K. (2004). A mathematical model of the effects of hypoxia on the cell-cycle of normal and cancer cells. *Journal of Theoretical Biology, 229*(3), 395–411. https://doi.org/10.1016/j.jtbi.2004.04.016

Albaghdadi, M. (2007). Baroreflex control of long-term arterial pressure. *Rev Bras Hipertens, 14*(4), 212–225.

Amin, R., Somers, V. K., McConnell, K., Willging, P., Myer, C., Sherman, M., … Daniels, S. (2008). Activity-adjusted 24-hour ambulatory blood pressure and cardiac remodeling in children with sleep disordered breathing. *Hypertension, 51*(1), 84–91. https://doi.org/10.1161/HYPERTENSIONAHA.107.099762

Bakris, G., & Sorrentino, M. (2018). Redefining hypertension—assessing the new blood-pressure guidelines. *New England Journal of Medicine, 378*(6), 497-499.

Barlas, Y. (2002). System Dynamics: Systemic Feedback Modeling for Policy Analysis in Knowledge for Sustainable Development–An. *Paris: Oxford*.

Bloch, M. J. (2016). Worldwide prevalence of hypertension exceeds 1.3 billion. *Journal of the American Society of Hypertension: JASH, 10*(10), 753.

Brunton, L. L., Chabner, B. A., & Knollmann, B. C. (2011). *Goodman and Gilman's The Pharmacological Basis of Therapeutics*. *Goodman and Gilman's The Pharmacological Basis of Therapeutics*. 12th ed. McGraw-Hill Co, New York.

Burns, T. W., Langley, P. E., Terry, B. E., Bylund, D. B., Hoffman, B. B., Tharp, M. D., … Fain, J. N. (1981). Pharmacological characterizations of adrenergic receptors in

human adipocytes. *The Journal of Clinical Investigation*, *67*(2), 467–75. https://doi.org/10.1172/JCI110055

Campese, V. M., Ye, S., Zhong, H., Yanamadala, V., Ye, Z., & Chiu, J. (2004). Reactive oxygen species stimulate central and peripheral sympathetic nervous system activity. *American Journal of Physiology-Heart and Circulatory Physiology*, *287*(2), H695–H703. https://doi.org/10.1152/ajpheart.00619.2003

Carl, D., & Sica, D. A. (2007). Obstructive sleep apnea, hypertension, and wakefulness-promoting agents. *Current hypertension reports*, *9*(4), 329-331.

Castorena-Gonzalez, J. A., Staiculescu, M. C., Foote, C., & Martinez-Lemus, L. A. (2014). Mechanisms of the inward remodeling process in resistance vessels: Is the actin cytoskeleton involved *Microcirculation*, *21*(3), 219–229. https://doi.org/10.1111/micc.12105

Chapleau, M. W., Hajduczok, G., & Abboud, F. M. (1989). Peripheral and central mechanisms of baroreflex resetting. *Clinical and Experimental Pharmacology & Physiology. Supplement*, *15*(1 989), 31–43. https://doi.org/10.1007/s00028-010-0082-y

Charkoudian, N., & Rabbitts, J. A. (2009). Sympathetic neural mechanisms in human cardiovascular health and disease. *Mayo Clinic Proceedings*, *84*(9), 822–830. https://doi.org/10.4065/84.9.822

Chatterjee, K., & Rouleau, J. L. (1981). Hemodynamic and metabolic effects of vasodilators, nitrates, hydralazine, prazosin and captopril in chronic ischemic heart failure. *Journal of Internal Medicine*, *210*(S651), 295-303.

Cheng, L., Ivanova, O., Fan, H. H., & Khoo, M. C. K. (2010). An integrative model of respiratory and cardiovascular control in sleep-disordered breathing. *Respiratory Physiology and Neurobiology*, *174*(1–2), 4–28. https://doi.org/10.1016/j.resp.2010.06.001

Clark, A. J. (1933). *Mode of action of drugs on cells*. Edward Arnold: London.

Clark, M. A., Finkel, R., Rey, J. A., & Whalen, K. (2012). *Lippincott's illustrated reviews: Pharmacology* (Vol. 526, pp. 530-541). Philadelphia: Wolters Kluwer.

Clutter, W. E., Bier, D. M., Shah, S. D., & Cryer, P. E. (1980). Epinephrine plasma metabolic clearance rates and physiologic thresholds for metabolic and hemodynamic actions in man. *Journal of Clinical Investigation*, *66*(1), 94–101. https://doi.org/10.1172/JCI109840

Colucci, W. S. (1982). Alpha-adrenergic receptor blockade with prazosin: consideration of hypertension, heart failure, and potential new applications. *Annals of internal medicine*, *97*(1), 67-77.

Colucci, W. S., Williams, G. H., & Braunwald, E. (1981). Clinical, hemodynamic, and neuroendocrine effects of chronic prazosin therapy for congestive heart failure. *Am Heart J*, *102*(3 Pt 2), 615–621. http://www.ncbi.nlm.nih.gov/pubmed/6115578, accessed in May 2019.

Costa, K. M., Accorsi-Mendonça, D., Moraes, D. J., & Machado, B. H. (2014). Evolution and physiology of neural oxygen sensing. *Frontiers in physiology*, *5*, 302.

Crinion, S. J., Ryan, S., & McNicholas, W. T. (2017). Obstructive sleep apnoea as a cause of nocturnal nondipping blood pressure: recent evidence regarding clinical importance and underlying mechanisms. *The European respiratory journal*, *49* (1).

Csordás, G., & Hajnóczky, G. (2009). SR/ER–mitochondrial local communication: calcium and ROS. *Biochimica et Biophysica Acta (BBA)-Bioenergetics*, *1787*(11), 1352-1362.

Cugini, P., Palma, L. Di, Simone, S. Di, Lucia, P., Battisti, P., Coppola, A., & Leone, G. (1993). Circadian rhythm of cardiac output, peripheral vascular resistance, and

related variables by a beat-to-beat monitoring. *Chronobiology International*, *10*(1), 73–78. https://doi.org/10.3109/07420529309064484

Cutler, M. J., Hamdan, A.-L., Hamdan, M. H., Ramaswamy, K., & Smith, M. L. (2002). Sleep apnea: from the nose to the heart. *The Journal of the American Board of Family Practice / American Board of Family Practice*, *15*(2), 128–141.

Dharmashankar, K., & Widlansky, M. E. (2010). Vascular endothelial function and hypertension: Insights and directions. *Current Hypertension Reports*, *12*(6), 448–455. https://doi.org/10.1007/s11906-010-0150-2

Daugherty, S. L., Powers, J. D., Magid, D. J., Tavel, H. M., Masoudi, F. A., Margolis, K. L., ... & Ho, P. M. (2012). Incidence and prognosis of resistant hypertension in hypertensive patients. *Circulation*, *125*(13), 1635-1642.

Dicarlo, S. E., & Bishop, V. S. (2001). Central baroreflex resetting as a means of increasing and decreasing sympathetic outflow and arterial pressure. *Annals of the New York Academy of Sciences*, *940*(1), 324-337.

Dictionary, A. H. (2007). The American Heritage Medical Dictionary.

Dopp, J. M., Reichmuth, K. J., & Morgan, B. J. (2007). Obstructive sleep apnea and hypertension: mechanisms, evaluation, and management. *Current hypertension reports*, *9*(6), 529.

Drager, L. F., Pereira, A. C., Barreto-Filho, J. A., Figueiredo, A. C., Krieger, J. E., Krieger, E. M., & Lorenzi-Filho, G. (2006). Phenotypic characteristics associated with hypertension in patients with obstructive sleep apnea. *Journal of Human Hypertension*, *20*(7), 523–528. https://doi.org/10.1038/sj.jhh.1002012

Elkayam, U., Lejemtel, T., Mathur, M., Ribner, H., Frishman, W., Strom, J., & Sonnenblick, E. (1979). Marked early attenuation of hemodynamic effects of oral prazosin therapy in chronic congestive heart failure. *American Journal of Cardiology*, *44*(September), 540–545.

Emdin, M., Mirizzi, G., Giannoni, A., Poletti, R., Iudice, G., Bramanti, F., & Passino, C. (2017). Prognostic significance of central apneas throughout a 24-hour period in patients with heart failure. *Journal of the American College of Cardiology*, *70*(11), 1351-1364.

Esler, M., Jackman, G., Bobik, A., Leonard, P., Kelleher, D. I. A. N. N. E., Skews, H., ... & Korner, P. (1981). Norepinephrine kinetics in essential hypertension. Defective neuronal uptake of norepinephrine in some patients. *Hypertension*, *3*(2), 149-156.

Fantini, S. (2014). Dynamic model for the tissue concentration and oxygen saturation of hemoglobin in relation to blood volume, flow velocity, and oxygen consumption: Implications for functional neuroimaging and coherent hemodynamics spectroscopy (CHS). *NeuroImage*, *85*, 202–221. https://doi.org/10.1016/j.neuroimage.2013.03.065

Fisher, D. A. (Ed.). (1998). *Endocrinology: test selection and interpretation*. Quest Diagnostics Incorporated.

Friedman, O., & Logan, A. G. (2009). Sympathoadrenal mechanisms in the pathogenesis of sleep apnea-related hypertension. *Current hypertension reports*, *11*(3), 212-216.

Frigy, A., & Kocsis, I. (2018). Hypertension and Sleep Apnea. In *Blood Pressure-From Bench to Bed*. Aise Seda Artis, IntechOpen, https://www.intechopen.com/books/blood-pressure-from-bench-to-bed/hypertension-and-sleep-apnea, accessed in May 2019.

Gao, L., Laude, K., & Cai, H. (2008). Mitochondrial Pathophysiology, Reactive Oxygen Species, and Cardiovascular Diseases. *Veterinary Clinics of North America - Small Animal Practice*, *38*(1), 137–155. https://doi.org/10.1016/j.cvsm.2007.10.004

Goldstein, D. S. (1983). Plasma catecholamines and essential hypertension. An analytical review. *Hypertension*, *5*(1), 86–99. https://doi.org/10.1161/01.HYP.5.1.86

Gorlach, A., Bertram, K., Hudecova, S., & Krizanova, O. (2015). Calcium and ROS: A mutual interplay. *Redox Biology*, *6*, 260–271. https://doi.org/10.1016/j.redox.2015.08.010

Goto, J. J., Gralla, E. B., Valentine, J. S., & Cabelli, D. E. (1998). Reactions of hydrogen peroxide with familial amyotrophic lateral sclerosis mutant human copper-zinc superoxide dismutases studied by pulse radiolysis. *Journal of Biological Chemistry*, *273*(46), 30104–30109.

Goya, T. T., Silva, R. F., Guerra, R. S., Lima, M. F., Barbosa, E. R. F., Cunha, P. J., … Ueno-Pardi, L. M. (2016). Increased Muscle Sympathetic Nerve Activity and Impaired Executive Performance Capacity in Obstructive Sleep Apnea. *Sleep*, *39*(1), 25–33. https://doi.org/10.5665/sleep.5310

Grassi, G. (2010). Sympathetic neural activity in hypertension and related diseases. *American Journal of Hypertension*, *23*(10), 1052–1060. https://doi.org/10.1038/ajh.2010.154

Guyton, A., & Hall, J. (2006). Textbook of medical physiology 11th edition Elsevier Saunders Inc. *Philadelphia PA*.

Hansen, J., & Sander, M. (2003). Sympathetic neural overactivity in healty humans after prolonged exposure to hypobaric hypoxia. *Journal of Physiology*, *546*(3), 921–929. https://doi.org/10.1113/jphysiol.2002.031765

Hasking, G. J., Esler, M. D., Jennings, G. L., Dewar, E., & Lambert, G. (1988). Norepinephrine spillover to plasma during steady-state supine bicycle exercise. Comparison of patients with congestive heart failure and normal subjects. *Circulation*, *78*(3 I), 516–521. https://doi.org/10.1161/01.CIR.78.3.516

Heuser, R. R., Schlaich, M., & Sievert, H. (Eds.). (2014). *Renal denervation: a new approach to treatment of resistant hypertension*. Springer.

Hill, A. V. (1909). The mode of action of nicotine and curari, determined by the form of the contraction curve and the method of temperature coefficients. *The Journal of physiology*, *39*(5), 361-373.

Hoffmann, C., Leitz, M. R., Oberdorf-Maass, S., Lohse, M. J., & Klotz, K. N. (2004). Comparative pharmacology of human β-adrenergic receptor subtypes—characterization of stably transfected receptors in CHO cells. *Naunyn-Schmiedeberg's archives of pharmacology*, *369*(2), 151-159.

Holtzman, J. L., Finley, D., Johnson, B., Berry, D. A., & Sirgo, M. A. (1986). The effects of single-dose atenolol, labetalol, and propranolol on cardiac and vascular function. *Clinical Pharmacology and Therapeutics*, *40*(3), 268–273. https://doi.org/10.1038/clpt.1986.174

Iftikhar, I. H., Valentine, C. W., Bittencourt, L. R., Cohen, D. L., Fedson, A. C., Gíslason, T., ... & Magalang, U. J. (2014). Effects of continuous positive airway pressure on blood pressure in patients with resistant hypertension and obstructive sleep apnea: a meta-analysis. *Journal of hypertension*, *32* (12), 2341. https://doi.org/10.1097/HJH.0000000000000372

Imperial E.S., Levy M.N., & Zieske H. (1961). Outflow Resistance as an Independent Determinant of Cardiac Performance. *Circulation Research*, *9*(6).

Kanagy, N. L. (2009). Vascular effects of intermittent hypoxia. *Ilar.J*, *50*(3), 282–288.

Karunajeewa, A. S., Abeyratne, U. R., Rathnayake, S. I., & Swarnkar, V. (2006, August). Dynamic data analysis in obstructive sleep apnea. In *Engineering in Medicine and Biology Society, 2006. EMBS'06. 28th Annual International Conference of the IEEE* (pp. 4510-4513). IEEE.

Katzung, B. G., & Trevor, A. J. (2015). Basic and clinical pharmacology 13th edition.Mc Graw Hill.

Kenakin, T. (2004). Principles: Receptor theory in pharmacology. *Trends in Pharmacological Sciences*, *25*(4), 186–192. https://doi.org/10.1016/j.tips.2004.02.012

Khan, S. A., Nanduri, J., Yuan, G., Kinsman, B., Kumar, G. K., Joseph, J., … Prabhakar, N. R. (2011). NADPH Oxidase 2 Mediates Intermittent Hypoxia-Induced Mitochondrial Complex I Inhibition: Relevance to Blood Pressure Changes in Rats. *Antioxidants & Redox Signaling*, *14*(4), 533–542. https://doi.org/10.1089/ars.2010.3213

Khoo, M. C. (1990). A model-based evaluation of the single-breath CO2 ventilatory response test. *Journal of Applied Physiology*, *68*(1), 393–399. https://doi.org/10.1152/jappl.1990.68.1.393

Klabunde, R. E. (2004). Cardiovascular Physiology Concepts. *Lippincott Williams & Wilkins*, 256. https://doi.org/citeulike-article-id:2086320

Koeners, M. P., Lewis, K. E., Ford, A. P., & Paton, J. F. (2016). Hypertension: a problem of organ blood flow supply–demand mismatch. *Future cardiology*, *12*(3), 339-349.

Konecny, T., Kara, T., & Somers, V. K. (2014). Obstructive sleep apnea and hypertension: an update. *Hypertension*, *63*(2), 203-209.

Koroboki, E., Manios, E., Psaltopoulou, T., Vemmos, K., Michas, F., Alexaki, E., & Zakopoulos, N. (2012). Original Research Circadian Variation of Blood Pressure and Heart Rate in Normotensives, White-Coat, Masked, Treated and Untreated Hypertensives. *Hellenic Journal of Cardiology*, *7*, 432–438.

Krieger, E. M. (1988). Mechanisms of Complete Baroreceptor Resetting in Hypertension. *Drugs*, *35*(6), 98–103. https://doi.org/10.2165/00003495-198800356-00014

Kuri, B. a. (2010). Regulation of Catecholamine Release From the Adrenal Medulla Under the Physiological Stress Response By, (January).Case Western Reserve University.

La Rovere, M. T., Pinna, G. D., & Raczak, G. (2008). Baroreflex sensitivity: measurement and clinical implications. *Annals of Noninvasive Electrocardiology, 13*(2), 191-207.

Lagerholm, B. C., & Thompson, N. L. (1998). Theory for ligand rebinding at cell membrane surfaces. *Biophysical Journal*, *74*(3), 1215–1228. https://doi.org/10.1016/S0006-3495(98)77836-1

Lahiri, S., Cherniak, N. S., & Fitzgerald, R. S. (Eds.). (2013). *Response and Adaptation to Hypoxia: Organ to Organelle*. Springer.

Lambert, E. A., Chatzivlastou, K., Schlaich, M., Lambert, G., & Head, G. A. (2014). Morning surge in blood pressure is associated with reactivity of the sympathetic nervous system. *American Journal of Hypertension*, *27*(6), 783–792. https://doi.org/10.1093/ajh/hpt273

Langley, J. N. (1905). On the reaction of cells and of nerve-endings to certain poisons, chiefly as regards the reaction of striated muscle to nicotine and to curari. *The Journal of physiology*, *33*(4-5), 374-413.

Larochelle, P., du Souich, P., Hamet, P., Larocque, P., & Armstrong, J. (1982). Prazosin plasma concentration and blood pressure reduction. *Hypertension*, *4*(1), 93–101.

Lattimore, J. D. L., Celermajer, D. S., & Wilcox, I. (2003). Obstructive sleep apnea and cardiovascular disease. *Journal of the American College of Cardiology*, *41*(9), 1429–1437. https://doi.org/10.1016/S0735-1097(03)00184-0

Lavie, P., Silverberg, D., Oksenberg, A., & Hoffstein, V. (2001). Obstructive sleep apnea and hypertension: From correlative to causative relationship. *Journal of Clinical Hypertension*, *3*(5), 296–301. https://doi.org/10.1111/j.1524-6175.2001.00491.x

LiDCO. (2011). Normal hemodynamic parameters. *Clinical Information*, 1–2. http://www.lidco.com/html/clinical/nhp.asp. accessed in May, 2019.

Linsell, C. R., Lightman, S. L., Mullen, P. E., Brown, M. J., & Causon, R. C. (1985). Circadian rhythms of epinephrine and norepinephrine in man. *Journal of Clinical Endocrinology and Metabolism*, *60*(6), 1210–1215. https://doi.org/10.1210/jcem-60-6-1210.

Lohmeier, T. E., Iliescu, R., Dwyer, T. M., Irwin, E. D., Cates, A. W., & Rossing, M. A. (2010). Sustained suppression of sympathetic activity and arterial pressure during chronic activation of the carotid baroreflex. *AJP: Heart and Circulatory Physiology*, *299*(2), H402–H409. https://doi.org/10.1152/ajpheart.00372.2010

López-Barneo, J., Ortega-Sáenz, P., Pardal, R., Pascual, A., Piruat, J. I., Durán, R., & Gómez-Díaz, R. (2009). Oxygen sensing in the carotid body. *Annals of the New York Academy of Sciences*, *1177*, 119–131. https://doi.org/10.1111/j.1749-6632.2009.05033.x

Lund-Johansen, P. (1983). Hemodynamic response: decrease in cardiac output vs reduction in vascular resistance. *Hypertension*, *5*(5 Pt 2), III49-57. http://www.ncbi.nlm.nih.gov/pubmed/6629461, accessed in May 2019.

Magosso, E., & Ursino, M. (2001). A mathematical model of CO2 effect on cardiovascular regulation. *American Journal of Physiology - Heart and Circulatory Physiology*, *281*(5), H2036–H2052. https://doi.org/10.1152/ajpheart.2001.281.5.H2036

Maher, P., & Schubert, D. (2000). Signaling by reactive oxygen species in the nervous system. *Cellular and Molecular Life Sciences CMLS*, *57*(8-9), 1287-1305.

Malpas, S. C. (2010). Sympathetic Nervous System Overactivity and Its Role in the Development of Cardiovascular Disease. Physiology *Reviews*, *90*(2), 513–557. https://doi.org/10.1152/physrev.00007.2009

Mansukhani, M. P., Kara, T., Caples, S. M., & Somers, V. K. (2014). Chemoreflexes, Sleep Apnea, and Sympathetic Dysregulation. *Current Hypertension Reports*, *16*(9), 1–12. https://doi.org/10.1007/s11906-014-0476-2

Martin, E., & Hine, R. (Eds.). (2015). *A dictionary of biology*. Oxford University Press, USA.

Meibohm, B. (Ed.). (2006). *Pharmacokinetics and pharmacodynamics of biotech drugs: principles and case studies in drug development*. John Wiley & Sons.

Michelini, L. C., O'Leary, D. S., Raven, P. B., & Nóbrega, A. C. L. (2015). Neural control of circulation and exercise: a translational approach disclosing interactions between central command, arterial baroreflex, and muscle metaboreflex. *American Journal of Physiology - Heart and Circulatory Physiology*, *309*(3), H381–H392. https://doi.org/10.1152/ajpheart.00077.2015

Monahan, K. D., Leuenberger, U. A., & Ray, C. A. (2006). Effect of repetitive hypoxic apnoeas on baroreflex function in humans. *Journal of Physiology*, *574*(2), 605–613. https://doi.org/10.1113/jphysiol.2006.108977

Motulsky, H., & Neubig, R. (2002). Analyzing radioligand binding data. *Current Protocols in Protein Science / Editorial Board, John E. Coligan ... [et al.]*, *Appendix 3*, Appendix 3H. https://doi.org/10.1002/0471140864.psa03hs21

Muenter Swift, N., Cutler, M. J., Fadel, P. J., Wasmund, W. L., Ogoh, S., Keller, D. M., ... & Smith, M. L. (2003). Carotid baroreflex function during and following voluntary apnea in humans. *American Journal of Physiology-Heart and Circulatory Physiology*, *285*(6), H2411-H2419.

Munch, P. A., Thoren, P. N., & Brown, A. M. (1987). Dual effects of norepinephrine and mechanisms of baroreceptor stimulation. *Circulation research*, *61*(3), 409-419.

Murphy, M. P. (2009). How mitochondria produce reactive oxygen species. *Biochemical Journal*, *417*(1), 1–13. https://doi.org/10.1042/BJ20081386

Narkiewicz, K., van de Borne, P. J. H., Pesek, C. a, Dyken, M. E., Montano, N., & Somers, V. K. (1999). Selective potentiation of peripheral chemorelfex sensitivity in obstructive sleep apnea. *Circulation*, *99*, 1183–1189.

Noble, M. I., Wyler, J., Milne, E. N., Trenchard, D., & Guz, A. (1969). Effect of changes in heart rate on left ventricular performance in conscious dogs. *Circulation Research*, *24*(2), 285–95. http://www.ncbi.nlm.nih.gov/pubmed/5764588, accessed in May 2019.

Noda, A., Yasuma, F., Okada, T., & Yokota, M. (1998). Circadian rhythm of autonomous activity in patients with obstructive sleep apnea syndrome. *Clinical Cardiology*, *21*(4), 271-276.

Okcay, A., Somers, V. K., & Caples, S. M. (2008). Obstructive sleep apnea and hypertension. *The Journal of Clinical Hypertension*, *10*(7), 549-555.

Packer, M., Medina, N., & Yushak, M. (1986). Comparative hemodynamic and clinical effects of long-term treatment with prazosin and captopril for severe chronic congestive heart failure secondary to coronary artery disease or idiopathic dilated cardiomyopathy. *American Journal of Cardiology*, *57*(15), 1323–1327. https://doi.org/10.1016/0002-9149(86)90212-2

Packer, M., Meller, J., Gorlin, R., & Herman, M. V. (1979). Differences in hemodynamic effects of nitroprusside and prazosin in severe chronic congestive heart failure. Evidence for a direct negative chronotropic effect of prazosin. *The American Journal of Cardiology*, *44*(2), 310–317. https://doi.org/10.1016/0002-9149(79)90322-9

Parmley, W. W., Chatterjee, K., Arnold, S., Rubin, S. A., Brundage, B. H., Williams, R. L., ... & Rouleau, J. (1981). Hemodynamic effects of prazosin in chronic heart failure. *American heart journal*, *102*(3), 622-625.

Paton, W. D. (1961). A theory of drug action based on the rate of drug-receptor combination. *Proceedings of the Royal Society of London B: Biological Sciences*, *154*(954), 21-69.

Perkins, J. P. (2012). *The Beta-adrenergic receptors*. Springer Science & Business Media.

Phillips, C., & O'Driscoll. (2013). Hypertension and obstructive sleep apnea. *Nature and Science of Sleep*, *39*(6), 43. https://doi.org/10.2147/NSS.S34841

Pickering, T. G. (2002), Sleep Apnea and Hypertension. The Journal of Clinical Hypertension, 4: 437-440. doi:10.1111/j.1524-6175.2002.01513.x

Pittman, R. N. (2011, April). Regulation of tissue oxygenation. In *Colloquium series on integrated systems physiology: from molecule to function* (Vol. 3, No. 3, pp. 1-100). Morgan & Claypool Life Sciences.

Poliner, L., Twieg, D., Parkey, R., Lewis, S., Dehmer, G., & Willerson, J. T. (1979, January). Radionuclide angiographic and hemodynamic assessment of Prazosin in patients with medically refractory heart-failure. *American Journal of Cardiology 43*, (2), 403-403.

Portaluppi, F., & Smolensky, M. H. (2007). Circadian rhythmic and environmental determinants of 24-hour blood pressure regulation in normal and hypertensive conditions. In *Blood pressure monitoring in cardiovascular medicine and therapeutics*(pp. 135-158). Humana Press.

Prabhakar, N. R., & Semenza, G. L. (2016). Regulation of carotid body oxygen sensing by hypoxia-inducible factors. *Pflügers Archiv-European Journal of Physiology*, *468*(1), 71-75.

Prabhakar, N. R., Kumar, G. K., & Peng, Y.-J. (2012). Sympatho-adrenal activation by chronic intermittent hypoxia. *Journal of Applied Physiology*, *113*(8), 1304–1310. https://doi.org/10.1152/japplphysiol.00444.2012

Qian, X., Yin, T., Li, T., Kang, C., Guo, R., Sun, B., & Liu, C. (2012). High levels of inflammation and insulin resistance in obstructive sleep apnea patients with hypertension. *Inflammation*, *35*(4), 1507–1511. https://doi.org/10.1007/s10753-012-9464-3

Range, N. (n.d.). Normal Hemodynamic Parameters and Laboratory Values Normal Hemodynamic Parameters – Adult.

Robertson, D. W., Biaggioni, I., Burnstock, G., Low, P., & Paton, J. F. (2012). Primer on the Autonomous Nervous System. Elsevier.

Rodela, T. M., & Wright, P. A. (2006). Metabolic and neuroendocrine effects on diurnal urea excretion in the mangrove killifish Rivulus marmoratus. *Journal of experimental biology*, *209*(14), 2704-2712.

Ruffolo, J. (2012). *The alpha-1 adrenergic receptors*. Springer Science & Business Media.

Salo, T. M., Jula, A. M., Piha, J. S., Kantola, I. M., Pelttari, L., Rauhala, E., … Viikari, J. S. A. (2000). Comparison of autonomous withdrawal in men with obstructive sleep apnea syndrome, systemic hypertension, and neither condition. *American Journal of Cardiology*, *85*(2), 232–238. https://doi.org/10.1016/S0002-9149(99)00638-4

Sanders, C. R. (2010). Biomolecular Ligand-Receptor Binding Studies: Theory, Practice, and Analysis. *Dept. of Biochemistry, Vanderbilt University*, 1–43. http://structbio.vanderbilt.edu/sanders/Binding_Principles_2010.pdf, accessed in May 2019.

Schieber, M., & Chandel, N. S. (2014). ROS function in redoz signaling and oxidative stress. *Current Biology*, *24*(10), R453–R462. https://doi.org/10.1016/j.cub.2014.03.034.ROS

Schofl, C., Becker, C., Prank, K., von zur Muhlen, A., Brabant, G., Scho, C., … Brabant, G. (1997). Twenty-four-hour rhythms of plasma catecholamines and their relation to

cardiovascular parameters in healthy young men. *European Journal of Endocrinology*, *137*(6), 675–83. https://doi.org/10.1530/eje.0.1370675

Schwinn, D. A., Johnston, G. I., Page, S. O., Mosley, M. J., Wilson, K. H., Worman, N. P., ... & Parry-Smith, D. J. (1995). Cloning and pharmacological characterization of human alpha-1 adrenergic receptors: sequence corrections and direct comparison with other species homologues. *Journal of Pharmacology and Experimental Therapeutics*, *272*(1), 134-142.

Shamsuzzaman, A. S., Gersh, B. J., & Somers, V. K. (2003). Obstructive sleep apnea: implications for cardiac and vascular disease. *Jama*, *290*(14), 1906-1914.

Sharpe, D. N., Coxon, R., DN, S., & R, C. (1982). Hemodynamic effects of captropril in chronic heart failure: efficacy of low-dose treatment and comparison with prazosin. *American Heart Journal*, *104*(5 Pt 2), 1164–1171. http://onlinelibrary.wiley.com/o/cochrane/clcentral/articles/267/CN-00029267/frame.html, accessed in May 2019.

Shatoor, A. S., Al-hashem, F., Elkarib, A., & Sakr, H. (2012). EC50 of adrenaline-atenolol : Functional agonist assay using Langendorff isolated rabbit heart tethered to powerLab data acquisition system, *6*(15), 1092–1098. https://doi.org/10.5897/AJPP12.123

Shimamoto, H., Shimamoto, Y., & Sakata, S. (1990). Influences of propranolol and atenolol on the circadian rhythm of heart rate in elderly patients with essential hypertension. *Clin Sci (Lond)*, *78*(4), 403–407. https://doi.org/10.1042/cs0780403

Snow, A. B., Khalyfa, A., Serpero, L. D., Capdevila, O. S., Kim, J., Buazza, M. O., & Gozal, D. (2009). Catecholamine alterations in pediatric obstructive sleep apnea: Effect of obesity. *Pediatric Pulmonology*, *44*(6), 559–567. https://doi.org/10.1002/ppul.21015

Souza, H. P., Liu, X., Samouilov, A., Kuppusamy, P., Laurindo, F. R. M., Zweier, J. A. Y. L., … Zweier, J. L. (2002). Quantitation of superoxide generation and substrate utilization by vascular NAD (P) H oxidase, *21224*, 466–474.

Stephenson, R. P. (1956). A modification of receptor theory. *British journal of pharmacology and chemotherapy*, *11*(4), 379-393.

Sterman, J. D. (2000). *Business dynamics: systems thinking and modeling for a complex world* (No. HD30. 2 S7835 2000).

Stern, N., Beahm, E., McGinty, D., Eggena, P., Littner, M., Nyby, M., … Sowers, J. R. (1985). Dissociation of 24-hour catecholamine levels from blood pressure in older men. *Hypertension (Dallas, Tex. : 1979)*, *7*(6 Pt 1), 1023–1029. https://doi.org/10.1161/01.HYP.7.6.1023

Stratton, J. R., Pfeifer, M. A., & Halter, J. B. (1987). The hemodynamic effects of sympathetic stimulation combined with parasympathetic blockade in man. *Circulation*, *75*(5), 922–929. https://doi.org/10.1161/01.CIR.75.5.922

Sun, J., Xu, L., Eu, J. P., Stamler, J. S., & Meissner, G. (2001). Classes of thiols that influence the activity of the skeletal muscle calcium release channel. Journal of Biological Chemistry, 276(19), 15625-15630.

Tamisier, R., Pépin, J. L., Rémy, J., Baguet, J. P., Taylor, J. A., Weiss, J. W., & Lévy, P. (2011). 14 Nights of Intermittent Hypoxia Elevate Daytime Blood Pressure and Sympathetic Activity in Healthy Humans. European Respiratory Journal, 37(1), 119–128. https://doi.org/10.1183/09031936.00204209

Ursino, M., 1998. Interaction between carotid baroregulation and the pulsating heart: a mathematical model. Am. J. Physiol. 275, H1733–H1747.

Ursino, M., & Magosso, E. (2003). Role of short-term cardiovascular regulation in heart period variability: a modeling study. *American Journal of Physiology-Heart and Circulatory Physiology*, *284*(4), H1479-H1493.

Vardhan, V., & Shanmuganandan, K. (2012). Hypertension and catecholamine levels in sleep apnoea. Medical Journal Armed Forces India, 68(1), 33–38. https://doi.org/10.1016/S0377-1237(11)60128-7

Vicentic, A., Robeva, A., Rogge, G., Uberti, M., & Minneman, K. P. (2002). Biochemistry and pharmacology of epitope-tagged α1-adrenergic receptor subtypes. *Journal of Pharmacology and Experimental Therapeutics*, *302*(1), 58-65.

Viitasalo, M., & Karjalainen, J. (1992). QT intervals at heart rates from 50 to 120 beats per minute during 24-hour electrocardiographic recordings in 100 healthy men. Effects of atenolol. *Circulation*, *86*(5), 1439-1442.

Von der Lippe, G., Ohm, O. J., & Lund-Johansen, P. (1981). Acute hemodynamic and long-term clinical effects of prazosin in the treatment of chronic congestive heart failure. *Acta Med.Scand.*, *210*(3), 213–216.

Voogel, A. J., Van Steenwijk, R. P., Karemaker, J. M., & Van Montfrans, G. A. (1999). Effects of treatment of obstructive sleep apnea on circadian hemodynamics. *Journal of the Autonomous Nervous System*, *77*(2–3), 177–183.

Westheim, A., Koss, A., & Sivertssen, E. (1986). Hemodynamic effects at rest and during exercise in long-term treatment with prazosin in chronic congestive heart failure. *Acta Medica Scandinavica*, *219*(5), 449–453.

White, W. B. (2003). Matching the Circadian Rhythms of Hypertension with Pharmacotherapy, *26*, 10–15.

White, W. B. (2007). Importance of blood pressure control over a 24-hour period. *Journal of Managed Care Pharmacy : JMCP*, *13*(8), 34–39.

Zhang, W., & Si, L. Y. (2012). Obstructive sleep apnea syndrome (OSAS) and hypertension: pathogenic mechanisms and possible therapeutic approaches. *Upsala*

journal of medical sciences, 117(4), 370-382. https://doi.org/10.3109/03009734.2012.707253

Zorov, D. B., Juhaszova, M., & Sollott, S. J. (2014). Mitochondrial Reactive Oxygen Species (ROS) and ROS-Induced ROS Release. *Physiological Reviews*, *94*(3), 909–950. https://doi.org/10.1152/physrev.00026.2013

APPENDIX A: MODEL EQUATIONS

Arterial_o2_sat(t) = Arterial_o2_sat(t - dt) + (o2_Sat_Adjustment_Rate) * dt

INIT Arterial_o2_sat = 97

UNITS: Unitless

INFLOWS:

o2_Sat_Adjustment_Rate = (implied_o2_sat-Arterial_o2_sat)/sat_AT

UNITS: per hour (1/hr)

Aten_Conc_Bound_Plas(t) = Aten_Conc_Bound_Plas(t - dt) + (Aten_Bound_Rate) * dt

INIT Aten_Conc_Bound_Plas = 0

UNITS: milligrams/l

INFLOWS:

Aten_Bound_Rate = (Des_Aten_Conc_Bound_Plas-Aten_Conc_Bound_Plas)/AT_Aten_Bound

UNITS: milligrams/hr-l

Average_Daily_O2_Ratio(t) = Average_Daily_O2_Ratio(t - dt) + (Oxygenation_rate) * dt

INIT Average_Daily_O2_Ratio = 1

UNITS: Unitless

INFLOWS:

Oxygenation_rate = (Oxygen_Demand_Supply_Ratio-Average_Daily_O2_Ratio)/AT_O2

UNITS: per hour (1/hr)

Average_Hourly_Sympathetic_Neuron_Activation(t) = Average_Hourly_Sympathetic_Neuron_Activation(t - dt) + (Bal_Rate) * dt

INIT Average_Hourly_Sympathetic_Neuron_Activation = 40

UNITS: burst

INFLOWS:

Bal_Rate = (Implied_SNA-Average_Hourly_Sympathetic_Neuron_Activation)/Bal_Time

UNITS: burst/hr

Average_Stroke_Volume(t) = Average_Stroke_Volume(t - dt) + (Adj_Rate_ASV) * dt

INIT Average_Stroke_Volume = 80

UNITS: milliliters/beat

INFLOWS:

Adj_Rate_ASV = (implied_Stroke_Volume-Average_Stroke_Volume)/(AT_ASV)

UNITS: milliliters/beat-hr

Baro_Smooth1(t) = Baro_Smooth1(t - dt) + (smooth_rate3) * dt

INIT Baro_Smooth1 = 87

UNITS: mmHg

INFLOWS:

smooth_rate3 = (BLood_Pressure-Baro_Smooth1)/AT_Baro

UNITS: mmhg/hr

Baro_Smooth2(t) = Baro_Smooth2(t - dt) + (smooth_rate4) * dt

INIT Baro_Smooth2 = 87

UNITS: mmHg

INFLOWS:

smooth_rate4 = (Baro_Smooth1-Baro_Smooth2)/AT_Baro

UNITS: mmhg/hr

BLood_Pressure(t) = BLood_Pressure(t - dt) + (Change_Rate_BP) * dt

INIT BLood_Pressure = 87

UNITS: mmHg

INFLOWS:

Change_Rate_BP = (implied_Bp-BLood_Pressure)/ATBP

UNITS: mmhg/hr

Conc_of_NonAbs_Aten(t) = Conc_of_NonAbs_Aten(t - dt) + (Aten_Dosage_Rate - Abs_Rate_of_Aten) * dt

INIT Conc_of_NonAbs_Aten = 0

UNITS: milligrams/l

INFLOWS:

Aten_Dosage_Rate = PULSE(Aten_Dosage* Bio_Aten/Volume_Distribution_of_Aten,6000,24)

UNITS: milligrams/hr-l

OUTFLOWS:

Abs_Rate_of_Aten = Abs_Ratio_of_aten*Conc_of_NonAbs_Aten

UNITS: milligrams/hr-l

Conc_of_NonAbs_Pro(t) = Conc_of_NonAbs_Pro(t - dt) + (Pro_Dosage_Rate - Abs_Rate_of_Pro) * dt

INIT Conc_of_NonAbs_Pro = 0

UNITS: mg/l

INFLOWS:

Pro_Dosage_Rate = Pulse(Pro_Dosage* Bio_Pro / Volume_distriburion_of_Pro,6000,24)

UNITS: mg/hr-l

OUTFLOWS:

Abs_Rate_of_Pro = Conc_of_NonAbs_Pro*Abs_ratio_of_Pro

UNITS: mg/hr-l

Diameter_of_Arterioles(t) = Diameter_of_Arterioles(t - dt) + (Dilatation_Rate - Constriction_Rate) * dt

INIT Diameter_of_Arterioles = 8*(10^-4)

UNITS: centimeter

INFLOWS:

Dilatation_Rate = (Implied_diameter-Diameter_of_arterioles)/(Diameter_AT)

UNITS: cm/hr

OUTFLOWS:

Constriction_Rate = (Diameter_of_arterioles-Implied_diameter)/Diameter_AT

UNITS: cm/hr

EP(t) = EP(t - dt) + (Trans_Rate - Clr_Rate_of_Ep) * dt

INIT EP = 40

UNITS: pg/ml

INFLOWS:

Trans_Rate = NEP*Trans_Rat_NE_to_E

UNITS: pg/hr-ml

OUTFLOWS:

Clr_Rate_of_Ep = EP*Clr_Rat_Ep

UNITS: pg/hr-ml

Expected_Loss_in_Ep(t) = Expected_Loss_in_Ep(t - dt) + (Net_Ep_Loss_Rate) * dt

INIT Expected_Loss_in_Ep = 400

UNITS: pg/ml-hour

INFLOWS:

Net_Ep_Loss_Rate = (Clr_rate_of_Ep-Expected_Loss_in_Ep)/AT_clr_rate_Ep

UNITS: pg/hour-hr-ml

Exp_Loss_in_Nep(t) = Exp_Loss_in_Nep(t - dt) + (Net_Nep_loss_rate) * dt

INIT Exp_Loss_in_Nep = 3600

UNITS: pg/ml-hour

INFLOWS:

Net_Nep_loss_rate = (Clr_rate_of_Nep-Exp_Loss_in_Nep)/AT_clr_rate_Nep

UNITS: pg/hour-hr-ml

Free_Aten_Conc(t) = Free_Aten_Conc(t - dt) + (Abs_Rate_of_Aten - Elim_Rate_of_Aten - Aten_Bound_Rate) * dt

INIT Free_Aten_Conc = 0

UNITS: milligrams/l

INFLOWS:

Abs_Rate_of_Aten = Abs_Ratio_of_aten*Conc_of_NonAbs_Aten

UNITS: milligrams/hr-l

OUTFLOWS:

Elim_Rate_of_Aten = Free_Aten_Conc*Elim_Rat_Aten

UNITS: milligrams/hr-l

Aten_Bound_Rate = (Des_Aten_Conc_Bound_Plas-Aten_Conc_Bound_Plas)/AT_Aten_Bound

UNITS: milligrams/hr-l

Free_Prozasin_Conc(t) = Free_Prozasin_Conc(t - dt) + (Abs_Rate_of_Pro - Elim_Rate_of_Pro - Pro_Bound_rate) * dt

INIT Free_Prozasin_Conc = 0

UNITS: mg/l

INFLOWS:

Abs_Rate_of_Pro = Conc_of_NonAbs_Pro*Abs_ratio_of_Pro

UNITS: mg/hr-l

OUTFLOWS:

Elim_Rate_of_Pro = Free_Prozasin_Conc*Elim_Rat_Pro

UNITS: mg/hr-l

Pro_Bound_rate = (Des_Pro_Conc_Bound_Plas-Pro_Conc_Bound_to_Plas)/AT_Pro_Bound

UNITS: mg/hr-l

Heart_Rate(t) = Heart_Rate(t - dt) + (Modification_rate) * dt

INIT Heart_Rate = 75

UNITS: beat/min

INFLOWS:

Modification_rate = (implied_heart_rate-Heart_Rate)/modification_time

UNITS: beat/hr-min

Heart_Rate_smoothed(t) = Heart_Rate_smoothed(t - dt) + (HR_Smooth_Rate) * dt

INIT Heart_Rate_smoothed = 75

UNITS: l/min

INFLOWS:

HR_Smooth_Rate = (Heart_Rate-Heart_Rate_smoothed)/Heart_Rate_delay

UNITS: l/hr-min

LTBP(t) = LTBP(t - dt) + (LTBP_smooth_rate) * dt

INIT LTBP = 87

UNITS: mmHg

INFLOWS:

LTBP_smooth_rate = (LTBP_Smooth2-LTBP)/AT_LTBP

UNITS: mmhg/hr

LTBP_Smooth1(t) = LTBP_Smooth1(t - dt) + (smooth_rate1) * dt

INIT LTBP_Smooth1 = 87

UNITS: mmHg

INFLOWS:

smooth_rate1 = (BLood_Pressure-LTBP_Smooth1)/AT_LTBP

UNITS: mmhg/hr

LTBP_Smooth2(t) = LTBP_Smooth2(t - dt) + (smooth_rate2) * dt

INIT LTBP_Smooth2 = 87

UNITS: mmHg

INFLOWS:

smooth_rate2 = (LTBP_Smooth1-LTBP_Smooth2)/AT_LTBP

UNITS: mmhg/hr

NEP(t) = NEP(t - dt) + (Spillover_Rate - Trans_Rate - Clr_rate_of_Nep) * dt

INIT NEP = 400

UNITS: pg/ml

INFLOWS:

Spillover_Rate = ((Des_EP-EP)/ATN)+Expected_Loss_in_Ep+Exp_Loss_in_Nep

UNITS: pg/hr-ml

OUTFLOWS:

Trans_Rate = NEP*Trans_Rat_NE_to_E

UNITS: pg/hr-ml

Clr_rate_of_Nep = NEP*Clr_Rat_Nep

UNITS: pg/hr-ml

Operation_point_of_Baroreceptor(t) = Operation_point_of_Baroreceptor(t - dt) + (Baro_smooth_rate) * dt

INIT Operation_point_of_Baroreceptor = 87

UNITS: mmHg

INFLOWS:

Baro_smooth_rate = (Baro_Smooth2-Operation_point_of_Baroreceptor)/AT_Baro

UNITS: mmhg/hr

Pro_Conc_Bound_to_Plas(t) = Pro_Conc_Bound_to_Plas(t - dt) + (Pro_Bound_rate) * dt

INIT Pro_Conc_Bound_to_Plas = 0

UNITS: mg/l

INFLOWS:

Pro_Bound_rate = (Des_Pro_Conc_Bound_Plas-Pro_Conc_Bound_to_Plas)/AT_Pro_Bound

UNITS: mg/hr-l

Total_Chemoreceptor_Concentration(t) = Total_Chemoreceptor_Concentration(t - dt) + (Prod_rate - Dest_rate) * dt

INIT Total_Chemoreceptor_Concentration = 100

UNITS: mg/l

INFLOWS:

Prod_rate = Implied_Prod_Ratio*Total_Chemoreceptor_Concentration*Eff_of_Chem_on_flows

UNITS: mg/hr-l

OUTFLOWS:

Dest_rate = Total_Chemoreceptor_Concentration*Implied_Dest_Ratio*Eff_of_Chem_on_flows

UNITS: mg/hr-l

Abs_Ratio_of_Aten = 0.1411

UNITS: per hour (1/hr)

Abs_ratio_of_Pro = 0.3943

UNITS: per hour (1/hr)

Ahi_dist = Ref_Ahi_dist*ratio_of_AHI_to_Ref_AHI

UNITS: per 20 minutes

Apnea_Hypopnea_Index = IF TIME<1680 THEN 30 ELSE 0

UNITS: Unitless

Ar_Sat = Arterial_o2_sat/ref_o2_arterial_sat

UNITS: Unitless

ATBP = 1

UNITS: hours (hr)

Aten_Binding_Ratio = 0.05

UNITS: Unitless

Aten_Dosage = 50

UNITS: milligrams (mg)

ATN = 1

UNITS: hour

AT_ASV = 1

UNITS: hour

AT_Aten_Bound = 1

UNITS: hour

AT_Baro = 8

UNITS: hour

AT_Clr_Rate_Ep = 1

UNITS: hour

AT_Clr_Rate_Nep = 1

UNITS: hour

AT_LTBP = 24

UNITS: hour

AT_O2 = 96

UNITS: hour

AT_Pro_Bound = 1

UNITS: hour

Bal_Time = 1

UNITS: hour

Bio_Aten = 0.56

UNITS: Unitless

Bio_Pro = 0.68

UNITS: Unitless

Cardiac_Output = Average_Stroke_Volume*Heart_Rate*unit_con_ml_to_l

UNITS: l/min

Chemo_Eff_on_SNA = GRAPH(Ratio_of_Tot_to_ref)

(1.00, 1.00), (1.02, 1.02), (1.04, 1.05), (1.06, 1.07), (1.08, 1.09), (1.10, 1.11), (1.12, 1.14), (1.14, 1.16), (1.16, 1.17), (1.18, 1.19), (1.20, 1.20), (1.22, 1.21), (1.24, 1.22), (1.26, 1.22), (1.28, 1.23), (1.30, 1.24), (1.32, 1.24), (1.34, 1.24), (1.36, 1.25), (1.38, 1.25), (1.40, 1.25)

UNITS: Unitless

Chemo_ref = 100

UNITS: mg/l

Clr_Rat_Ep = 10

UNITS: 1/hour

Clr_Rat_Nep = 9

UNITS: 1/hour

Cl_Of_Aten = 10.2

UNITS: l/hour

Cl_Of_Pro = 12.6

UNITS: l/hour

Com_Fac_A1 = 1/(1+(EPI/KD_EP_A1)+(NEPI/KD_NEP_A1)+(Free_Prozasin_Conc/KD_of_Pro))

UNITS: Unitless

Com_Fac_Beta_1 = 1/(1+(EPI/KD_EP_B1)+(NEPI/KD_NEP_B1)+(Free_Aten_Conc/KD_of_atenolol))

UNITS: Unitless

Daily_O2_Ratio_Eff = GRAPH(Average_Daily_O2_Ratio)

(0.00, 0.45), (0.1, 0.46), (0.2, 0.48), (0.3, 0.51), (0.4, 0.55), (0.5, 0.6), (0.6, 0.66), (0.7, 0.73), (0.8, 0.81), (0.9, 0.9), (1.00, 1.00)

UNITS: Unitless

Des_Aten_Conc_Bound_Plas = Free_Aten_Conc*Aten_Binding_Ratio

UNITS: mg/l

Des_EP = Average_Hourly_Sympathetic_Neuron_Activation*Productivity_of_each_neuron

UNITS: pg/ml

Des_Pro_Conc_Bound_Plas = Free_Prozasin_Conc*Pro_Binding_Ratio

UNITS: mg/l

Diameter_AT = 1

UNITS: hours (hr)

Duration_of_Ahi = 1/120

UNITS: per 20 minutes

EC50_EP_for_B1 = 23.6*(10^3)/(5.454*10^6)

UNITS: mg/l

EC50_NEP_for_B1 = 236*(10^3)/(5.914*10^6)

UNITS: mg/l

EC_50_NEP_for_A1 = 15*(10^3)/(5.914*10^6)

UNITS: mg/l

Effect_of_Tot_B1_Res_on_Heart_Rate = GRAPH(Tot_B1_Res/Ref_Tot_B1_Res)

(0.00, 0.6), (0.0741, 0.61), (0.148, 0.63), (0.222, 0.66), (0.296, 0.7), (0.37, 0.75), (0.444, 0.81), (0.519, 0.871), (0.593, 0.935), (0.667, 1.00), (0.741, 1.06), (0.815, 1.13), (0.889, 1.19), (0.963, 1.25), (1.04, 1.29), (1.11, 1.33), (1.19, 1.37), (1.26, 1.41), (1.33, 1.44), (1.41, 1.48), (1.48, 1.51), (1.56, 1.54), (1.63, 1.57), (1.70, 1.59), (1.78, 1.61), (1.85, 1.64), (1.93, 1.65), (2.00, 1.65)

UNITS: Unitless

Effect_Tot_A1_Res_on_Diameter = GRAPH(Tot_A1_Res/Ref_Tot_A1_Res)

(0.00, 1.17), (0.1, 1.16), (0.2, 1.16), (0.3, 1.15), (0.4, 1.14), (0.5, 1.12), (0.6, 1.10), (0.7, 1.08), (0.8, 1.06), (0.9, 1.03), (1.00, 1.00), (1.10, 0.97), (1.20, 0.943), (1.30, 0.923), (1.40, 0.91), (1.50, 0.902), (1.60, 0.896), (1.70, 0.891), (1.80, 0.887), (1.90, 0.884), (2.00, 0.883)

UNITS: Unitless

Eff_of_Baro = GRAPH(Ratio_of_BP_to_BOP)

(0.1, 1.32), (0.19, 1.31), (0.28, 1.29), (0.37, 1.26), (0.46, 1.21), (0.55, 1.15), (0.64, 1.10), (0.73, 1.06), (0.82, 1.03), (0.91, 1.01), (1, 1.00), (1.09, 0.99), (1.18, 0.97), (1.27, 0.94), (1.36, 0.9), (1.45, 0.85), (1.54, 0.79), (1.63, 0.74), (1.72, 0.71), (1.81, 0.69), (1.90, 0.68)

UNITS: Unitless

Eff_Of_Blood_Pressure_on_O2_Uptake = GRAPH(Ratio_Of_Blood_Pressure)

(0.00, 0.66), (0.1, 0.68), (0.2, 0.712), (0.3, 0.776), (0.4, 0.832), (0.5, 0.88), (0.6, 0.92), (0.7, 0.952), (0.8, 0.976), (0.9, 0.988), (1.00, 1.00), (1.10, 1.01), (1.20, 1.02), (1.30, 1.05), (1.40, 1.08), (1.50, 1.12), (1.60, 1.17), (1.70, 1.22), (1.80, 1.29), (1.90, 1.32), (2.00, 1.34)

UNITS: Unitless

Eff_of_Chem_on_flows = GRAPH(Ratio_of_Tot_to_ref)

(1.00, 4.48), (1.01, 4.45), (1.02, 4.36), (1.02, 4.12), (1.03, 3.88), (1.04, 3.40), (1.05, 2.80), (1.06, 2.20), (1.07, 1.72), (1.08, 1.36), (1.08, 1.12), (1.09, 1.03), (1.10, 1.00)

UNITS: Unitless

Eff_Of_Chem_on_Prod_rat = GRAPH(Ratio_of_Tot_to_ref)

(1.00, 1.00), (1.01, 0.997), (1.02, 0.991), (1.03, 0.982), (1.04, 0.97), (1.05, 0.95), (1.06, 0.93), (1.07, 0.918), (1.08, 0.909), (1.09, 0.903), (1.10, 0.9)

UNITS: Unitless

Eff_of_F&L = GRAPH(time mod 24)

(0.00, 0.89), (1.00, 0.878), (2.00, 0.873), (3.00, 0.878), (4.00, 0.89), (5.00, 0.908), (6.00, 0.932), (7.00, 0.963), (8.00, 0.999), (9.00, 1.03), (10.0, 1.06), (11.0, 1.09), (12.0, 1.11), (13.0, 1.12), (14.0, 1.12), (15.0, 1.12), (16.0, 1.11), (17.0, 1.09), (18.0, 1.06), (19.0, 1.03), (20.0, 0.999), (21.0, 0.963), (22.0, 0.932), (23.0, 0.908), (24.0, 0.89)

UNITS: Unitless

Eff_of_filling_time_on_ASV = GRAPH(Heart_Rate/reference_heart_rate)

(0.4, 1.25), (0.457, 1.25), (0.514, 1.24), (0.571, 1.22), (0.629, 1.19), (0.686, 1.15), (0.743, 1.10), (0.8, 1.05), (0.857, 1.00), (0.914, 0.953), (0.971, 0.909), (1.03, 0.87), (1.09, 0.834), (1.14, 0.8), (1.20, 0.776), (1.26, 0.753), (1.31, 0.732), (1.37, 0.712), (1.43, 0.694), (1.49, 0.676), (1.54, 0.661), (1.60, 0.645), (1.66, 0.633), (1.71, 0.624), (1.77, 0.615), (1.83, 0.61), (1.89, 0.606), (1.94, 0.603), (2.00, 0.6)

UNITS: Unitless

Eff_Of_Oxygen_Rat = GRAPH(Oxygen_Demand_Supply_Ratio)

(0.5, 1.49), (0.55, 1.49), (0.6, 1.48), (0.65, 1.48), (0.7, 1.47), (0.75, 1.46), (0.8, 1.43), (0.85, 1.38), (0.9, 1.26), (0.95, 1.14), (1.00, 1.00), (1.05, 0.861), (1.10, 0.791), (1.15, 0.767), (1.20, 0.756), (1.25, 0.747), (1.30, 0.739), (1.35, 0.733), (1.40, 0.728), (1.45, 0.725), (1.50, 0.723)

UNITS: Unitless

Eff_Of_Workload = GRAPH(Heart_Rate_smoothed/reference_heart_rate)

(0.75, 0.85), (0.762, 0.85), (0.775, 0.851), (0.787, 0.851), (0.8, 0.853), (0.812, 0.856), (0.825, 0.86), (0.838, 0.865), (0.85, 0.872), (0.863, 0.88), (0.875, 0.891), (0.888, 0.904), (0.9, 0.919), (0.913, 0.937), (0.925, 0.952), (0.938, 0.965), (0.95, 0.976), (0.963, 0.984), (0.975, 0.991), (0.988, 0.996), (1.00, 1.00), (1.01, 1.00), (1.03, 1.00), (1.04, 1.01), (1.05, 1.01)

UNITS: Unitless

Elim_Rat_Aten = Cl_Of_Aten/Volume_Distribution_of_Aten

UNITS: per hour (1/hr)

Elim_Rat_Pro = Cl_of_Pro/Volume_distriburion_of_Pro

UNITS: per hour (1/hr)

EPI = unit_converter_pgml_to_mgl*(EP)

UNITS: mg/l

EP_rat_occ_B1 = (EPI/KD_EP_B1)*Com_Fac_Beta_1

UNITS: Unitless

Heart_Rate_Delay = 24

UNITS: hours (hr)

Implied_Bp = Systemic_Vascular_Resis*Cardiac_Output

UNITS: mmHg

Implied_Dest_Ratio = Daily_O2_Ratio_Eff*Ref_Dest_ratio

UNITS: per hour (1/hr)

Implied_diameter = Effect_Tot_A1_Res_on_diameter*reference_diameter

UNITS: centimeter

implied_heart_rate = reference_heart_rate*Effect_of_Tot_B1_Res_on_Heart_Rate

UNITS: beat/min

Implied_o2_sat = perc_of_breathing*ref_o2_arterial_sat

UNITS: Unitless

Implied_Oxygen_uptake = Ref_O2_uptake * Eff_Of_Blood_Pressure_on_O2_Uptake * Ar_Sat

UNITS: picomolar/hour

Implied_Oxygen_Usage = Eff_Of_workload * ref_Oxygen_Usage * (Eff_of_F&L)

UNITS: picomolar/hour

Implied_Prod_Ratio = Eff_Of_Chem_on_prod_rat*Ref_Prod_Ratio

UNITS: per hour (1/hr)

Implied_SNA = Ref_Sna*Eff_of_Baro*Eff_Of_Oxygen_Rat*Chemo_Eff_on_SNA

UNITS: burst

Implied_Stroke_Volume = ref_Stroke_Volume*Eff_of_filling_time_on_ASV

UNITS: milliliters/beat

KD_EP_A1 = 251.18*(10^3)/(5.914*10^6)

UNITS: mg/l

KD_EP_B1 = (3970)*(10^3)/(5.454*10^6)

UNITS: mg/l

KD_NEP_A1 = 199.52*(10^3)/(5.914*10^6)

UNITS: mg/l

KD_NEP_B1 = 3570*10^3/(10^6*5.914)

UNITS: mg/l

KD_of_atenolol = (388)*266.336*(10^-9)*(10^3)*100/7.75

UNITS: mg/l

KD_of_Pro = 10.2*(10^-9)*(10^3)*383.401*10/7

UNITS: mg/l

modification_time = 1

UNITS: hour

NEPI = unit_converter_pgml_to_mgl*(NEP)

UNITS: mg/l

NEP_rat_occ_A1 = NEPI*Com_Fac_A1/KD_NEP_A1

UNITS: Unitless

NEP_rat_occ_B1 = (NEPI/KD_NEP_B1)*Com_Fac_Beta_1

UNITS: Unitless

Oxygen_Demand_Supply_Ratio = Implied_Oxygen_uptake/Implied_Oxygen_Usage

UNITS: Unitless

Perc_of_Breathing = (1-duration_of_Ahi*Ahi_dist)

UNITS: Unitless

Productivity_of_each_neuron = 1

UNITS: pg/ml-burst

Pro_Binding_Ratio = 0.95

UNITS: Unitless

Pro_Dosage = 0.5

UNITS: milligrams (mg)

ratio_of_AHI_to_Ref_AHI = Apnea_Hypopnea_Index/Ref_Ahi

UNITS: Unitless

Ratio_Of_Blood_Pressure = (BLood_Pressure/ref_blood_Pressure)

UNITS: Unitless

Ratio_of_BP_to_BOP = BLood_Pressure/Operation_point_of_Baroreceptor

UNITS: Unitless

Ratio_of_Resis_Change = (reference_diameter/Diameter_of_arterioles)^4

UNITS: Unitless

Ratio_of_Tot_to_ref = Total_Chemoreceptor_Concentration/Chemo_ref

UNITS: Unitless

reference_diameter = 8*(10^-4)

UNITS: centimeter

reference_heart_rate = 75

UNITS: beat/min

Ref_Ahi = 54

UNITS: Unitless

Ref_Ahi_dist = GRAPH((Time) mod 24)

(0.00, 0.4), (0.333, 2.00), (0.667, 5.60), (1.00, 12.0), (1.33, 22.0), (1.67, 28.4), (2.00, 32.0), (2.33, 33.6), (2.67, 34.0), (3.00, 34.0), (3.33, 33.6), (3.67, 32.0), (4.00, 28.4), (4.33, 22.0), (4.67, 12.0), (5.00, 5.60), (5.33, 2.00), (5.67, 0.4), (6.00, 0.00), (6.33, 0.00), (6.67, 0.00), (7.00, 0.00), (7.33, 0.00), (7.67, 0.00), (8.00, 0.00), (8.33, 0.00), (8.67, 0.00), (9.00, 0.00), (9.33, 0.00), (9.67, 0.00), (10.0, 0.00), (10.3, 0.00), (10.7, 0.00), (11.0, 0.00), (11.3, 0.00), (11.7, 0.00), (12.0, 0.00), (12.3, 0.00), (12.7, 0.00), (13.0, 0.00), (13.3, 0.00), (13.7, 0.00), (14.0, 0.00), (14.3, 0.00), (14.7, 0.00), (15.0, 0.00), (15.3, 0.00), (15.7, 0.00), (16.0, 0.00), (16.3, 0.00), (16.7, 0.00), (17.0, 0.00), (17.3, 0.00), (17.7, 0.00), (18.0, 0.00), (18.3, 0.00), (18.7, 0.00), (19.0, 0.00), (19.3, 0.00), (19.7, 0.00), (20.0, 0.00), (20.3, 0.00), (20.7, 0.00), (21.0, 0.00), (21.3, 0.00), (21.7, 0.00), (22.0, 0.00), (22.3, 0.00), (22.7, 0.00), (23.0, 0.00), (23.3, 0.00), (23.7, 0.00), (24.0, 0.00)

UNITS: per 20 minutes

ref_Blood_Pressure = 87

UNITS: mmHg

Ref_Dest_ratio = 0.05

UNITS: per hour (1/hr)

ref_o2_arterial_sat = 97

UNITS: Unitless

Ref_O2_uptake = 15*(10^5)

UNITS: picomolar/hour

ref_Oxygen_Usage = 15*(10^5)

UNITS: picomolar/hour

Ref_Prod_Ratio = 0.05

UNITS: per hour (1/hr)

Ref_Sna = 40

UNITS: burst

Ref_Stroke_Volume = 80

UNITS: milliliters/beat

Ref_Svr = 14.5

UNITS: mmHg-min/l

Ref_Tot_A1_Res = 0.155713802459758

UNITS: Unitless

Ref_Tot_B1_Res = 0.0184748782940904

UNITS: Unitless

Res_E_on_B1 = (KD_EP_B1/EC50_EP_for_B1)*EP_rat_occ_B1

UNITS: Unitless

Res_NE_on_B1 = (KD_NEP_B1/EC50_NEP_for_B1)*NEP_rat_occ_B1

UNITS: Unitless

Sat_AT = 1

UNITS: hour

Systemic_Vascular_Resis = Ratio_of_Resis_Change*ref_Svr

UNITS: mmHg-min/l

Tot_A1_Res = (NEP_rat_occ_A1*KD_NEP_A1/EC_50_NEP_for_A1)

UNITS: Unitless

Tot_B1_Res = (Res_E_on_B1+Res_NE_on_B1)

UNITS: Unitless

Trans_Rat_NE_to_E = 1

UNITS: 1/hour

unit_converter_pgml_to_mgl = (10^-6)

UNITS: mg-ml/pg-l

unit_con_ml_to_l = 0.001

UNITS: l/ml

Volume_distriburion_of_Pro = 42

UNITS: liters (l)

Volume_Distribution_of_Aten = 67

UNITS: liters (l)